

# Multi-gram Synthesis of Trioxanes Enabled by a Supercritical CO<sub>2</sub> Integrated Flow Process

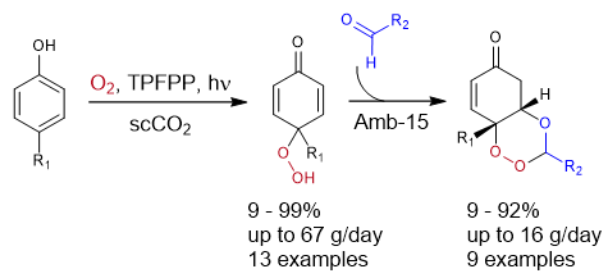
Lingqiao Wu,<sup>a</sup> Bruna Lacerda Da Silva Abreu,<sup>a</sup> Alexander J. Blake,<sup>a</sup> Laurence J. Taylor,<sup>a</sup> William Lewis,<sup>a</sup> Stephen P. Argent,<sup>a</sup> Martyn Poliakoff,<sup>a</sup> Hamza Boufroua\*<sup>a</sup> and Michael W. George.\*<sup>a</sup>

<sup>a</sup>School of Chemistry, University of Nottingham, University Park, Nottingham, NG7 2RD, UK

**Email:** [mike.george@nottingham.ac.uk](mailto:mike.george@nottingham.ac.uk) and [hamza.boufroua@nottingham.ac.uk](mailto:hamza.boufroua@nottingham.ac.uk)

## TOC graphic

### Telescoped Continuous Flow Process



## Abstract

Photochemical synthesis of highly reactive hydroperoxides and their conversion into useful products, such as 1,2,4-trioxanes, is of wide interest for synthetic organic chemistry and pharmaceutical manufacturing, particularly because of their relevance as potential antimalarial and anticancer treatments e.g. Artemisinin. One class of antimalarial drugs is based on 1,2,4-trioxane scaffolds, although production of such compounds on a gram scale is challenging due to their instability in oxidisable solvents. Furthermore, current methods employ either solid oxidants, which makes continuous processing problematic, or molecular oxygen, requiring long reaction times of up to 48 hours. Here we report a new multi-gram continuous approach using a custom-built high-pressure sapphire photoreactor to make trioxanes via the de-aromatisation of *para*-substituted phenols by photo-generated singlet oxygen in supercritical CO<sub>2</sub>. The CO<sub>2</sub> also gives improved mixing with O<sub>2</sub> and lower viscosity, thereby improving penetration into the pores of the solid acid catalyst used for the formation of the trioxanes. We show the capabilities of a 5.2 mL reactor to scale up the reaction to 67 g/day. This synthetic approach provides a platform to rapidly access high value compounds under flow conditions, with high atom efficiencies, excellent yields, short reaction times, and without the need for isolation of hazardous intermediates.

Keywords: Singlet oxygen, Supercritical CO<sub>2</sub>, De-aromatisation, 1,2,4-Trioxanes, Telescoped Synthesis, Continuous Flow.

## Introduction

The oxidative de-aromatisation of phenols is a desirable strategy to access valuable precursors in the synthesis of more complex architectures such as natural products.<sup>1</sup> When singlet oxygen is used, oxidative de-aromatisation of phenols gives rise to peroxyquinols. These key intermediates have been used for the formation of natural products. More specifically, they have been exploited in the formation of 1,2,4-trioxanes<sup>2-5</sup> by reaction of *para*-peroxyquinols with aldehydes, which are important molecules that bear an endoperoxide motif which exhibits biological activities. This moiety appears to be a key pharmacophore<sup>6-9</sup> in combating malaria.<sup>10,11</sup>

The synthesis of peroxide and 1,2,4-trioxanes can be problematic due to their potentially explosive properties, e.g. triacetone triperoxide (TATP).<sup>12</sup> Thus, there is a need to develop new antimalarial compounds. Minimizing the financial and environmental costs of manufacturing such compounds is a major goal since it is the aim to supply any antimalarial treatment at a price that will permit widespread use in economically developing countries.<sup>13</sup> In addition to antimalarial activity, recent reports have also shown that such compounds may be useful as antitumor agents<sup>14-17</sup> and may have  $\beta$ -cell reactivation activity which is of relevance to diabetes therapy.<sup>18-19</sup> Moreover, *para*-peroxyquinols are valuable as intermediates in their own right for the preparation of diverse range of synthetic scaffolds.<sup>20</sup>

Griesbeck and co-workers<sup>21</sup> have an outstanding record in developing methodologies to access new trioxanes including the use of both chemically and photochemically generated singlet oxygen, <sup>1</sup>O<sub>2</sub>, to access spirofused and annulated cyclic peroxides of varying ring size so as to examine their conformational and thermal stability. More generally, the synthesis of 1,2,4-trioxanes has been achieved by the de-aromatisation of phenol using <sup>1</sup>O<sub>2</sub> which can be generated either photochemically<sup>21</sup> or chemically<sup>22</sup> (e.g. from commercially available Oxone, (KHSO<sub>5</sub>)). Therefore the use of <sup>1</sup>O<sub>2</sub> on-scale would open up very economical routes to high value compounds but, unfortunately, all of this work has involved batch reactions which are hard to scale-up both on safety grounds (e.g. larger inventories of hazardous intermediates) and the more generic problems of scaling-up photochemical reactions. However, the recent resurgence of photochemistry<sup>23-31</sup> is driving the design of new flow photoreactors,<sup>32-46</sup> many of which enable effective and safe addition of gases such as photochemically generated <sup>1</sup>O<sub>2</sub>.<sup>28, 32-40</sup> Here we demonstrate that continuous flow synthesis in supercritical CO<sub>2</sub> (scCO<sub>2</sub>) overcomes many of the scale-up problems confronting more

traditional approaches to making trioxanes, including full miscibility with gaseous O<sub>2</sub>, the long lifetime of <sup>1</sup>O<sub>2</sub>, together with the non-flammability and chemical inertness of CO<sub>2</sub> to deliver a wide range of trioxanes on a multi-gram scale.

## Results and Discussion

### General Strategy

Our route to 1,2,4-trioxanes involves an integrated two-step flow synthesis in scCO<sub>2</sub> via a telescoped process. First a photo-oxidation to de-aromatise *para*-substituted phenols, generating peroxyquinols which are then reacted with a series of aldehydes to form the corresponding cyclic endoperoxides: 1,2,4-trioxanes, thereby minimising the quantity of potentially unstable peroxyquinols in the system at any one time. To fully exploit the use of scCO<sub>2</sub> in the flow synthesis of trioxanes, the phenol precursors and aldehydes need to be pumped into the flow system to mix with scCO<sub>2</sub> and O<sub>2</sub> and, since many of these compounds are solids, a co-solvent is required. The challenge has been to find a solvent which can be used for both stages of the process, because, at the small scale of these experiments, a solvent change between the two stages would be difficult if not impossible. Figure 1 shows a schematic view of the entire flow reactor.

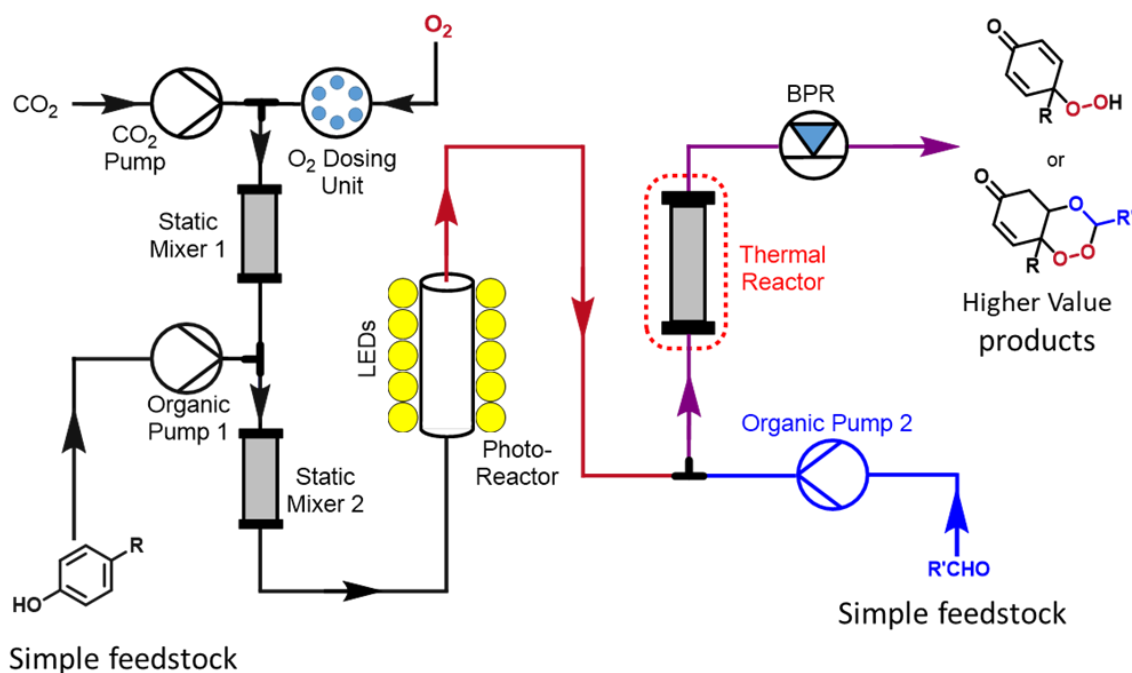


**Figure 1.** Simplified diagram of our high pressure continuous flow setup for dearomatisation followed by the acid-catalysed reaction with aldehydes to make 1,2,4-trioxanes. CO<sub>2</sub> is supplied from a chilled CO<sub>2</sub> Pump and O<sub>2</sub> is dosed in at a known rate via a Rheodyne Dosage Unit. The Static Mixer 1 consists of a stainless steel tubular reactor loaded with sand to promote the mixing of CO<sub>2</sub> and O<sub>2</sub>. The reagents and photosensitizer are pumped by Organic Pump 1 and then mixed with gases in Static Mixer 2, which is also a stainless steel tube filled with sand. The mixture is then flowed upwards through a high-pressure sapphire tube reactor, which is filled with glass beads to enhance mixing, and finally irradiated by these arrays of white light LEDs. Downstream of the photoreactor, there is an electrically-heated Thermal Reactor, (shown in purple) consisting of a stainless steel tubular reactor loaded with a solid catalyst. A second optional Organic Pump is attached before the thermal reactor. The product mixture then passes through a back pressure

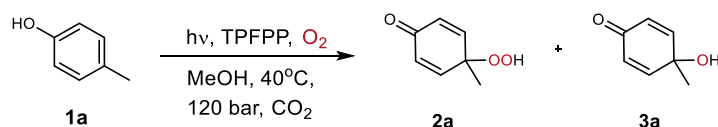
regulator, BPR, before further analysis is carried out. (A full diagram of each set-up and the information about the LEDs set are provided in the ESI).

### Photo-oxidation of *para*-cresol using MeOH as co-solvent

In order to optimise the first stage of the process, different conditions were screened for the photo-oxidation of *para*-cresol with O<sub>2</sub> to form the peroxide with 5,10,15,20-tetrakis(pentafluorophenyl)porphyrin (TPFPP) as the photosensitiser, using scCO<sub>2</sub> with MeOH (40°C, 120 bar). MeOH was initially chosen as the co-solvent to minimise the risk of precipitation of both the substrate and product in scCO<sub>2</sub>. The first challenge was to minimize the formation of reduced peroxyquinol which could react further during the second step and necessitate a complicated separation from the desired trioxanes. There are also potential issues with dehydration forming quinone methide which might lead to acid-catalysed polymerisation in the thermal reactor.

Our initial attempt to form the de-aromatised methyl peroxyquinol **2a** afforded the desired product with a yield of 35% with a residence time of 7 minutes (Table 1, entry 1). Increasing the residence time by a factor of four increased the yield to 72% (Table 1, entry 2). The addition of different bases TEA, DBU and K<sub>2</sub>CO<sub>3</sub> failed to increase the formation of the peroxide product substantially but did increase the yield of undesired reduced product **3a** up to nearly 10% (See ESI). Surprisingly, increasing the concentration of starting material gave improved yields (Table 1, entries 3 & 4), permitting the formation of *para*-peroxyquinol with an excellent yield of 96%, increasing the concentration of the starting solution to 5 M in MeOH caused blockages on prolonged running (>4 hrs).

**Table 1.** Optimisation of de-aromatisation of *para*-cresol **1a**, in continuous flow in high pressure system using scCO<sub>2</sub> and MeOH as a co-solvent.



Entry	Conc of <b>1a</b> (M)	TPFPP ratio <sup>a</sup> (mol%)	CO <sub>2</sub> pump (mL/min)	Residence time (min)	Conv. of <b>1a</b> (%)	Yield <sup>b</sup> of <b>2a</b> (%)
1 <sup>c</sup>	0.1	0.1	0.37	7	43	35
2	0.1	0.1	0.15	26	76	72
3	2.0	0.1	0.15	26	97	91
4	3.0	0.05	0.15	26	97	96

All the experiments were performed using MeOH as a co-solvent and the photoreactor is filled with glass beads (6 mm O. D.). The flow rate of organic pump 1 was 0.05 mL/min. Zero conversion and yield were obtained in two control experiments, one without light and one without TPFPP. [a]: The ratio of TPFPP to **1a**. [b]: Yields were measured by <sup>1</sup>H NMR using biphenyl as internal standard. [c]: This experiment was conducted in a half-length photoreactor (10 mm O. D., 120 mm length) instead of (10 mm O. D., 240 mm length).

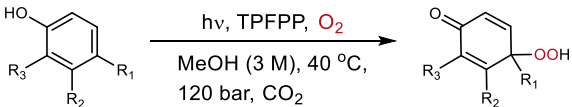
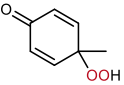
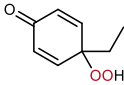
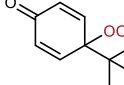
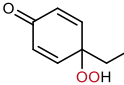
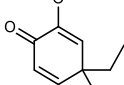
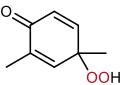
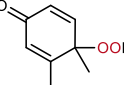
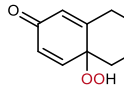
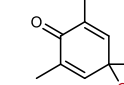
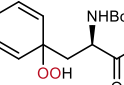
A key question is what is the role of the scCO<sub>2</sub> in this reaction. Although the CO<sub>2</sub> is above its critical temperature and pressure (31°C, 7.4 MPa), this does not automatically mean that the whole reaction mixture is supercritical or even monophasic, because the phase behavior of multicomponent mixtures is more complex than for a pure substance.<sup>47</sup> The situation is further complicated for a reaction mixture, since its composition changes during the reaction, especially

when a permanent gas is consumed.<sup>48,49</sup> In the case of this de-aromatisation, the phase behavior studies on the mixtures at the start of the reaction described in the ESI show that, except at the highest concentration of *para*-cresol and O<sub>2</sub> (3.0 M), the mixture is monophasic. At 3.0 M, small bubbles of gas are observed. This means that even under these conditions, the bulk of the reaction mixture is in the liquid phase. It is what is often described as a “*gas-expanded liquid*”; that is a liquid with a reduced density compared to that of the organic solvent.<sup>50</sup> Under these conditions, the CO<sub>2</sub> will be playing several roles: (i) it increases the miscibility of the O<sub>2</sub>, photosensitizer, and *para*-cresol bringing them all into a single phase thereby removing most mass transport limitations; even at the highest concentration, the reaction mixture will become monophasic after only a small proportion of the O<sub>2</sub> is consumed. (ii) it will lengthen the lifetime of <sup>1</sup>O<sub>2</sub> compared to that in pure MeOH. (iii) it will lower viscosity which will aid penetration into the pores of the solid acid catalyst in the downstream reactions of the peroxide.

### **Extending the scope of the photo-oxidation with MeOH as a co-solvent**

Following the optimisation of the de-aromatisation of *para*-cresol **1a**, we expanded the scope of the reaction to prepare *para*-peroxyquinols derivatives (Table 2). These compounds were synthesised initially using the optimised conditions described in Table 1. However, for some substrates the concentration of the starting material was lowered to 1 M due to substrate solubility in MeOH. As shown in Table 2, phenols bearing different alkyl substituents in the *para* position have been obtained with excellent yields (93-99%) and high productivity (Table 2, compounds **2a-2f**) in relatively short residence time (26 mins). The reaction of *para-tert*-butylphenol **1c** gave 59% yield of the peroxyquinol **2c** and, to the best of our knowledge, this is the first time that this compound has been reported. Although this yield is somewhat lower than for the other compounds, it may be due to the bulkiness of the *tert*-butyl group. Phenols bearing more functionalised groups gave *para*-peroxyquinols with more moderate yields (30-46%) (Table 2, compound **2d** and **2f**). Phenols bearing electron-withdrawing groups (-NO<sub>2</sub>, -CF<sub>3</sub>) or benzylic alcohols in the *para* position do not undergo de-aromatisation under conventional conditions and, disappointingly, they did not dearomatize under our conditions either.

**Table 2.** Substrate scope for the de-aromatisation of phenols in scCO<sub>2</sub> with MeOH as the co-solvent.

	
<b>1a-1j</b>	<b>2a-2j</b>
	Yield <sup>a</sup> (%) Productivity <sup>b</sup> (g/day)
	<b>2a</b> 96% 47 g/day
	<b>2b</b> 93% 55 g/day
	<b>2c*</b> 59% (55%) 8 g/day
	<b>2d*</b> 46% (44%) 6 g/day
	<b>2e</b> 85% 34 g/day
	<b>2f</b> 94% 55 g/day
	<b>2g</b> >99% (99%) 66 g/day
	<b>2h</b> >99% 67 g/day
	<b>2i*</b> >99% 12 g/day
	<b>2j*</b> 26% (30%) 7 g/day

All experiments were conducted with a concentration of TPFPP of 0.05 mol% at 40°C and 120 bar using CO<sub>2</sub> and MeOH as solvents. The yields in brackets are isolated yields. All other yields were calculated from <sup>1</sup>H NMR spectroscopy, using biphenyl as an internal standard. \*Due to solubility issues of the corresponding phenols in MeOH, the concentration of the starting solution was 1M instead of 3M. [a]: Maximum yield were obtained when the flow rate of the organic pumps 1 was 0.05 mL/min and the flow rate of CO<sub>2</sub> was 0.15 mL/min. [b]: For compounds **2a**, **2b**, **2f**, **2g** and **2h** maximum productivities were obtained when flow rate of the organic pump 1 was 0.1 mL/min and the flow rate of CO<sub>2</sub> pump was 0.3 mL/min. For all experiments, the photoreactor was 10 mm O. D., 240 mm length, filled with glass beads (6 mm O. D.) and the reactor free volume was ca. 5.2 mL. Further experimental details are given in the ESI.

The structure of **2a**, prepared by our approach, have been confirmed by X-ray of a crystal that was obtained by evaporating the co-solvent from the unpurified solution emerging from the Back Pressure Regulator (BPR). The structure determination confirmed the structure of **2a**, shown in Figure 2. Interestingly, **2a** crystallises as centrosymmetric dimers linked by a pair of intermolecular

hydrogen bonds characterised by an H2 to O3 distance of 1.96 (2) Å. Further details are given in the ESI.

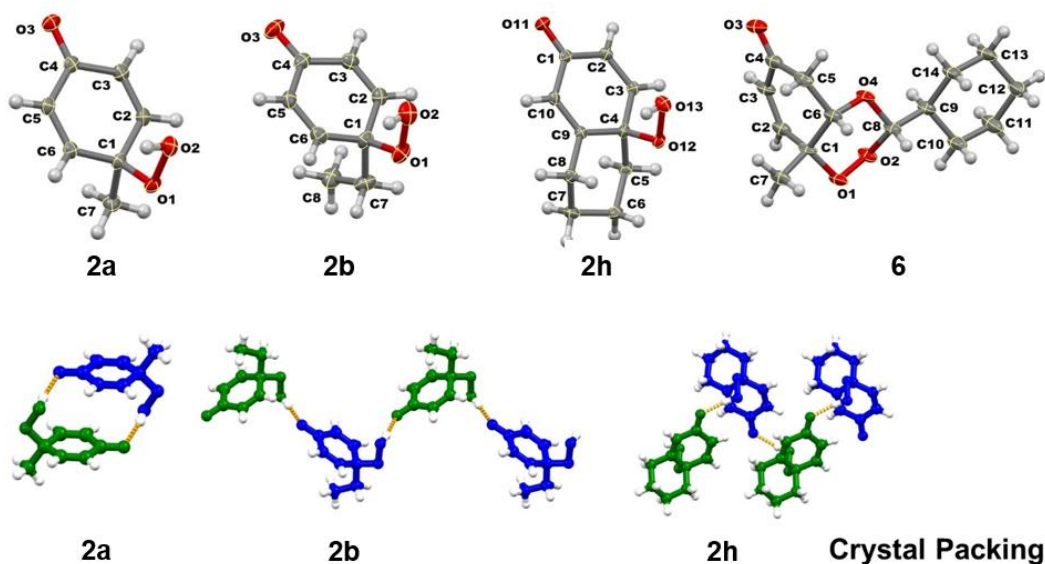
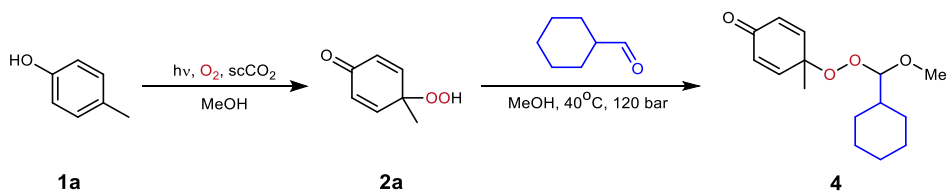


**Figure 2:** Molecular structures of the peroxyquinols **2a**, **2b** and **2h** and, on the right, the 1,2,4-trioxane **6** with anisotropic displacement ellipsoids set at 50% probability. Below is a crystal packing of **2a**, **2b** and **2h**. Note that **2a** forms doubly hydrogen-bonded dimers while **2b** and **2h** form hydrogen-bonded chains. All four single-crystal X-ray structures were obtained from crystals which formed in the solution emerging from the back pressure regulator of the flow reactor sufficiently pure that they did not require any further purification. Bond lengths and angles for all four structures are tabulated in the ESI.

### Multi-step process for trioxane formation

Next, we examined the formation of 1,2,4-trioxanes, obtained by reacting the *para*-peroxyquinol with cyclohexanecarboxaldehyde following an acetalisation/oxa-Michael cascade under acidic conditions. Unfortunately, our first attempt to access the 1,2,4-trioxane structure was not successful. The presence in excess of MeOH, a nucleophilic solvent, appears to be detrimental to the acid-catalysed step, thus blocking the cascade that would have given rise to the desired 1,2,4-trioxane product (Scheme 1). Such issues are often found in telescoped continuous flow processes, where two linked reactions require two different solvents and where a switch of solvent is then needed.<sup>51</sup> In our case we wanted to be able to keep the same solvent for both stages.<sup>52,53</sup>

**Scheme 1:** Reaction *para*-peroxyquinol with aldehyde under acidic conditions using MeOH as co-solvent.

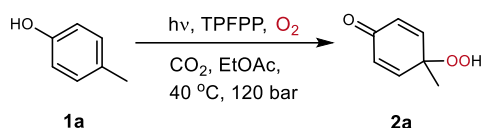


In this particular example, we expected that the first step to be favoured by using a polar protic solvent while the second step requires a non-nucleophilic solvent. Previously reported examples described accessing 1,2,4-trioxanes with good results in dichloromethane.<sup>6</sup> However, the use of a halogenated solvent is not compatible with our approach, particularly because of potential corrosion of the high pressure apparatus.<sup>54</sup> Hence, our strategy was to screen different solvents for the photo-oxidation step. We found that  $^1\text{O}_2$  has an acceptable lifetime<sup>55</sup> in ethyl acetate (EtOAc), a polar aprotic solvent which can be considered to be a greener solvent.<sup>56</sup>

#### **Optimisation of photo-oxidation step using EtOAc as co-solvent**

Therefore, in order to synthesise 1,2,4-trioxanes via the de-aromatisation of phenol derivatives, EtOAc was employed instead of the protic solvent, MeOH. The results in Table 3 demonstrates that *para*-peroxyquinol **2a** could be obtained in a reasonable yield. Unlike in MeOH, the yield of **2a**, was low when a high concentration of **1a** (e.g. 3.0 M) was used probably because some polymerisation was observed, (Table 3, entry 1). No polymerisation was observed and 69% yield was obtained at 1.0 M (Table 2, entry 2) but a higher yield was found when *tert*-butanol was used as a protic additive in EtOAc (Table 3, entry 3). The best yields were obtained when using 2 equivalents of hexafluoroisopropanol (HFIP), with 1.0 M concentration of substrate using 0.3 mol% of TPFPP and a residence time of 26 min (Table 3, entry 4). Presumably HFIP is a better proton donor, with a lower pKa than MeOH and *tert*-butanol, and the conjugate base of HFIP is less nucleophilic than that of *tert*-butanol due to its two electrowithdrawing  $\text{CF}_3$  groups.<sup>57</sup> In addition, HFIP may have a synergic effect, increasing the acidity of Amberlyst-15 in the next step of 1,2,4-trioxane formation.<sup>58</sup>

**Table 3.** Optimisation of de-aromatisation of *para*-cresol **1a**, in continuous flow in high pressure system using scCO<sub>2</sub> and EtOAc as co-solvent.



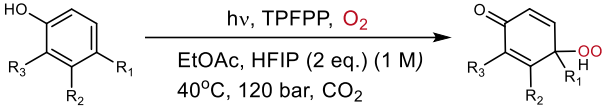
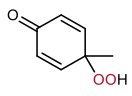
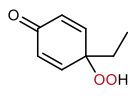
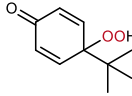
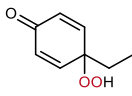
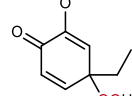
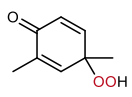
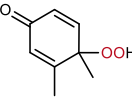
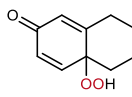
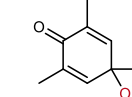
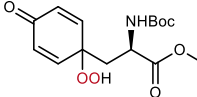
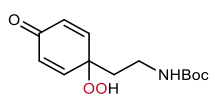
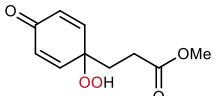
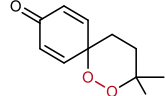
Entry	Conc. of <b>1a</b> <sup>a</sup> (M)	TPFPP <sup>b</sup> (mol%)	Residence time (min) <sup>c</sup>	Conv. of <b>1a</b> (%)	Yield of <b>2a</b> (%)
<b>1</b>	3.0	0.05	26	94	54
<b>2</b>	1.0	0.3	15	69	69
<b>3<sup>d</sup></b>	1.0	0.3	26	86	78
<b>4<sup>e</sup></b>	1.0	0.3	26	95	94

All experiments were conducted at 40 °C and 120 bar, using CO<sub>2</sub> and EtOAc as solvents. The flow rate of organic pump 1 was 0.05 mL/min, the flow rate of CO<sub>2</sub> was 0.15 mL/min (residence time of 26 min) or 0.3 mL/min (residence time of 15 min). The photoreactor was 10 mm O. D., 240 mm length, filled with glass beads (6 mm O. D.). The yields and conversions were calculated from <sup>1</sup>H NMR spectroscopy, using biphenyl as internal standard. [a]: The concentration of **1a** in EtOAc. [b]: The ratio of TPFPP to **1a**. [c]: Residence time of photo-oxidation step in the photoreactor. [d]: Addition of 2 equivalents of *t*-BuOH into the starting solution. [e]: addition of 2 equivalents of HFIP added in the starting solution. An expanded version of this Table can be found in the ESI.

#### Widening the scope of the photo-oxidation of *para*-cresol using EtOAc and HFIP

Having established optimal conditions for de-aromatisation using EtOAc doped with HFIP (Table 3, entry 4), the scope of the reaction was expanded with a variety of phenols (Table 4). Low to excellent yields of *para*-peroxyquinols were obtained (9-99%). Primary and secondary *para*-substituted phenols gave excellent yields (94-99%), whilst *para-tert*-butyl phenol **1c** resulted in a moderate yield most likely due to steric hindrance. Di- and tri- substituted phenols also gave excellent yields (88-99%) presumably due to the positive inductive effect, injecting electrons in the aromatic ring (Table 4, compounds **2e** and **2g**). Reasonable to low yields were obtained with phenols bearing functionalised chains in the *para* position (Table 4, compounds **2j-2m**).

**Table 4.** Substrate scope for the de-aromatisation of phenols in scCO<sub>2</sub> using EtOAc and HFIP (2 equivalents) as a mixed co-solvent.

	
<b>1a-1m</b>	<b>2a-2m</b>
	Yield <sup>a</sup> (%) Productivity (g/day)
	<b>2a</b> 94% (92%) 9 g/day
	<b>2b</b> >99% 11 g/day
	<b>2c*</b> 49% 3 g/day
	<b>2d</b> 49% 6 g/day
	<b>2e</b> 56% 11 g/day
	<b>2e</b> 88% 10 g/day
	<b>2f</b> >99% 11 g/day
	<b>2g</b> 47% 6 g/day
	<b>2h</b> >99% (99%) 12 g/day
	<b>2j*</b> 9% 1 g/day
	<b>2k*</b> 42% (43%) 8 g/day
	<b>2l</b> 58% (51%) 9 g/day
	<b>2m<sup>b</sup></b> 62% 4 g/day

All experiments were conducted with a concentration of TPFPP of 0.3 mol% at 40°C and 120 bar using CO<sub>2</sub>, EtOAc and HFIP (2 eq.) as solvents. The yields were calculated from <sup>1</sup>H NMR spectroscopy, using biphenyl as internal standard. The yields in bracket are isolated yields. No ortho-oxidation was observed. <sup>a</sup>The concentration of the starting phenol was 0.5 M instead of 1.0 M in these cases because of solubility issues of those phenols in EtOAc and HFIP (2 eq.), [a]: For maximum yield, the flow rate of organic pumps 1 was 0.05 mL/min, the flow rate of CO<sub>2</sub> was 0.15 mL/min. For all experiments, the photoreactor was 10 mm O. D., 240 mm length, filled with glass beads (6 mm O. D.) and reactor free volume was ca. 5.2 mL. [b]: This compound has been obtained as an hemiacetal that spontaneously formed after the photo-oxidation reaction. Further experimental details are given in the ESI.

### Optimisation of 1,2,4-trioxane formation

The next step was to optimise trioxane formation in EtOAc. We suspected that both the amount of catalyst (Amberlyst-15) and the temperature would affect the cyclisation step. However, the most

important factor appeared to be efficient mixing of the *para*-peroxyquinol and aldehyde prior to encountering the solid acid catalyst, presumably because mixing reduces the decomposition of **2a** when interacting with Amberlyst-15 in the thermal reactor which was used in upflow for this stage of the process (see Figure 1). Thus, a ca. 60% yield of the desired 1,2,4-trioxane **5** was obtained with 0.75 g Amberlyst-15 with an additional 0.85 g of glass beads (1.5-2 mm), filling the remaining volume of the reactor below the Amberlyst-15 to act as a pre-mixer. Only slight heating was required; 30–40°C was sufficient.

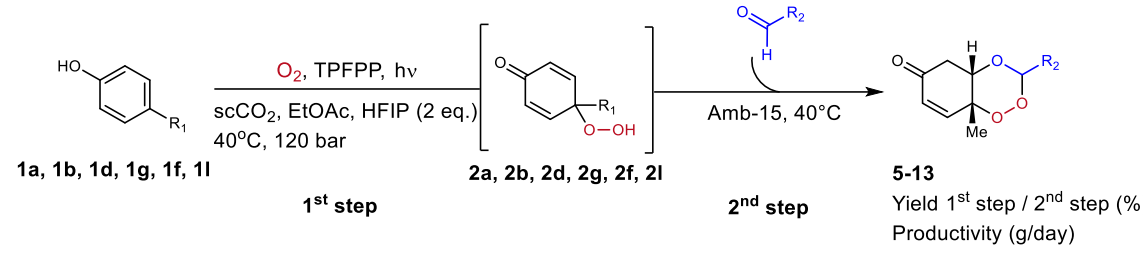
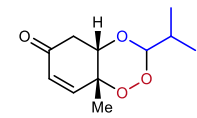
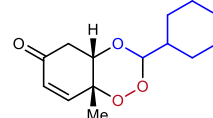
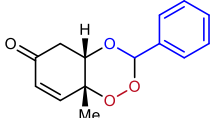
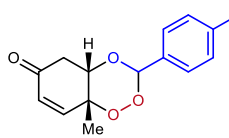
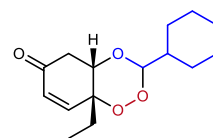
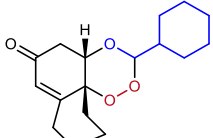
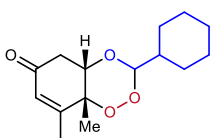
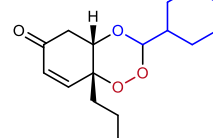
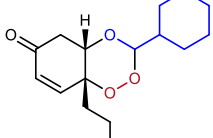
After optimisation of the continuous two-stage process in our multistep equipment using the EtOAc/HFIP/CO<sub>2</sub> mixed solvent system, the yields were raised to 95% for the dearomatisation of *para*-cresol **1**, with an overall 88% yield for the two-stage formation of trioxane **6**. When the reactor chain was run for 8 hours with a feed of **1a** (1.0 M in EtOAc), 4.2 grams of crystalline **6** were obtained after recrystallisation of the crude product.

### **Expanding the scope of the multi-step formation of trioxanes from *para*-substituted phenols**

We then explored reacting with **1** with different aldehydes, as a strategy for the synthesis 1,2,4-trioxanes from *para*-phenol derivatives in our high-pressure system. With a system pressure of 120 bar and temperatures of 40°C in both the photoreactor and the thermal reactor, alkyl aldehydes reacted with **2a** to afford 1,2,4-trioxanes **5** and **6** with excellent yields and high productivities (Table 5). Aromatic aldehydes, such as benzaldehyde or *para*-methylbenzaldehyde reacted under the same conditions to afford respectively 1,2,4-trioxanes **7** and **8** with somewhat lower yields but, nevertheless, with useful productivities (Table 5 upper).

Cyclohexanecarboxaldehyde was chosen in order to screen the effectiveness of our reactor for the formation of trioxanes using phenols with different functional groups. The choice was based on the observation that this aldehyde gave an excellent yield for the thermal step (88%) and is less prone to polymerisation than isobutyraldehyde. The results, summarised in the lower part of Table 5, show that the least reactive phenol gave a productivity of 4 g/day and all but one of the others gave much higher productivities which are large compared to those normally achieved by many other lab-scale routes to such trioxanes.

**Table 5.** Substrate scope for the 1,2,4-trioxanes formation.

	1 <sup>st</sup> step	2 <sup>nd</sup> step	5-13 Yield 1 <sup>st</sup> step / 2 <sup>nd</sup> step (%) Productivity (g/day)
			<p><b>5</b> 95 / 97% 14 g/day</p> <p><b>6</b> 95 / 88% 15 g/day</p> <p><b>7</b> 95 / 28% 5 g/day</p>
			<p><b>8</b> 95 / 21% 4 g/day</p> <p><b>9</b> 99 / 72% 14 g/day</p> <p><b>10</b> 47 / 19% 4 g/day</p>
			<p><b>11</b> 99 / 85% 16 g/day</p> <p><b>12</b> 58 / 90% 12 g/day</p> <p><b>13</b> 55 / 75% 9 g/day</p>

*Compounds 5-8: screening different aldehydes for the cyclisation of para-peroxyquinol in the thermal reactor. Compounds 9-13: screening different para-phenols for the cyclisation with cyclohexanecarboxaldehyde. In both parts, the numbers (e.g. 55/75%) give respectively the yields for the first stage and for both stages combined in our process. The productivity also refers to the two steps being run as a single continuous process. These results were obtained when the flow rates of the organic pump 1 and 2 were 0.05 mL/min and the flow rate of CO<sub>2</sub> pump was 0.15 mL/min. For all experiments, the photoreactor was 10 mm O. D., 240 mm length, filled with glass beads (6 mm O. D.) and reactor free volume was ca. 5.2 mL. The thermal reactor was ¼ inch O. D., 1 mm wall thickness and 156 mm length. The thermal reactor was filled with 0.75 g of Amb-15 and 0.85 g of glass beads (2 mm O. D.) and reactor volume was ca. 0.8 mL. The temperature of the thermal reactor was set at 40 °C*

## Conclusions

In summary, we have described the successful continuous photoinitiated de-aromatisation of para-phenol derivatives with singlet oxygen and the synthesis of 1,2,4-trioxanes in a high-pressure CO<sub>2</sub>

continuous flow reactor on a multi-gram scale. Although the reactors are small, ca. 20 mL, they have proved to be capable of producing relatively large quantities of peroxyquinols and trioxanes compared to conventional organic chemistry methodologies. Addressing challenges in sustainability is likely to need new approaches.<sup>59</sup> Photochemistry has long been recognized as a potentially more sustainable way of making chemicals<sup>60</sup> and more recently photochemistry has been highlighted as having a possible role to play in realizing a circular economy.<sup>61</sup> More specifically, our approach is greener than more traditional methods such as those with oxone or hypervalent iodine catalysts because it generates little waste. It involves a greener reagent (singlet oxygen, photogenerated from the renewable feedstock, gaseous O<sub>2</sub>) and renewable solvents (supercritical CO<sub>2</sub> and EtOAc). It also satisfies four of the “12 Principles of Green Chemistry”, including avoiding the generation of waste, synthesis without unnecessary derivatisation, the use of catalysis instead of stoichiometric reagents, and by using continuous flow, increasing the safety of the process. These productivities for *para*-peroxyquinols and 1,2,4-trioxanes are promising for easy further scale-up, and present considerable opportunities for the synthesis of new potential anti-malarial and anticancer candidates.

## Experimental

**Reagents:** Compounds were purchased in reagent grade from commercial suppliers and used without further purification, unless otherwise stated.

**Purification methods:** For the purification of new compounds, flash chromatography was used otherwise noted. The solvent mixture used to eluent the products were cyclohexane/EtOAc or *n*-pentane/EtOAc. Two methods were used, flash chromatography and automatic flash chromatography (TELEDYNE ISCO, P/N 69-3873-244). *Procedure for the automatic flash chromatography:* Firstly, two different solvents were chosen and used to prime the system starting with the polar solvent to the less polar one. Then, a dry pre-loaded solid cartridge with silica was placed into the solid sample position; the appropriate RediSep Rf Gold® silica gel column was loaded on to the system; then running the separation. Different fractions were obtained. Further identification was made after removing the solvents.

**<sup>1</sup>H and <sup>13</sup>C NMR spectra:** Proton nuclear magnetic resonance (<sup>1</sup>H NMR) spectra and proton-decoupled carbon nuclear magnetic resonance (<sup>13</sup>C {<sup>1</sup>H} NMR) spectra were recorded at 25 °C (unless stated otherwise) on AV-400 (400 MHz), AV (III) 400 (400 MHz) or AV (III) 500 (500 MHz). Chemical shifts for proton are reported in parts per million (ppm) downfield from tetramethylsilane and are referenced to residual protium in the NMR solvent according to values reported in the literature.

**General information about the high-pressure equipment:** As far as we are aware, there is no commercially available equivalent of the reactor system used in this work which, apart from the photo-reactor itself, was assembled from commercially available parts and components. Although conceptually simple, the system needs careful design and assembly to ensure safe operation. Details of the equipment required for this work and other experimental details are to be found in the ESI.

**Safety Warning:** In the ESI, we give further details of the equipment used to carry out this work at Nottingham but the Authors give no undertaking as to the suitability of this equipment when used in other laboratories, particularly because national and local safety regulations may vary between locations. The equipment described is not necessarily, the only type that could be used, nor possibly the best available. It is the responsibility of each researcher to check the suitability and safety of their own equipment for such experiments in their laboratories. Additional safety issues that need to be considered are the use of potentially flammable co-solvents in the presence of oxygen at high pressure. Further details of the equipment methodology and equipment required for this work together with other experimental details are to be found in the ESI.

If the reactions were to be scaled-up further, one would have to consider the possible thermal instability of the peroxide products.

### Author Contributions

MWG led and supervised this research. HB initially proposed this approach to trioxane formation and oversaw the characterisation of the products. LQW and BLDA carried out the majority of the reactions. AJB, LJT, WL, SPA carried out the X-ray structure determinations. MP advised on the reactor design and supercritical fluid aspects of the project. All of the authors contributed to the writing of this paper.

### Conflicts of Interest.

There are no conflicts to declare

### Acknowledgments

We thank the EPSRC grant (EP/P013341/1) for funding this work and the University of Nottingham Vice-Chancellor's Scholarship Scheme for supporting L.Q.W. and B.L.D.A. We indebted to Professor Ross M. Denton and Dr Trevor Laird for helpful discussions. We are grateful to Messrs Richard Wilson, Richard Meehan, Matthew McAdam, Ben Clarke and Mark Guyler for their technical support.

### Supporting Information

Equipment diagram and set-up, typical procedure for high-pressure equipment, experiment optimization in batch, phase behaviour study, supplementary optimisation experiments, <sup>1</sup>H and <sup>13</sup>C NMR spectra and crystallographic data.

### References

- 1 Quideau, S.; Pouységu, L.; Deffieux, D. Oxidative dearomatization of phenols: why, how and what for? *Synlett* **2008**, *4*, 467–495.
- 2 Barradas, S.; Carreño, M. C.; González-López, M.; Latorre, A.; Urbano, A. Direct stereocontrolled synthesis of polyoxygenated hydrobenzofurans and hydrobenzopyrans from *p*-peroxy quinols. *Org. Lett.* **2007**, *9*, 5019–5022.
- 3 Roche, S. P.; Porco, J. A. Dearomatization strategies in the synthesis of complex natural products. *Angew. Chem. Int. Ed.* **2011**, *50*, 4068–4093.
- 4 Barradas, S.; Hernández-Torres, G.; Urbano, A.; Carreño, M. C. Total synthesis of natural *p*-quinol cochinchinenone. *Org. Lett.* **2012**, *14*, 5952–5955.
- 5 Park, K. H.; Chen, D. Y-K. A desymmetrization-based approach to morphinans: application in the total synthesis of oxycodone. *Chem. Commun.* **2018**, *54*, 13018–13021.
- 6 Rubush, D. M.; Morges, M. A.; Rose, B. J.; Thamm, D. H.; Rovis, T. An asymmetric synthesis of 1,2,4-trioxane anticancer agents via desymmetrization of peroxyquinols through a Brønsted acid catalysis cascade. *J. Am. Chem. Soc.* **2012**, *134*, 13554–13557.
- 7 Lévesque, F.; Seeberger, P.H. Continuous-flow synthesis of the anti-malaria drug artemisinin. *Angew. Chem. Int. Ed.* **2012**, *51*, 1706–1709.
- 8 Kopetzki, D.; Lévesque, F.; Seeberger, P.H. A continuous-flow process for the synthesis of artemisinin. *Chem. Eur. J.* **2013**, *19*, 5450–5456.
- 9 Triemer, S.; Gilmore, K.; Vu, G. T.; Seeberger, P. H.; Seidel-Morgenstern, A. Literally green chemical synthesis of artemisinin from plant extracts. *Angew. Chem. Int. Ed.* **2018**, *57*, 5525–5528.

- 10 World Health Organisation. Malaria. <https://www.who.int/news-room/fact-sheets/detail/malaria>, 2020.
- 11 Tiwari, M. K.; Chaudhary, S. Artemisinin-derived antimalarial endoperoxides from bench-side to bed-side: chronological advancements and future challenges. *Med. Res. Rev.* **2020**, *40*, 1220–1275.
- 12 Klapötke, T. M. *Chemistry of high-energy materials*, 3rd ed.; Walter de Gruyter: Berlin, 2015.
- 13 Paddon, C. J.; Keasling, J. D. Semi-synthetic artemisinin: a model for the use of synthetic biology in pharmaceutical development. *Nature Rev. Microbiol.* **2014**, *12*, 355–367.
- 14 Efferth, T. Cancer combination therapies with artemisinin-type drugs. *Biochem. Pharmacol.* **2017**, *139*, 56–70.
- 15 Fröhlich, T.; Ndreshkjana, B.; Muenzner, J. K.; Reiter, C.; Hofmeister, E.; Mederer, S.; Fatfat, M.; El-Baba, C.; Gali-Muhtasib, H.; Schneider-Stock, R.; Tsogoeva, S. B. Synthesis of novel hybrids of thymoquinone and artemisinin with high activity and selectivity against colon cancer. *ChemMedChem.* **2017**, *12*, 226–234.
- 16 Crespo-Ortiz M. P.; Wei, M. Q. Antitumor activity of artemisinin and its derivatives: from a well-known antimalarial agent to a potential anticancer drug. *J. Biomed. Biotechnol.* **2012**, *247597*, 1–18.
- 17 Efferth, T.; Dunstan, H.; Sauerbrey, A.; Miyachi, H.; Chitambar, C. R. The anti-malarial artesunate is also active against cancer. *Int. J. Oncol.* **2001**, *18*, 767–773.
- 18 Li, J.; Casteels, T.; Frogne, T.; Ingvorsen, C.; Honoré, C.; Courtney, M.; Huber, K. V. M.; Schmitner, N.; Kimmel, R. A.; Romanov, R. A.; Sturtzel, C.; Lardeau, C.-H.; Klughammer, J.; Farlik, M.; Sdelci, S.; Vieira, A.; Avolio, F.; Briand, F.; Baburin, I.; Májek, P.; Pauler, F. M.; Penz, T.; Stukalov, A.; Gridling, M.; Parapatics, K.; Barbieux, C.; Berishvili, C.; Spittler, A.; Colinge, J.; Bennett, K. L.; Hering, S.; Sulpice, T.; Bock, C.; Distel, M.; Harkany, T.; Meyer, D.; Superti-Furga, G.; Collombat, P.; Hecksher-Sørensen, J.; Kubicek, S. Artemisinins target GABAA receptor signaling and impair  $\alpha$  cell identity. *Cell* **2017**, *168*, 86–100.
- 19 van der Meulen, T.; Lee, S.; Noordeloos, E.; Donaldson, C. J.; Adams, M. W.; Noguchi, G. M.; Mawla A. M.; Huising, M. O. Artemether does not turn  $\alpha$  cells into  $\beta$  cells. *Cell Metab.* **2018**, *27*, 218–225.
- 20 Endo, K.; Seya, K.; Hikino, H. Biogenesis-like transformation of salidroside to renygol and its related cyclohexyletanoids of *Forsythia suspensa*. *Tetrahedron* **1989**, *45*, 3673–3682.
- 21 Eske, A.; Ecker, S.; Fendinger, C.; Goldfuss, B.; Jonen, M.; Lefarth, J.; Neudörfl, J.-M.; Spilles, M.; Griesbeck, A. G. Spiro-fused and annulated 1,2,4-trioxepane-, 1,2,4-trioxocane-, and 1,2,4-trioxonane-cyclohexadienones: cyclic peroxides with unusual ring conformation dynamics. *Angew. Chem. Int. Ed.* **2018**, *57*, 13770–13774.
- 22 Carreño, M. C.; González-López M.; Urbano, A. Oxidative de-aromatization of *para*-alkyl phenols into *para*-peroxyquinols and *para*-quinols mediated by oxone as a source of singlet oxygen. *Angew. Chem. Int. Ed.* **2006**, *45*, 2737–2741.
- 23 Skubi, K. L.; Blum T. R.; Yoon, T. P. Dual catalysis strategies in photochemical synthesis. *Chem. Rev.* **2016**, *116*, 10035–10074.
- 24 Romero, N. A.; Nicewicz, D. A. Organic photoredox catalysis. *Chem. Rev.* **2016**, *116*, 10075–10166.
- 25 Remy, R.; Bochet, C. G. Arene-alkene cycloaddition. *Chem. Rev.* **2016**, *116*, 9816–9849.
- 26 Ravelli, D.; Protti, S.; Fagnoni, M. Carbon–carbon bond forming reactions via photogenerated intermediates. *Chem. Rev.* **2016**, *116*, 9850–9913.
- 27 Kärkäs, M. D.; Porco, J. A.; Stephenson, C. R. J. Photochemical approaches to complex chemotypes: applications in natural product synthesis. *Chem. Rev.* **2016**, *116*, 9683–9747.
- 28 Hone, C. A.; Roberge D. M.; Kappe, C. O. The use of molecular oxygen in pharmaceutical manufacturing: is flow the way to go? *ChemSusChem* **2017**, *10*, 32–41.
- 29 Ghogare, A. A.; Greer, A. Using singlet oxygen to synthesize natural products and drugs. *Chem. Rev.* **2016**, *116*, 9994–10034.
- 30 Chen, M.; Zhong, M. J.; Johnson, J. A. Light-controlled radical polymerization: mechanisms, methods, and applications. *Chem. Rev.* **2016**, *116*, 10167–10211.

- 31 Cambie, D.; Bottecchia, C.; Straathof, N. J. W.; Hessel, V.; Noel, T. Applications of continuous-flow photochemistry in organic synthesis, material science, and water treatment. *Chem. Rev.* **2016**, *116*, 10276–10341.
- 32 Wu, L.; Lee, D. S.; Boufroura, H.; Poliakoff, M.; George, M. W. Photooxidation of fulvenes in a continuous flow photoreactor using carbon dioxide as a solvent. *ChemPhotoChem* **2018**, *2*, 580–585.
- 33 Wu, L.; Abada, Z.; Lee, D. S.; Poliakoff, M.; George, M. W. Combining engineering and chemistry for the selective continuous production of four different oxygenated compounds by photo-oxidation of cyclopentadiene using liquid and supercritical CO<sub>2</sub> as solvents. *Tetrahedron* **2018**, *74*, 3107–3112.
- 34 Ioannou, G. I.; Montagnon, T.; Kalaitzakis, D.; Pergantis, S. A.; Vassilikogiannakis, G. One-pot synthesis of diverse  $\gamma$ -lactam scaffolds facilitated by a nebulizer-based continuous flow photo-reactor. *ChemPhotoChem* **2017**, *1*, 173–177
- 35 Amara, Z.; Bellamy, J. F. B.; Horvath, R.; Miller, S. J.; Beeby, A.; Burgard, A.; Rossen, K.; Poliakoff, M.; George, M. W. Applying green chemistry to the photochemical route to artemisinin. *Nature. Chem.* **2015**, *7*, 489–495.
- 36 Bourne, R. A.; Han, X.; Chapman, A. O.; Arrowsmith, N. J.; Kawanami, H.; Poliakoff, M.; George, M. W. Homogeneous photochemical oxidation via singlet O<sub>2</sub> in supercritical CO<sub>2</sub>. *Chem. Commun.* **2008**, *37*, 4457–4459.
- 37 Van Gerven, T.; Mul, G.; Moulijn, J.; Stankiewicz, A. A review of intensification of photocatalytic processes. *Chem. Eng. Process.* **2007**, *46*, 781–789.
- 38 Jähnisch, K.; Dingerdissen, U. Photochemical generation and [4+2]-cycloaddition of singlet oxygen in a falling-film micro reactor. *Chem. Eng. Technol.* **2005**, *28*, 426–427.
- 39 Dionysiou, D. D.; Balasubramanian, G.; Suidan, M. T.; Khodadoust, A. P.; Baudin, I.; Laine, M. Rotating disk photocatalytic reactor: development, characterization, and evaluation for the destruction of organic pollutants in water. *Water Res.* **2000**, *34*, 2927–2940.
- 40 Gemoets, H. P. L.; Su, Y.; Shang, M.; Hessel, V.; Luqueb, R.; Noël, T. Liquid phase oxidation chemistry in continuous-flow microreactors. Liquid phase oxidation chemistry in continuous-flow microreactors. *Chem. Soc. Rev.* **2016**, *45*, 83–117.
- 41 Hall, J. F. B.; Bourne, R. A.; Han, X.; Earley, J. H.; Poliakoff, M.; George, M. W. Synthesis of antimalarial trioxanes via continuous photo-oxidation with <sup>1</sup>O<sub>2</sub> in supercritical CO<sub>2</sub>. *Green Chem.* **2013**, *15*, 177–180.
- 42 Lee, D. S.; Amara, Z.; Clark, C. A.; Xu, Z. Y.; Kakimpa, B.; Morvan, H. P.; Pickering, S. J.; Poliakoff, M.; George, M. W. Continuous Photo-Oxidation in a Vortex Reactor: Efficient Operations Using Air Drawn from the Laboratory. *Org. Process Res. Dev.* **2017**, *21*, 1042–1045.
- 43 Rehm, T. H. Reactor Technology Concepts for Flow Photochemistry. *ChemPhotoChem* **2020**, *4*, 235–254.
- 44 Politano, F.; Oksdath-Mansilla, G. Light on the Horizon: Current Research and Future Perspectives in Flow Photochemistry. *Org. Process Res. Dev.* **2018**, *22*, 1045–1062.
- 45 Clark, C. A.; Lee, D. S.; Pickering, S. J.; Poliakoff, M.; George, M. W. A Simple and Versatile Reactor for Photochemistry. *Org. Process. Res. Dev.* **2016**, *20*, 1792–1798.
- 46 DeLaney, E. N.; Lee, D. S.; Elliot, L. D.; Jin, J.; Booker-Milburn, K. I.; Poliakoff, M.; George, M. W. A laboratory-scale annular continuous flow reactor for UV photochemistry using excimer lamps for discrete wavelength excitation and its use in a wavelength study of a photodecarboxylative cyclisation. *Green Chem.* **2017**, *19*, 1431–1438.
- 47 McHugh, M. A.; Krukonis, V. J. *Supercritical Fluid Extraction: Principles and Practice*, 2nd ed.; Butterworth-Heinemann: Boston, MA, 1994.
- 48 Ke, J.; Han, B. X.; George, M. W.; Yan, H. K.; Poliakoff, M. How does the critical point change during a chemical reaction in supercritical fluids? A study of the hydroformylation of propene in supercritical CO<sub>2</sub>. *J. Am. Chem. Soc.* **2001**, *123*, 3661–3670.
- 49 Ke, J.; Sánchez-Vicente, Y.; Akien, G. R.; Novitskiy, A. A.; Comak, G.; Bagratashvili, V. N.; George, M. W.; Poliakoff, M. Detecting phase transitions in supercritical mixtures: an enabling tool for greener chemical reactions. *Proc. R. Soc. A* **2010**, *466*, 2799–2818.

- 50 Akien, G. R.; Poliakoff, M. A critical look at reactions in class I and II gas-expanded liquids using CO<sub>2</sub> and other gases. *Green Chem.* **2009**, *11*, 1083–1100.
- 51 Deadman, B. J.; Battilocchio, C.; Sliwinskia, E.; Steven V. Ley, S. V. A prototype device for evaporation in batch and flow chemical processes. *Green Chem.* **2013**, *15*, 2050–2055.
- 52 Webb, D.; Jamison, T. F. Continuous flow multi-step organic synthesis. *Chem. Sci.* **2010**, *1*, 675–680.
- 53 Akwi, F. M.; Watts, P. Continuous flow chemistry: where are we now? Recent applications, challenges and limitations. *Chem. Commun.* **2018**, *54*, 13894–13928.
- 54 Hoar, T.; Jacob, W. Breakdown of passivity of stainless steel by halide ions. *Nature*, **1967**, *216*, 1299–1301.
- 55 Foote, C. S.; Clennan, E. L. Properties and reactions of singlet dioxygen. In *Active oxygen in chemistry*; Foote, C. S.; Valentine, J. S.; Greenberg, A.; Liebman, J. F., Eds.; Springer: Dordrecht, Netherlands, 1995; pp 105–140.
- 56 Prat, D.; Hayler, J.; Wells, A. A survey of solvent selection guides. *Green Chem.* **2014**, *16*, 4546–4551.
- 57 Ebersson, L.; Hartshorn, M. P.; Persson, O. 1,1,1,3,3,3-Hexafluoropropan-2-ol as a solvent for the generation of highly persistent radical cations. *J. Chem. Soc., Perkin Trans. 2* **1995**, *9*, 1735–1744.
- 58 Vuković, V. D.; Richmond, E.; Wolf, E.; Moran, J. Catalytic Friedel–Crafts reactions of highly electronically deactivated benzylic alcohols. *Angew. Chem. Int. Ed.* **2017**, *56*, 3085–3089.
- 59 Poliakoff, M.; Licence, P.; George, M. W. A new approach to sustainability: a moore's law for chemistry. *Angew. Chem. Int. Ed.* **2018**, *57*, 12590–12591.
- 60 Ciamician, G. The photochemistry of the future. *Science* **1912**, *36*, 385–394.
- 61 Poliakoff, M.; George M. W. Manufacturing chemicals with light: any role in the circular economy? *Phil. Trans. R. Soc. A* **2020**, *378*, 20190260.

## Supplementary Information

### **Multi-gram Synthesis of Trioxanes Enabled by a Supercritical CO<sub>2</sub> Integrated Flow Process**

Lingqiao Wu,<sup>a</sup> Bruna L. Abreu,<sup>a</sup> Alexander J. Blake,<sup>a</sup> Laurence J. Taylor,<sup>a</sup> William Lewis,<sup>a</sup> Stephen P. Argent,<sup>a</sup> Martyn Poliakoff,<sup>a</sup> Hamza Boufroua\*<sup>a</sup> and Michael W. George\*<sup>a</sup>

<sup>a</sup>School of Chemistry, University of Nottingham, University Park, Nottingham, NG7 2RD U.K.

# Table of Contents

<b>General Information</b> .....	<b>4</b>
<b>Equipment Diagram and set-up</b> .....	<b>5</b>
<b>Typical procedure for high-pressure equipment</b> .....	<b>10</b>
<b>Procedure in batch experiments</b> .....	<b>12</b>
<b>Phase Behaviour study</b> .....	<b>15</b>
<b>Supplementary synthesis</b> .....	<b>18</b>
Optimisation of the amount of TPFPP in scCO <sub>2</sub> and EtOAc system.....	18
The results of photo-oxidation of <i>para</i> -cresol with powerful LED light .....	18
<b>NMR Data</b> .....	<b>20</b>
<b>Description of the products</b> .....	<b>20</b>
4-Hydroperoxy-4-methylcyclohexa-2,5-dien-1-one. ( <b>2a</b> ) .....	20
4-Hydroxy-4-methylcyclohexa-2,5-dien-1-one. ( <b>3a</b> ) .....	20
4-Ethyl-4-hydroperoxycyclohexa-2,5-dien-1-one. ( <b>2b</b> ) .....	20
4-Ethyl-4-hydroxycyclohexa-2,5-dien-1-one ( <b>3b</b> ) .....	21
4-( <i>tert</i> -Butyl)-4-hydroperoxycyclohexa-2,5-dien-1-one. ( <b>2c</b> ).....	21
4-Hydroperoxy-4-(2-methoxyethyl)cyclohexa-2,5-dien-1-one. ( <b>2d</b> ).....	22
4-Ethyl-4-hydroperoxy-2-methoxycyclohexa-2,5-dien-1-one. ( <b>2e</b> ) .....	22
4-hydroperoxy-2,4-dimethylcyclohexa-2,5-dien-1-one. ( <b>2f</b> ).....	22
4-Hydroperoxy-3,4-dimethylcyclohexa-2,5-dien-1-one ( <b>2g</b> ) .....	23
4a-Hydroperoxy-5,6,7,8-tetrahydronaphthalen-2(4aH)-one. ( <b>2h</b> ).....	23
4-Hydroperoxy-2,4,6-trimethylcyclohexa-2,5-dien-1-one. ( <b>2i</b> ) .....	24
Methyl (tert-butoxycarbonyl)-L-tyrosinate. ( <b>1j</b> ).....	24
Methyl (S)-2-((tert-butoxycarbonyl)amino)-3-(1-hydroperoxy-4-oxocyclohexa-2,5-dien-1-yl)propanoate. ( <b>2j</b> ).....	24
tert-Butyl (4-hydroxyphenethyl)carbamate. ( <b>1k</b> ).....	25
tert-Butyl (2-(1-hydroperoxy-4-oxocyclohexa-2,5-dien-1-yl)ethyl) carbamate. ( <b>2k</b> ) .....	25
Methyl 3-(1-hydroperoxy-4-oxocyclohexa-2,5-dien-1-yl)propanoate. ( <b>2l</b> ).....	26
3-Hydroxy-3-methyl-1,2-dioxaspiro[5.5]undeca-7,10-dien-9-one / 4-Hydroperoxy-4-(3-oxobutyl)cyclohexa-2,5-dien-1-one. ( <b>2m</b> ).....	26
3-Isopropyl-8a-methyl-4a,8a-dihydrobenzo[e][1,2,4]trioxin-6(5H)-one. ( <b>5</b> ) <sup>[S4]</sup> .....	27
3-Cyclohexyl-8a-methyl-4a,8a-dihydrobenzo[e][1,2,4]trioxin-6(5H)-one. ( <b>6</b> ) .....	27
8a-Methyl-3-phenyl-4a,8a-dihydrobenzo[e][1,2,4]trioxin-6(5H)-one. ( <b>7</b> ).....	28
8a-Methyl-3-( <i>p</i> -tolyl)-4a,8a-dihydrobenzo[e][1,2,4]trioxin-6(5H)-one. ( <b>8</b> ) .....	28
3-Cyclohexyl-8a-ethyl-4a,8a-dihydrobenzo[e][1,2,4]trioxin-6(5H)-one. ( <b>9</b> ).....	29
3-Cyclohexyl-4a,5,8,9,10,11-hexahydro-6H-naphtho[1,8a-e][1,2,4]trioxin-6-one. ( <b>10</b> ).....	29
3-Cyclohexyl-8,8a-dimethyl-4a,8a-dihydrobenzo[e][1,2,4]trioxin-6(5H)-one. ( <b>11</b> ) .....	30
Methyl 3-(3-cyclohexyl-6-oxo-5,6-dihydrobenzo[e][1,2,4]trioxin-8a(4aH)-yl)propanoate ( <b>12</b> ).....	30
3-Cyclohexyl-8a-(2-methoxyethyl)-4a,8a-dihydrobenzo[e][1,2,4]trioxin-6(5H)-one. ( <b>13</b> ).....	31
<b>NMR Spectra</b> .....	<b>32</b>
4-Hydroperoxy-4-methylcyclohexa-2,5-dien-1-one. ( <b>2a</b> ) .....	32
4-Hydroxy-4-methylcyclohexa-2,5-dien-1-one. ( <b>3a</b> ) .....	33
4-Ethyl-4-hydroperoxycyclohexa-2,5-dien-1-one. ( <b>2b</b> ) .....	34

4-Ethyl-4-hydroxycyclohexa-2,5-dien-1-one ( <b>3b</b> ) .....	35
4-( <i>tert</i> -Butyl)-4-hydroperoxycyclohexa-2,5-dien-1-one. ( <b>2c</b> ).....	36
4-Hydroperoxy-4-(2-methoxyethyl)cyclohexa-2,5-dien-1-one. ( <b>2d</b> ).....	37
4-Ethyl-4-hydroperoxy-2-methoxycyclohexa-2,5-dien-1-one. ( <b>2e</b> ) .....	38
4-Hydroperoxy-2,4-dimethylcyclohexa-2,5-dien-1-one. ( <b>2f</b> ) .....	39
4-Hydroperoxy-3,4-dimethylcyclohexa-2,5-dien-1-one ( <b>2g</b> ) .....	40
4a-Hydroperoxy-5,6,7,8-tetrahydronaphthalen-2(4aH)-one. ( <b>2h</b> ).....	41
4-Hydroperoxy-2,4,6-trimethylcyclohexa-2,5-dien-1-one. ( <b>2i</b> ) .....	42
Methyl ( <i>tert</i> -butoxycarbonyl)- <i>L</i> -tyrosinate. ( <b>1j</b> ).....	43
Methyl ( <i>S</i> )-2-(( <i>tert</i> -butoxycarbonyl)amino)-3-(1-hydroperoxy-4-oxocyclohexa-2,5-dien-1-yl)propanoate. ( <b>2j</b> ).....	44
<i>tert</i> -Butyl (4-hydroxyphenethyl) carbamate. ( <b>1k</b> ).....	45
<i>tert</i> -Butyl (2-(1-hydroperoxy-4-oxocyclohexa-2,5-dien-1-yl)ethyl) carbamate. ( <b>2k</b> ) .....	46
Methyl 3-(1-hydroperoxy-4-oxocyclohexa-2,5-dien-1-yl)propanoate. ( <b>2l</b> ).....	47
3-Hydroxy-3-methyl-1,2-dioxaspiro[5.5]undeca-7,10-dien-9-one / 4-Hydroperoxy-4-(3-oxobutyl)cyclohexa-2,5-dien-1-one. ( <b>2m</b> ).....	48
3-Isopropyl-8a-methyl-4a,8a-dihydrobenzo[e][1,2,4]trioxin-6(5H)-one. ( <b>5</b> ).....	49
3-Cyclohexyl-8a-methyl-4a, 8a-dihydrobenzo[e][1,2,4]trioxin-6(5H)-one. ( <b>6</b> ) .....	50
8a-Methyl-3-phenyl-4a, 8a-dihydrobenzo[e][1,2,4]trioxin-6(5H)-one. ( <b>7</b> ).....	51
8a-Methyl-3-( <i>p</i> -tolyl)-4a,8a-dihydrobenzo[e][1,2,4]trioxin-6(5H)-one. ( <b>8</b> ) .....	52
3-Cyclohexyl-8a-ethyl-4a,8a-dihydrobenzo[e][1,2,4]trioxin-6(5H)-one. ( <b>9</b> ).....	53
3-Cyclohexyl-4a,5,8,9,10,11-hexahydro-6H-naphtho[1,8a-e][1,2,4]trioxin-6-one. ( <b>10</b> ).....	54
3-Cyclohexyl-8,8a-dimethyl-4a,8a-dihydrobenzo[e][1,2,4]trioxin-6(5H)-one. ( <b>11</b> ) .....	55
Methyl 3-(3-cyclohexyl-6-oxo-5,6-dihydrobenzo[e][1,2,4]trioxin-8a(4aH)-yl)propanoate. ( <b>12</b> ).....	56
3-Cyclohexyl-8a-(2-methoxyethyl)-4a,8a-dihydrobenzo[e][1,2,4]trioxin-6(5H)-one. ( <b>13</b> ).....	57
<b>Crystallography Data .....</b>	<b>58</b>
Crystal ( <b>2a</b> ).....	58
Crystal ( <b>2b</b> ).....	59
Crystal ( <b>2h</b> ).....	60
Crystal ( <b>6</b> ).....	61
Single Crystal X-ray Diffraction Experimental .....	62
Single Crystal X-ray Diffraction Refinement Details .....	64
<b>References.....</b>	<b>65</b>

## General Information

**Reagents** were purchased in reagent grade from commercial suppliers and used without further purification, unless otherwise stated.

**Purification methods:** Thin layer chromatography (TLC) using pre-coated aluminium plates covered with 0.20 mm silica gel with fluorescent indicator visualised upon UV irradiation ( $\lambda = 254$  nm) or  $\text{KMnO}_4$  stain, was used for reaction monitoring and product detection.

For the purification of new compounds, flash chromatography was used otherwise noted. The solvent mixture used to eluent the products were cyclohexane/EtOAc or *n*-pentane/EtOAc. Two methods were used, flash chromatography and automatic flash chromatography. The automatic flash chromatography machine was purchased from TELEDYNE ISCO (P/N 69-3873-244). The procedure for the automatic flash chromatography is described. Firstly, two different solvents were chosen and used to prime the system starting with the polar solvent to the less polar one. Following the system priming a dry pre-loaded solid cartridge with silica was placed into the solid sample position; the appropriate RediSep Rf Gold® silica gel column was loaded on to the system; then running the separation. Different fractions were obtained. Further identification was made after removing the solvents.

**$^1\text{H}$  and  $^{13}\text{C}$  NMR spectra:** Proton nuclear magnetic resonance ( $^1\text{H}$  NMR) spectra and proton-decoupled carbon nuclear magnetic resonance ( $^{13}\text{C}$   $\{^1\text{H}\}$  NMR) spectra were recorded at 25 °C (unless stated otherwise) on AV-400 (400 MHz), AV (III) 400 (400 MHz) or AV (III) 500 (500 MHz) spectrometers at the University of Nottingham nuclear magnetic resonance facility. Chemical shifts for proton are reported in parts per million (ppm) downfield from tetramethylsilane and are referenced to residual protium in the NMR solvent according to values reported in the literature.<sup>[S1]</sup>

Chemical shifts for carbon are reported in parts per million downfield from tetramethylsilane and are referenced to the carbon resonances of the solvent. The solvent peak was referenced to 7.26 ppm for  $^1\text{H}$  and 77.16 ppm for  $^{13}\text{C}$  in  $\text{CDCl}_3$ .

Data are represented as follows: chemical shift, integration, multiplicity (s = singlet, d = doublet, t = triplet, q = quartet, dd = doublet doublet, ddd = doublet doublet doublet, dt = doublet triplet, tdt = triplet doublet triplet, m = multiplet), coupling constants in Hertz (Hz). In the case of compounds containing fluorine atoms, it should be noted that  $^{13}\text{C}$  NMR experiments were obtained without  $^{19}\text{F}$  decoupling. NMR spectra were processed with MestReNova Software.

**High Resolution Mass Spectra (HRMS)** were recorded on a Bruker microTOF II.

**Safety Warning:** These reactions involve high pressures and require appropriately rated apparatus and with due regard to the potentially explosive reaction between  $\text{O}_2$  and organic compounds. Below, we give further details of the equipment used to carry out this work at Nottingham but the Authors give no undertaking as to the suitability of this equipment when used in other laboratories, particularly because national and local safety regulations may vary between locations. The equipment described is not necessarily, the only type that could be used, nor possibly the best available. It is the responsibility of each researcher to check the suitability and safety of their own equipment for such experiments in their laboratories.

## Equipment Diagram and set-up

**General information about the equipment:** As far as we are aware, there is no commercially available equivalent of the reactor system used in this work which, apart from the photo-reactor itself, was assembled from commercially available parts and components. Although conceptually simple, the system needs careful design and assembly to ensure safe operation.

The high-pressure continuous flow rigs for photo-oxidation were built using HPLC pumps, connecting tubes, mixers, a custom-built sapphire tube reactor, and cooling bath. Temperatures were monitored by thermocouples and system pressure was set and controlled by a back-pressure regulator. System pressure, CO<sub>2</sub> pressure and O<sub>2</sub> pressure were monitored by pressure transducers. All continuous flow experiments described in this paper were carried out using the rig described below. The rig diagrams are shown in Figure S1-S4.

Compressed CO<sub>2</sub> was delivered from a chilled CO<sub>2</sub> pump (Jasco TM PU-1580-CO<sub>2</sub> pump; note that liquid CO<sub>2</sub> is too compressible at room temperature to be pumped in this way) and O<sub>2</sub> was dosed at a known rate via a Rheodyne dosage unit (alternatively one could use an appropriately pressure rated mass-flow controller. Mixers M1 and M2 (78 mm, ¼ inch O. D., SS316 tubes) were loaded with one gram of sand each. CO<sub>2</sub> and O<sub>2</sub> were mixed in the first static mixer M1 and then the organic stream was added by OP1 (organic pump 1, Jasco TM PU-980 HPLC pump) into the gases mixture before entering into the second mixer M2. The second reagent was feed by OP2 (organic pump 2, Jasco TM PU-980 HPLC pump) if necessary.

The fluid mixture entered then into the high-pressure sapphire tube reactor (the tubing itself was purchased from Saint-Gobain Crystals, 10 mm O.D., 1 mm wall thickness, 120-480 mm long; loaded with desired glass beads, 6 mm O. D.) following an up-flow method. The sapphire tube was irradiated with visible light by LEDs, which were controlled by LED controllers. LED lights were composed of three banks of liquid cooled LED aluminium blocks each containing five chips (Citizen Electronics Co. Ltd) irradiating for 1000 lumen per chip. The blocks were cooled with a chiller. Due to the heat generated by the LED lights, a secondary cooling bath was used to pump coolant around the sapphire tube to ensure the desired temperature in the reactor. Thus, LEDs can be positioned as close as possible to the sapphire tube assuring a high efficient irradiation. Photo-reactor 1 refers to the association of the sapphire tube, LEDs and aluminium blocks. The Photo-reactor was followed by a thermal reactor 2, which is constructed from a stainless-steel tubing and fittings (Swagelock, 156 mm, ¼ inch SS 316 tubes). The system pressure was controlled continuously by a back-pressure regulator (BPR, Jasco TM BP-1580-81). Finally, once the reaction mixture passed the BPR, the products can be collected for further analysis. The whole system has pressure trips to cut the electrical power if the pressure exceeds pre-set safety limits.

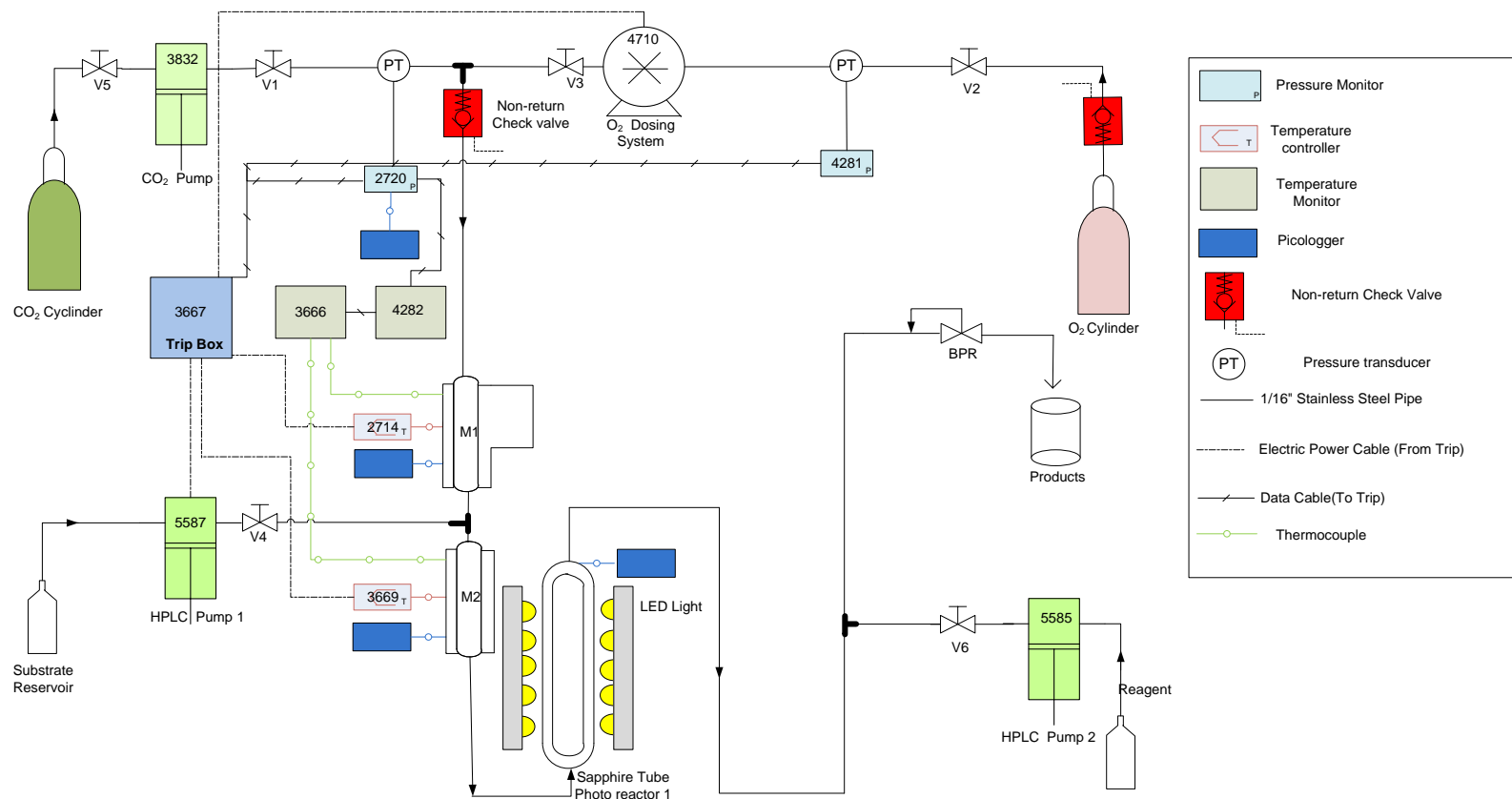


**Figure S1.** The diagram of the high-pressure rig for the synthesis of products-setup-1. This is a general high-pressure continuous flow reactor using CO<sub>2</sub> as a solvent. CO<sub>2</sub> and O<sub>2</sub> were mixed in M1, then the organic solution was introduced by organic pump 1 meeting the gases in the second mixer M2. A second organic pump was used to pump more solvent to avoid the blockage in the BPR. The solution was irradiated by white LEDs in the photo-reactor (Saint-Gobain Crystals, 10 mm O.D., 1 mm wall thickness, 240 mm long) before flowing out from BPR. Non-return check valves were used to prevent the organic stream from large amount of oxygen. Pressure and temperature monitors were connected to the Piclogger which stores the pressure and temperature data for the system. Trip box is used to cut the electrical power to the various components whenever the system pressure or temperature exceeded safe limits.

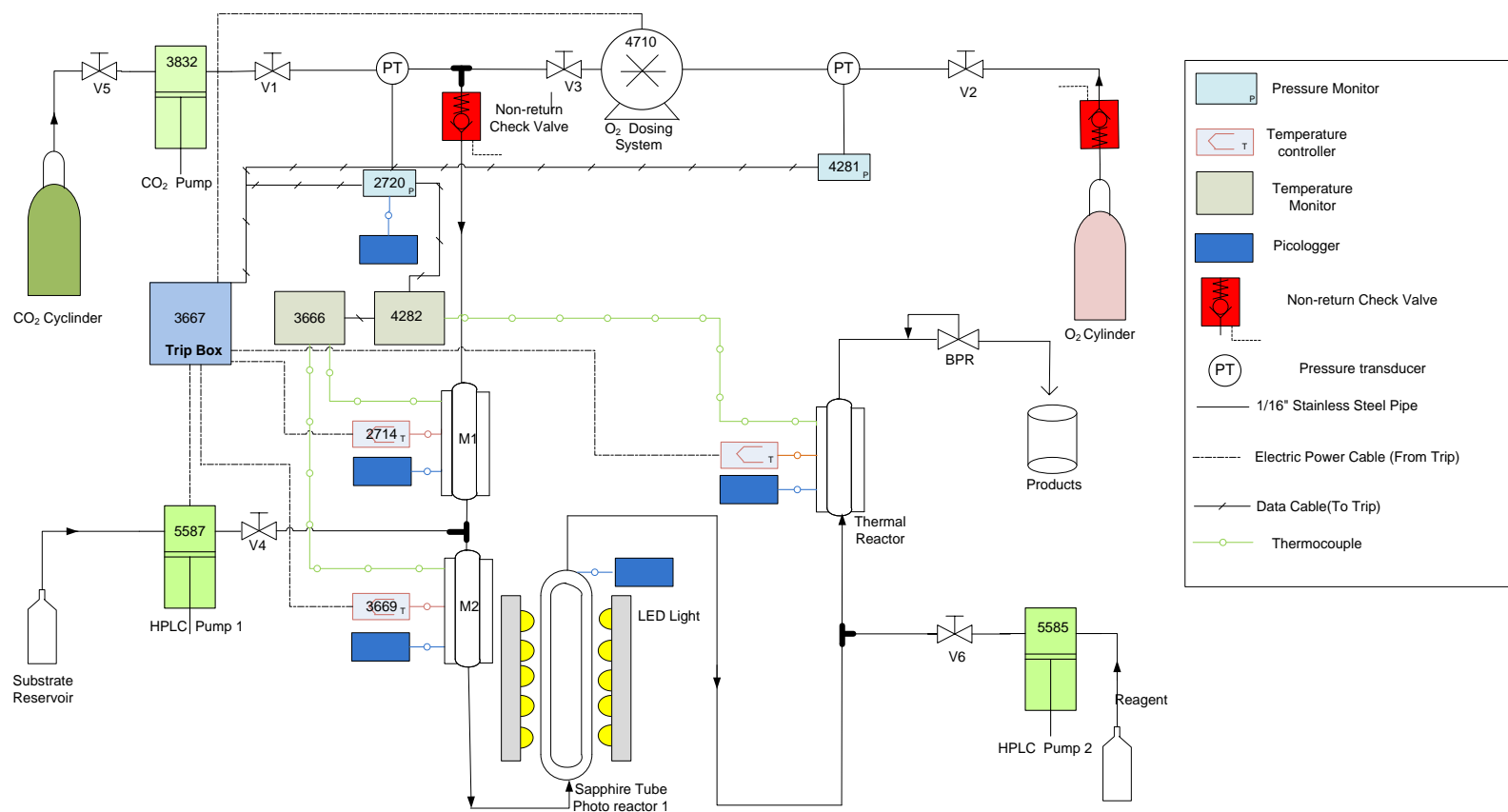


**Figure S2.** The diagram of the high-pressure rig for the synthesis of products-setup-2. The difference between setup-2 and setup-1 was that a thermal reactor (78 mm, ¼ inch O. D., SS316 tubes) was added between photoreactor and BPR, for the cyclisation of para-peroxylquinol derivatives with different aldehydes.

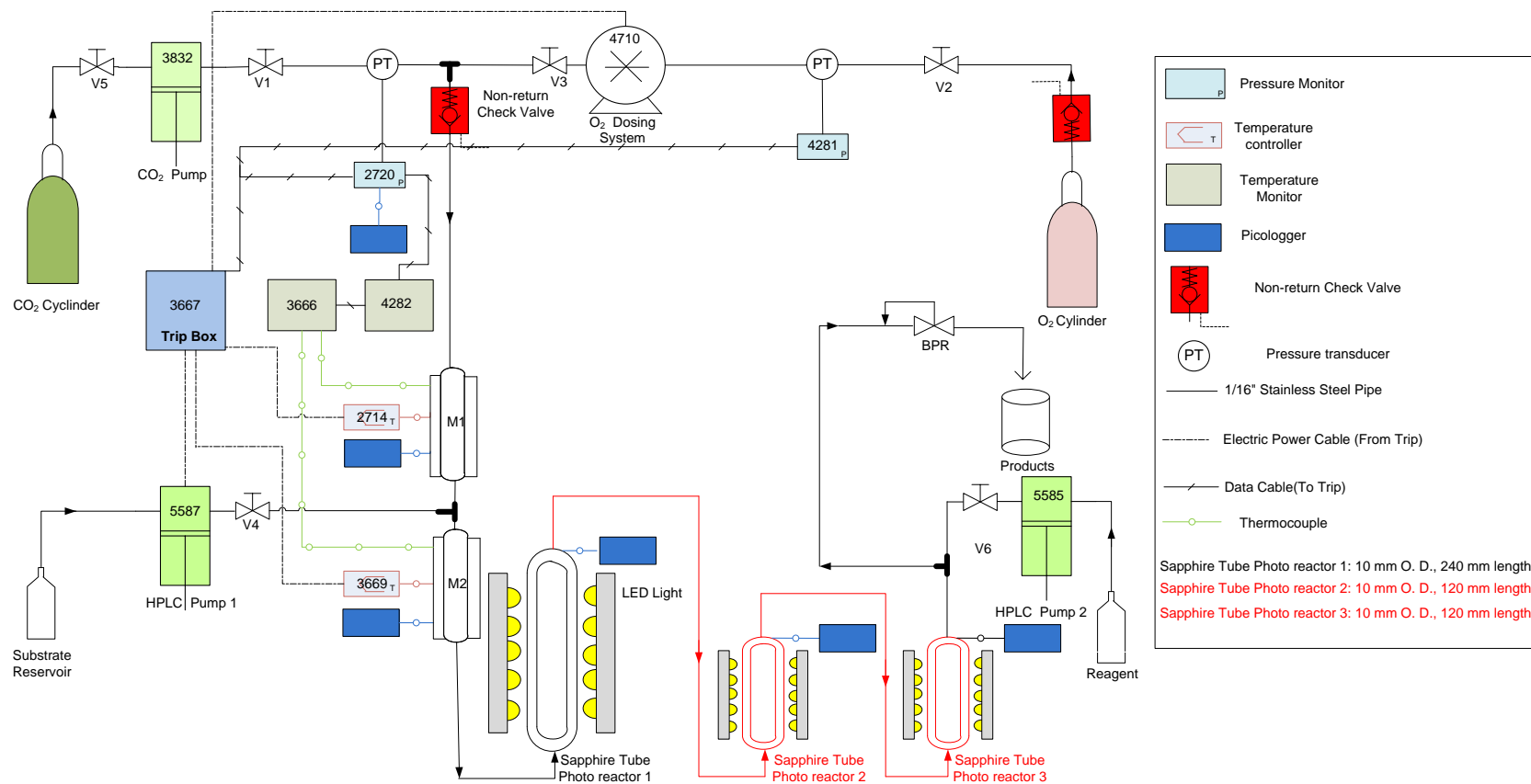


**Figure S3.** The diagram of the high-pressure rig for the synthesis of products-setup-3. The difference between setup-3 and setup-1 was that two extra photoreactors (Saint-Gobain Crystals, 10 mm O.D., 1 mm wall thickness, 120 mm long) were connected with previous photoreactor 1 in series to extend the irradiation time in the photoreactor.

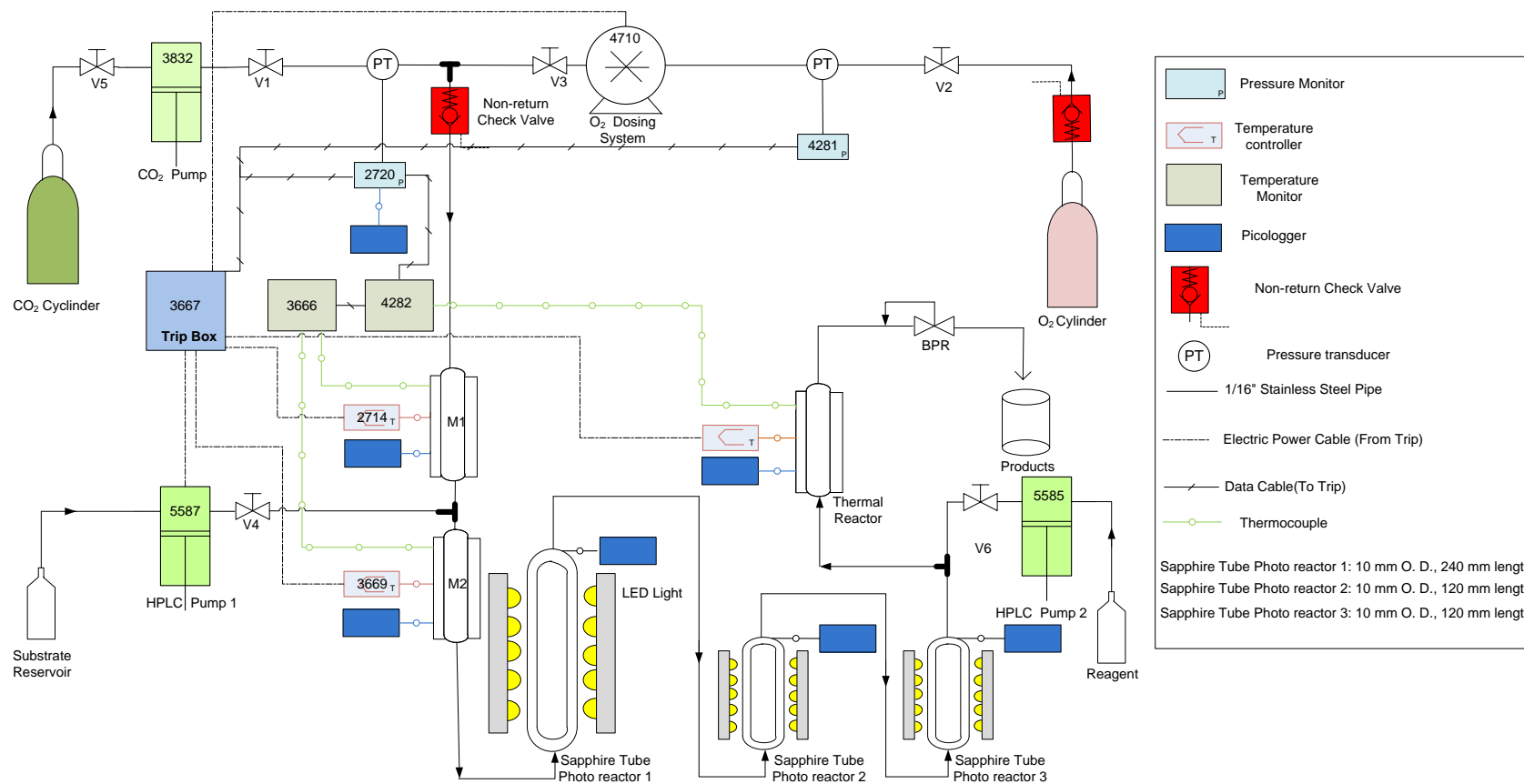


**Figure S4.** The diagram of the high-pressure rig for the synthesis of products-setup-4. The difference between setup-4 and setup-1 was that a thermal reactor and two photoreactors were connected in series as shown in the diagram to obtain longer irradiation time and cyclisation of para-peroxyquinol derivatives with different aldehydes.

## Typical procedure for the high-pressure equipment (Figs S1 –S4)

- *Start-up procedure:*
  1. Mixers heaters M1, M2 and the thermal reactor were set to 40 °C and switched on.
  2. Cooling bath were set to 35 °C and turned on.
  3. Then the Rheodyne dosing unit was set to a switching time of 16 seconds.
  4. The set pressure on the BPR was fixed at 120 bar and the valve V5 was opened.
  5. The CO<sub>2</sub> pump was set to 0.15 mL/min (unless otherwise mentioned) and the organic pump was set to 0.05 mL/min.
  6. Afterwards the CO<sub>2</sub> pump was started and the valve V1 was opened allowing CO<sub>2</sub> to enter the system.
  7. A feedstock of EtOAc (unless otherwise mentioned) was pumped into the system and valve V4 was opened.
  8. The system was allowed to settle for 30 minutes to reach set temperatures and pressure. As soon as the system had reached equilibrium, the Rheodyne dosing unit was started and valve V2 and V3 were opened allowing O<sub>2</sub> to enter the system.
  9. Normally a good mixing of O<sub>2</sub> and CO<sub>2</sub> is obtained 30 minutes after letting O<sub>2</sub> enter into the system.
  10. At this point the LEDs light source was turned on and the photoreactor 1 was allowed to stabilise to the desired temperature: 40 °C. Then the organic pump feedstock was changed to a freshly prepared mixture of organic materiel dissolved into EtOAc (or MeOH) at the chosen concentration.
  11. After allowing the system to equilibrate, the rig was under starting conditions.
  12. After one hour holding the conditions described above, three samples were taken for each condition, sample was submitted to <sup>1</sup>H NMR in the appropriate deuterated solvent with mesitylene/biphenyl as internal standard.

- *Shutdown and cleaning procedures:*
  1. To shut down and clean the rig the following procedure was followed. The LEDs light source was turned off.
  2. Valve V4 was closed and then the HPLC was stopped.
  3. Valve V2 and V3 were closed and the Rheodyne dosing unit was turned off.
  4. After ten minutes the mixers heaters and chillers were switched off.
  5. The system was allowed to return to room temperature while flushing with CO<sub>2</sub>.
  6. The system was allowed to return to atmospheric pressure by slowly reducing the set pressure value fixed at the BPR in roughly 20 bar increments with 10 seconds approximatively between each value. Valve V1 was then closed and the CO<sub>2</sub> pump was stopped.
  7. Finally, the system was purged with organic solvent (EtOAc or MeOH) at a flow rate of 1 mL/min for 40 minutes.

**Safety Note:** *Special care is required before restarting any pressure system such as this one after an unscheduled shut-down (e.g. when the power is cut-off by the pressure trip). The pressure should be fully released and the system purged with an inert gas before re-pressurizing.*

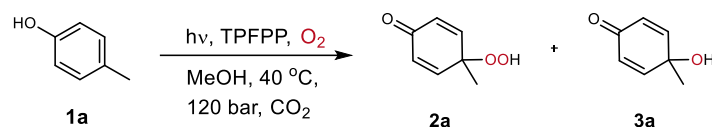
**Procedure for the synthesis of *para*-peroxyquinol derivatives:** The desired concentration of starting material was pumped into the rig by organic pump 1 at the desired flow rate; a second pump delivered more solvent after the photoreactor to avoid the blockage in the BPR. The *para*-peroxyquinol derivatives crude could be collected after BPR, ready to be isolated using flash chromatography and identified.

**Procedure for the synthesis of 1,2,4-trioxane derivatives:** As described in the procedure for the synthesis of *para*-peroxyquinol derivatives, instead of pumping the pure solvent from the second pump, the desired aldehyde dissolved in the solvent was pumped at the same flow rate as organic pump 1.

## Procedure in batch experiments

In a round bottle flask, 1 mmol of *para*-cresol (**1a**) was dissolved in the desired solvent to prepare 0.067 M of the solution. To this solution, 0.05-0.1 mol % of TPFPP to **1a** was added. Oxygen was provided from a balloon loaded with pure oxygen at atmospheric pressure. The mixture was irradiated by white LED light at room temperature for a time period of 4-5 hours. The crude was purified with using Cyclohexane/EtOAc to eluent products using Automatic Flash Chromatography after removing the solvent. For the reaction with co-catalyst, 0.5 equivalent co-catalyst was added into the solution before irradiation.

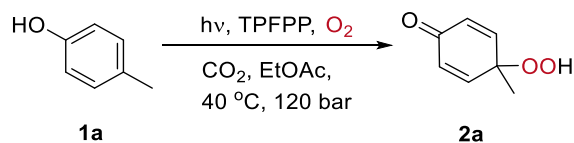
**Table S1.** Optimisation of de-aromatisation of para-cresol **1a**, in continuous flow in high pressure system using CO<sub>2</sub> and MeOH as a co-solvent (full table)



Entry	Conc of 1a (M)	Co-catalyst	CO <sub>2</sub> pump (mL/min)	Residence time (min)	Conv. of 1a (%)	Yield of 2a (%)	Yield of 3a (%)
1 <sup>a</sup>	0.1	-	0.37	7	43	35	-
2	0.1	-	0.15	26	76	72	-
3 <sup>b</sup>	0.1	TEA (5 mol%)	0.15	26	78	77	-
4	0.1	DBU (5 mol%)	0.15	26	89	82	5
5	0.1	K <sub>2</sub> CO <sub>3</sub> (5 mol%)	0.15	26	93	76	8
6	0.1	DBU (20 mol%)	0.15	26	92	81	9
7	2.0	-	0.15	26	97	91	1
8	3.0	-	0.15	26	97	96	<1
9 <sup>c</sup>	3.0	-	0.3	13	96	78	<1
10 <sup>d</sup>	5.0	-	0.15	26	96	94	-

All the experiments were performed using MeOH as the co-solvent, and the molar ratio of TPFPP was 0.1 mol% of **1** (entries 1-7) and 0.05 mol % of **1** (entries 8-10), the flow rate of organic pump was 0.05 mL/min unless otherwise stated. [a]: This experiment was conducted in a half-length photoreactor (10 mm o. d., 120 mm length). [b]: H<sub>2</sub>O (12.5 mol%) was added. [c]: the flow rate of the organic pump was 0.1 mL/min. [d]: The BPR was blocked after running for 4 hours. The yield was calculated by <sup>1</sup>H NMR using biphenyl as internal standard.

**Tables S2.** Optimisation of de-aromatisation of para-cresol **1a**, in continuous flow in high pressure system using CO<sub>2</sub> and EtOAc as a co-solvent (full table)



Entry	Conc. of <b>1a</b> <sup>a</sup> (M)	TPFPP <sup>b</sup> (mol%)	Residence Time (min) <sup>c</sup>	Conv. of <b>1a</b> (%)	Yield of <b>2a</b> (%)
<b>1</b>	3.0	0.05	15	80	41
<b>2</b>	3.0	0.05	26	94	54
<b>3</b>	1.0	0.1	15	41	41
<b>4</b>	1.0	0.3	15	69	69
<b>5</b>	1.0	0.1	26	72	68
<b>6</b>	2.0	0.1	15	88	51
<b>7<sup>d</sup></b>	1.0	0.3	26	86	78
<b>8<sup>e</sup></b>	1.0	0.3	26	95	94

All experiments were conducted at 40 °C and 120 bar, using CO<sub>2</sub> and EtOAc as solvents, The flow rate of organic pump 1 was 0.05 mL/min, the flow rate of CO<sub>2</sub> was 0.15 mL/min (26 min) or 0.3 mL/min (15 min). The photoreactor was 10 mm O. D., 240 mm length, filled with glass beads (6 mm O. D.), the yield and conversion were calculated from <sup>1</sup>H NMR spectroscopy, using biphenyl as internal standard. [a]: The concentration of **1** in EtOAc. [b]: The ratio of TPFPP to **1a**. [c]: Residence Time of photo-oxidation step in the photoreactor. [d]: Addition of 2 equivalents of t-BuOH into the starting solution. [e]: with 2 equivalent HFIP added in the starting solution.

## Phase Behaviour study

In order to mimic the conditions in the process of de-aromatisation, the phase behaviour was studied in the high-pressure continuous flow reactor (Figure S5), in the absence of irradiation by LED light, at 120 bar and 40 °C with the sapphire tube (240 mm length, 10 mm O. D.) was loaded with glass beads in the same configuration as was used for the photoreactions. The results are summarised in Table S1.

Firstly, CO<sub>2</sub>/MeOH system was studied; 62 % of CO<sub>2</sub> and 38 % MeOH were fully miscible, with a 1:1 molar ratio of the substrate (*para*-cresol **1a**) to O<sub>2</sub>. With neither *para*-cresol **1a** nor O<sub>2</sub> present, a single phase was observed (Table S1, entry 1). Then, pumping the *para*-cresol **1a** solution at 3.9 %, CO<sub>2</sub> (59.6 %) and MeOH (36.5 %), without O<sub>2</sub>, the mixture was still in a single phase with an initial 3.0 M concentration of *para*-cresol **1a** in MeOH, (TableS1, entry 2). However, when O<sub>2</sub> was introduced (3.8 %) and *para*-cresol **1a** (3.8 %), two phases were observed for these four components (CO<sub>2</sub>, MeOH, O<sub>2</sub> and *para*-cresol **1a**) (Tale S1, entries 3-4).

Then, decreasing the mole fraction of O<sub>2</sub> in CO<sub>2</sub>/MeOH from 3.8 % to 2.0 %, we a single phase occurred, even after adding 2 % of *para*-cresol **1a** (Table S1, entries 5–8). During of all these processes, *para*-cresol **1a** was highly soluble in the CO<sub>2</sub> + MeOH system. However, two phases were observed when the mole fraction of O<sub>2</sub> was > 2.7 %. This problem was only transient in our photochemical experiments, since all the O<sub>2</sub> was consumed, even starting with high O<sub>2</sub> concentrations.

**Table S3.** The results for phase behaviour studies in the CO<sub>2</sub> system<sup>a</sup>.

Entry	Equivalent Concentration of	Mole fraction of each component %				Phase behaviour	Pressure (bar)	Temperature (°C)
	1a in MeOH, O <sub>2</sub> :Sub=1:1	CO <sub>2</sub>	MeOH	O <sub>2</sub>	Substrate			
	(mol:mol)							
1	-	62.0	38	0	0	A single phase	120	40
2	3.0 M	59.6	36.5	0	3.9	A single phase	120	40
3	3.0 M	59.6	36.5	3.9	0	Two phases <sup>b</sup>	120	40
4	3.0 M	57.3	35.1	3.8	3.8	Two phases <sup>b</sup>	120	40
5	2.5 M	60.3	36.3	3.3	0	Two phases <sup>b</sup>	120	40
6	2.0 M	61.1	36.2	2.7	0	Two phases <sup>b</sup>	120	40
7	1.5 M	62	36	2	0	Single phase	120	40
8	1.5 M	60.7	35.3	2	2	Single phase	120	40

[a]: Phase studies carried out in the absence of irradiation by the LEDs; the photosensitizer was omitted since its concentration is so low that it would not be expected to affect the phase behaviour.

[b]: "Two phases" means that some bubbles were observed in the up-flow sapphire tube reactor.

### Phase behaviour studies

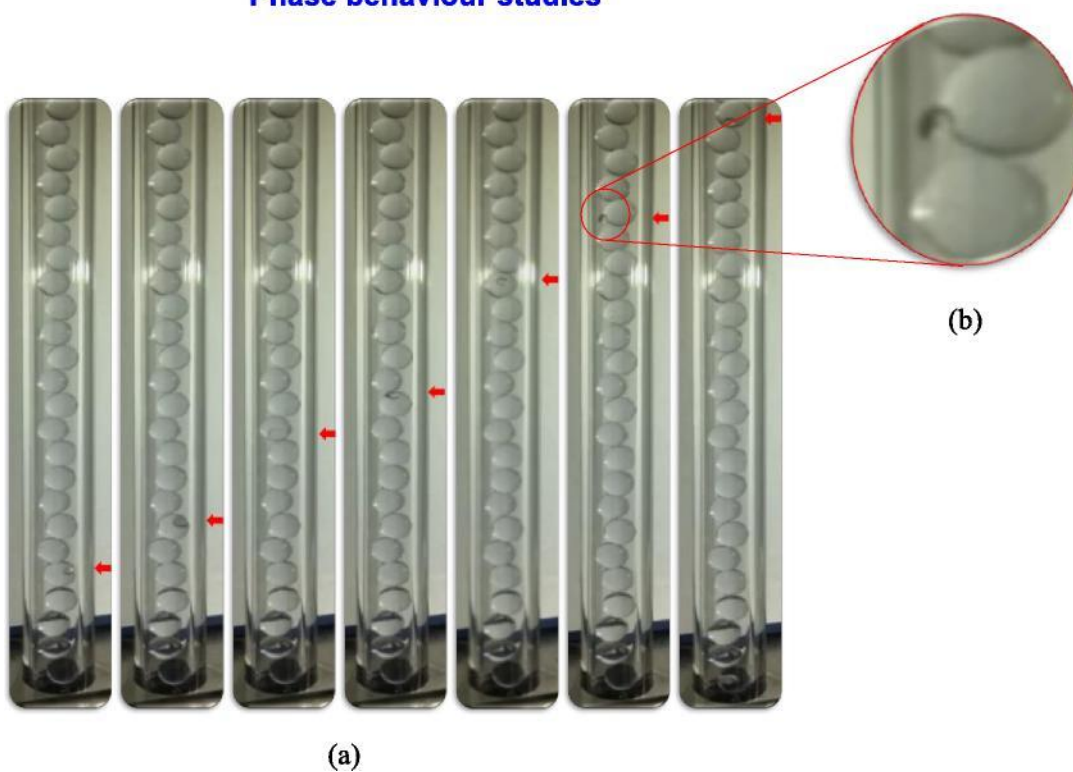


**Figure S5.** An example of two phases under the conditions of Table S3, entry 4. (a) A bubble (arrowed) is moving upwards as the time evolves from left to right; (b) Magnified picture to show the bubble more clearly.

## Supplementary synthesis

A brief study was carried out into the effect of the amount of TPFPP in scCO<sub>2</sub> and EtOAc system

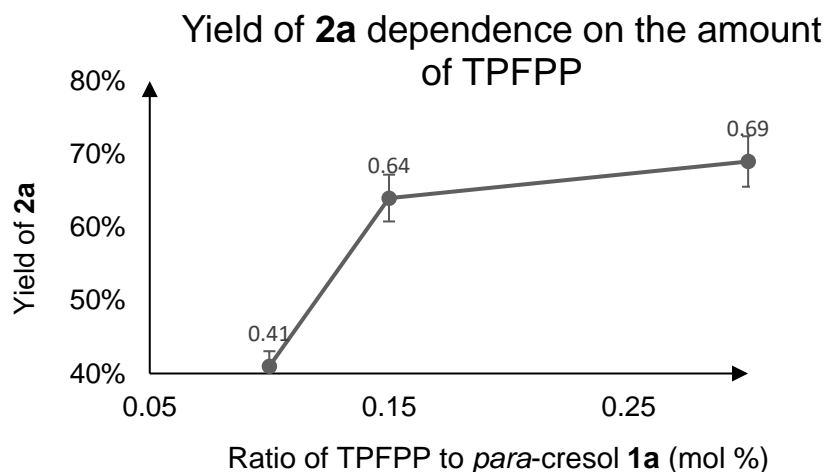


**Figure S6.** Showing how the yield of **2a** depends on the amount of TPFPP in EtOAc and CO<sub>2</sub>. These experiments were conducted in the setup shown in Figure S2. The system pressure was 120 bar. The photoreactor (40 °C) was 10 mm O. D., 240 mm length, filled with glass beads (6 mm O. D.), the flow rate of organic pump 1 was 0.05 mL/min, the flow rate of CO<sub>2</sub> pump was 0.3 mL/min. The concentration of **1a** in EtOAc was 1.0 M, the residence time was 15 min, The switching time of Rheodyne for oxygen was 15.9 seconds; using biphenyl as an internal standard.

The results of photo-oxidation of *para*-cresol with powerful LED light

When we employed more powerful LED lights (8000 lumens for each chip, 3 chips for each LED), one powerful LED and five normal LED (1000 lumens for each chip, each LED with 5 chips) at the same time to irradiate the photoreactor, the conversion of **1a** was 89 %. The residence time was 9 min in the photo-oxidation step, with 64 % overall yield of **2b** the flow rates of organic pump 1 and CO<sub>2</sub> pump were held at 0.1 mL/min, 0.45 mL/min, respectively. Others conditions also were tested, but polymerisation was observed when employing a longer residence time, 26 min as previously shown in Table S4..

**Table S4.** The results of photo-oxidation of **1a** with powerful LED light.<sup>a</sup>

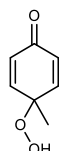
Entry	Flow Rate (mL/min)		Residence Time <sup>b</sup>	Conversion <sup>c</sup>	Yield of <b>2a</b> <sup>c</sup>
	Org. Pump 1	CO <sub>2</sub> Pump			
1	0.05	0.15	26 min	97 %	58%
2	0.05	0.3	15 min	97 %	35 %
3	0.1	0.45	9 min	89 %	69 %
4	0.1	0.6	7 min	89 %	54 %
5	0.15	0.52	8 min	89 %	80 %

[a]: All experiments were performed at 40 °C, 120 bar. The concentration of TPFPP to **1a** was 0.3 mol %. The switching time of Rheodyne for oxygen was 15.9 seconds. [b]: represents Residence Time in the photoreactor. [c]: Yield was calculated by <sup>1</sup>H NMR spectroscopy, using biphenyl as an internal standard.

## NMR Data

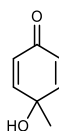
### Description of the products

#### 4-Hydroperoxy-4-methylcyclohexa-2,5-dien-1-one. (2a) <sup>[S2]</sup>



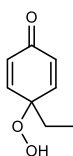
- The product was purified using flash chromatography column and eluted with a mixture of EtOAc/Cyclohexane (1:1)
- White solid
- **<sup>1</sup>H NMR** (400 MHz, CDCl<sub>3</sub>) δ 8.34 (s, 1H), 6.94 – 6.87 (m, 2H), 6.33 – 6.26 (m, 2H), 1.42 (s, 3H).
- **<sup>13</sup>C NMR** (101 MHz, CDCl<sub>3</sub>) δ 185.5, 149.7, 130.5, 78.7, 22.9.
- **HRMS** (ESI, m/z): calc for C<sub>7</sub>H<sub>8</sub>O<sub>3</sub> [M]<sup>+</sup>: 140.0473, found: 140.0472.

#### 4-Hydroxy-4-methylcyclohexa-2,5-dien-1-one.(3a) <sup>[S3]</sup>



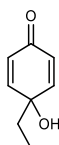
- The product was purified using flash chromatography column and eluted with a mixture of EtOAc/Cyclohexane (1:1)
- White solid
- **<sup>1</sup>H NMR** (400 MHz, CDCl<sub>3</sub>) δ 6.92 – 6.82 (m, 2H), 6.12 – 6.02 (m, 2H), 1.46 (s, 3H).
- **<sup>13</sup>C NMR** (101 MHz, CDCl<sub>3</sub>) δ 185.8, 152.6, 127.1, 67.2, 26.8.
- **HRMS** (ESI, m/z): calc for C<sub>7</sub>H<sub>8</sub>O<sub>2</sub> [M+H]<sup>+</sup>: 125.0597, found:125.0590.

#### 4-Ethyl-4-hydroperoxycyclohexa-2,5-dien-1-one. (2b) <sup>[S4]</sup>



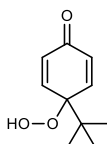
- White crystal
- **<sup>1</sup>H NMR** (400 MHz, CDCl<sub>3</sub>) δ 8.75 (s, 1H), 6.96 – 6.75 (m, 2H), 6.39 – 6.30 (m, 2H), 1.74 (q, *J* = 7.6 Hz, 2H), 0.85 (t, *J* = 7.6 Hz, 3H).
- **<sup>13</sup>C NMR** (101 MHz, CDCl<sub>3</sub>) δ 186.2, 149.4, 131.4, 82.4, 29.0, 7.9.
- **HRMS** (ESI, *m/z*): calc for C<sub>8</sub>H<sub>10</sub>O<sub>3</sub> [M-H]<sup>-</sup>: 153.0557, found: 153.0551

#### 4-Ethyl-4-hydroxycyclohexa-2,5-dien-1-one (3b).



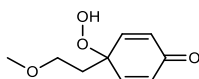
- The crude was purified with eluent (Cyclohexane/EtOAc) by autosampler Flash Chromatography after solvent removal.
- White solid
- **<sup>1</sup>H NMR** (400 MHz, CDCl<sub>3</sub>) δ 7.10 (d, *J* = 8.4 Hz, 2H), 6.79 (d, *J* = 8.4 Hz, 2H), 4.84 (broad s, 1H), 2.61 (q, *J* = 7.7 Hz, 2H), 1.24 (t, *J* = 7.6 Hz, 3H).
- **<sup>13</sup>C NMR** (101 MHz, CDCl<sub>3</sub>) δ 153.5, 136.7, 129.0, 115.2, 28.1, 16.0.
- **HRMS** (ESI, *m/z*): calc for C<sub>8</sub>H<sub>10</sub>O<sub>2</sub> [M-H]<sup>-</sup>: 153.0557, found: 153.0551.

#### 4-(*tert*-Butyl)-4-hydroperoxycyclohexa-2,5-dien-1-one. (2c)



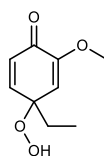
- The product was purified using flash chromatography column and eluted with a mixture of EtOAc/Cyclohexane (1:1)
- White solid
- **<sup>1</sup>H NMR** (400 MHz, CDCl<sub>3</sub>) δ 8.11 (s, 1H), 7.06 (d, *J* = 10.4 Hz, 2H), 6.39 (d, *J* = 10.4 Hz, 2H), 1.03 (s, 9H).
- **<sup>13</sup>C NMR** (101 MHz, CDCl<sub>3</sub>) δ 185.4, 149.0, 132.3, 85.9, 39.7, 26.1.
- **HRMS** (ESI, *m/z*) calc for C<sub>10</sub>H<sub>14</sub>O<sub>3</sub>Na [M + Na]<sup>+</sup>: 205.0835, found: 205.0833.

#### 4-Hydroperoxy-4-(2-methoxyethyl)cyclohexa-2,5-dien-1-one. (2d)



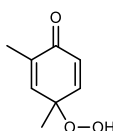
- The product was purified using flash chromatography column and eluted with a mixture of EtOAc/Cyclohexane (1:1)
- White solid
- **<sup>1</sup>H NMR** (400 MHz, CDCl<sub>3</sub>) δ 9.47 (s, 1H), 6.96 (d, *J* = 10.2 Hz, 2H), 6.29 (d, *J* = 10.2 Hz, 2H), 3.47 (t, *J* = 5.9 Hz, 2H), 3.31 (s, 3H), 2.03 (t, *J* = 5.9 Hz, 2H).
- **<sup>13</sup>C NMR** (101 MHz, CDCl<sub>3</sub>) δ 185.8, 148.3, 130.4, 79.7, 67.5, 58.9, 36.4.
- **HRMS** (ESI, *m/z*) calc for C<sub>9</sub>H<sub>12</sub>O<sub>4</sub>Na [M + Na]<sup>+</sup>: 207.0628, found: 207.0627.

#### 4-Ethyl-4-hydroperoxy-2-methoxycyclohexa-2,5-dien-1-one. (2e)



- The crude was purified with eluent (Cyclohexane/EtOAc) by autosampler Flash Chromatography after solvent removal.
- Yellow solid
- **<sup>1</sup>H NMR** (400 MHz, CDCl<sub>3</sub>) δ 8.23 (s, 1H), 6.85 (dd, *J* = 10.1, 2.7 Hz, 1H), 6.35 (d, *J* = 10.0 Hz, 1H), 5.66 (d, *J* = 2.8 Hz, 1H), 3.70 (s, 3H), 1.79 (q, *J* = 7.7 Hz, 2H), 0.87 (t, *J* = 7.6 Hz, 3H).
- **<sup>13</sup>C NMR** (101 MHz, CDCl<sub>3</sub>) δ 181.3, 152.9, 149.6, 130.5, 114.5, 84.2, 55.2, 29.9, 8.1.
- **HRMS** (ESI, *m/z*): calc for C<sub>9</sub>H<sub>12</sub>O<sub>4</sub> [M+H]<sup>+</sup>: 185.0808, found: 185.0800.

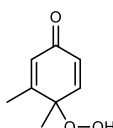
#### 4-hydroperoxy-2,4-dimethylcyclohexa-2,5-dien-1-one. (2f) <sup>[S5]</sup>



- The crude was purified with eluent (Cyclohexane/EtOAc) by autosampler Flash Chromatography after solvent removal.
- White solid

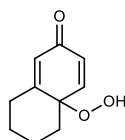
- **<sup>1</sup>H NMR** (400 MHz, CDCl<sub>3</sub>) δ 8.16 (d, *J* = 2.0 Hz, 1H), 6.87 (dd, *J* = 10.0, 3.1 Hz, 2H), 6.66 (dd, *J* = 3.0, 1.5 Hz, 1H), 6.28 (d, *J* = 10.0 Hz, 2H), 1.92 (d, *J* = 1.5 Hz, 5H), 1.40 (s, 5H).
- **<sup>13</sup>C NMR** (101 MHz, CDCl<sub>3</sub>) δ 186.3, 149.4, 144.8, 137.2, 130.2, 79.0, 23.0, 15.9.
- **HRMS** (ESI, *m/z*): calc for C<sub>8</sub>H<sub>10</sub>O<sub>3</sub> [M-H]<sup>-</sup>: 153.0557, found: 153.0541.

#### 4-Hydroperoxy-3,4-dimethylcyclohexa-2,5-dien-1-one (2g)



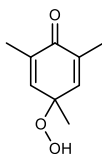
- The product was purified using flash chromatography column and eluting with a gradient of EtOAc/Cyclohexane (3:7 to 7:3)
- White solid
- **<sup>1</sup>H NMR** (400 MHz, CDCl<sub>3</sub>) δ 9.51 (s, 1H), 6.93 (d, *J* = 10.0 Hz, 1H), 6.22 (d, *J* = 10.0 Hz, 1H), 6.11 (s, 1H), 2.08 (s, 3H), 1.35 (s, 3H).
- **<sup>13</sup>C NMR** (101 MHz, CDCl<sub>3</sub>) δ 186.66 (s), 161.50 (s), 151.92 (s), 129.66 (s), 128.12 (s), 80.46 (s), 22.43 (s), 18.12 (s).
- **HRMS** (ESI) *m/z* calc [C<sub>8</sub>H<sub>10</sub>O<sub>3</sub>Na]<sup>+</sup> [M + Na]<sup>+</sup>: 177.0522, found 177.0523.

#### 4a-Hydroperoxy-5,6,7,8-tetrahydronaphthalen-2(4aH)-one. (2h) <sup>[S4]</sup>



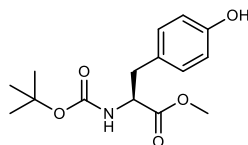
- The crude was purified with eluent (Cyclohexane/EtOAc) by autosampler Flash Chromatography after solvent removal.
- White solid
- **<sup>1</sup>H NMR** (400 MHz, CDCl<sub>3</sub>) δ 7.85 (s, 1H), 6.81 (d, *J* = 9.9 Hz, 1H), 6.31 (dd, *J* = 10.0, 2.0 Hz, 1H), 6.19 (t, *J* = 1.8 Hz, 1H), 2.70 – 2.59 (m, 1H), 2.42 (d, *J* = 12.9 Hz, 1H), 2.24 – 2.15 (m, 1H), 2.09 – 2.00 (m, 1H), 1.79 (tt, *J* = 13.7, 4.0 Hz, 1H), 1.62 (d, *J* = 13.7 Hz, 1H), 1.52 – 1.34 (m, 2H).
- **<sup>13</sup>C NMR** (101 MHz, CDCl<sub>3</sub>) δ 186.5, 161.4, 149.2, 131.1, 126.4, 79.8, 37.0, 32.4, 28.0, 20.6.
- **HRMS** (ESI, *m/z*): calc for C<sub>10</sub>H<sub>12</sub>O<sub>3</sub> [M+H]<sup>+</sup>: 181.0859, found: 181.0855.

#### 4-Hydroperoxy-2,4,6-trimethylcyclohexa-2,5-dien-1-one. (2i)



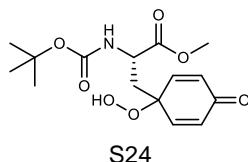
- The product was purified using flash chromatography column and eluted with a mixture of EtOAc/Cyclohexane (1:1)
- Off-white solid
- **<sup>1</sup>H NMR** (400 MHz, CDCl<sub>3</sub>) δ 8.28 (bs, 1H), 6.64 (s, 2H), 1.90 (s, 6H), 1.36 (s, 3H).
- **<sup>13</sup>C NMR** (101 MHz, CDCl<sub>3</sub>) δ 186.9, 144.6, 136.8, 78.7, 23.1, 16.1.
- **HRMS** (ESI, *m/z*) calc for C<sub>9</sub>H<sub>12</sub>O<sub>3</sub>Na [M + Na]<sup>+</sup>: 191.0679, found: 191.0683.

#### Methyl (tert-butoxycarbonyl)-L-tyrosinate.<sup>[S6]</sup> (1j)



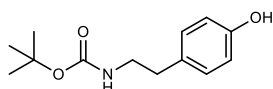
- The product was purified using flash chromatography column and eluted with a mixture of EtOAc/Cyclohexane (3:7)
- White solid
- **<sup>1</sup>H NMR** (400 MHz, CDCl<sub>3</sub>) δ 6.95 (d, *J* = 8.3 Hz, 2H), 6.72 (d, *J* = 8.3 Hz, 2H), 6.16 (s, 1H), 5.03 (d, *J* = 8.4 Hz), 4.53 (dt, *J* = 8.4, 6.0 Hz), 3.71 (s, 3H), 3.07 – 2.99 (dd, *J* = 14.0, 6.0 Hz, 1H), 2.99 – 2.91 (dd, *J* = 14.0, 6.0 Hz, 1H), 1.41 (s, 9H).
- **<sup>13</sup>C NMR** (101 MHz, CDCl<sub>3</sub>) δ 172.8, 155.5, 155.3, 130.5, 127.6, 115.6, 80.4, 54.7, 52.4, 37.7, 28.4.
- **HRMS** (ESI, *m/z*) calc for C<sub>15</sub>H<sub>21</sub>N<sub>1</sub>O<sub>5</sub>Na [M + Na]<sup>+</sup>: 318.1312, found: 318.1313.

#### Methyl (S)-2-((tert-butoxycarbonyl)amino)-3-(1-hydroperoxy-4-oxocyclohexa-2,5-dien-1-yl)propanoate. (2j)



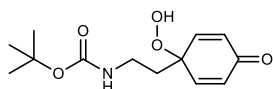
- The product was purified using flash chromatography column and eluted with a mixture of EtOAc/Cyclohexane (1:1)
- White solid
- **<sup>1</sup>H NMR** (400 MHz, CD<sub>3</sub>OD) δ 7.00 – 6.94 (m, 2H), 6.31 (d, *J* = 10.0 Hz, 1H), 6.22 (d, *J* = 10.0 Hz, 1H), 4.20 (dd, *J* = 10.2, 3.2 Hz, 1H), 3.70 (s, 3H), 2.34 (dd, *J* = 14.2, 3.2 Hz, 1H), 2.05 (dd, *J* = 14.2, 10.2 Hz, 1H), 1.41 (s, 9H).
- **<sup>13</sup>C NMR** (101 MHz, CD<sub>3</sub>OD) δ 187.4, 173.7, 157.4, 151.1, 150.2, 132.0, 130.7, 80.8, 80.6, 52.9, 50.9, 39.4, 28.7.
- **HRMS** (ESI, *m/z*) calc for C<sub>15</sub>H<sub>21</sub>N<sub>1</sub>O<sub>7</sub>Na [M + Na]<sup>+</sup>: 350.1210, found: 350.1210.

### tert-Butyl (4-hydroxyphenethyl)carbamate.<sup>[S7]</sup> (1k)



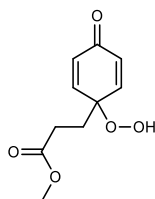
- The product was purified using flash chromatography column and eluting with a gradient of EtOAc/Cyclohexane (1:4 to 3:7)
- White solid
- **<sup>1</sup>H NMR** (400 MHz, CDCl<sub>3</sub>) δ 7.02 (d, *J* = 8.4 Hz, 2H), 6.81 (d, *J* = 8.4 Hz, 2H), 4.70 (bs, 1H), 3.35 (m, 2H), 2.72 (t, *J* = 6.9 Hz, 2H), 1.47 (s, 9H).
- **<sup>13</sup>C NMR** (101 MHz, CDCl<sub>3</sub>) δ 156.5, 155.0, 130.3, 129.9, 115.6, 79.8, 42.2, 35.4, 28.5.
- **HRMS** (ESI, *m/z*): calc for C<sub>13</sub>H<sub>20</sub>NO<sub>3</sub> [M + H]<sup>+</sup>: 238.1438, found: 238.1441.

### tert-Butyl (2-(1-hydroperoxy-4-oxocyclohexa-2,5-dien-1-yl)ethyl) carbamate. (2k)



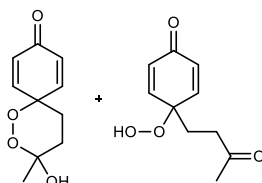
- The product was purified using flash chromatography column and eluted with a mixture of EtOAc/Cyclohexane (1:1)
- Colorless oil
- **<sup>1</sup>H NMR** (400 MHz, CDCl<sub>3</sub>) δ 10.10 (s, 1H), 6.94 (d, *J* = 10.2 Hz, 2H), 6.31 (d, *J* = 10.2 Hz, 2H), 4.83 (bs, 1H), 3.20 – 3.15 (m, 2H), 1.96 – 1.92 (m, 2H), 1.40 (s, 9H).
- **<sup>13</sup>C NMR** (101 MHz, CDCl<sub>3</sub>) δ 185.6, 156.3, 148.1, 131.0, 80.3, 80.1, 36.7, 35.6, 28.5.
- **HRMS** (ESI, *m/z*) calc for C<sub>13</sub>H<sub>19</sub>N<sub>1</sub>O<sub>5</sub>Na [M + Na]<sup>+</sup>: 292.1155, found: 292.1152.

### Methyl 3-(1-hydroperoxy-4-oxocyclohexa-2,5-dien-1-yl)propanoate. (2l)



- The product was purified using flash chromatography column and eluting with a gradient of EtOAc/Cyclohexane (3:7 to 7:3)
- Off-white solid
- **<sup>1</sup>H NMR** (400 MHz, CDCl<sub>3</sub>): δ 9.37 (s, 1H), 6.88 (d, *J* = 10.2 Hz, 2H), 6.32 (d, *J* = 10.2 Hz, 2H, O=CCH), 3.65 (s, 3H), 2.33 (t, *J* = 7.7 Hz, 2H), 2.08 (t, *J* = 7.7 Hz, 2H).
- **<sup>13</sup>C NMR** (101 MHz, CDCl<sub>3</sub>): δ 185.7, 173.4, 148.2, 131.3, 80.6, 52.2, 30.7, 28.4.
- **HRMS** (ESI) *m/z* calc for [C<sub>10</sub>H<sub>13</sub>O<sub>5</sub>]<sup>+</sup> ([M + H]<sup>+</sup>): 213.0757, found 213.0763.

### 3-Hydroxy-3-methyl-1,2-dioxaspiro[5.5]undeca-7,10-dien-9-one / 4-Hydroperoxy-4-(3-oxobutyl)cyclohexa-2,5-dien-1-one. (2m)



- The product was purified using flash chromatography column, with a mixture of EtOAc/Cyclohexane (3:7 to 7:3)
- Yellow oil

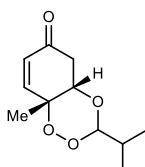
#### Spirocycle

- **<sup>1</sup>H NMR** (400 MHz, CDCl<sub>3</sub>): δ 7.40 (dd, *J* = 10.5, 3.1 Hz, 1H), 6.79 (dd, *J* = 10.3, 3.1 Hz, 1H), 6.27 (dd, *J* = 10.5, 1.8 Hz, 1H), 6.25 (dd, *J* = 10.3, 1.8 Hz, 1H), 4.21 (s, 1H), 2.24 – 2.14 (m, 1H), 1.96 – 1.91 (m, 2H), 1.65 – 1.59 (m, 1H), 1.44 (s, 3H).
- **<sup>13</sup>C NMR** (101 MHz, CDCl<sub>3</sub>): δ 185.5, 146.3, 145.6, 130.5, 128.6, 99.9, 75.4, 29.7, 28.9, 25.2.
- **HRMS** (ESI) *m/z* calc for [C<sub>10</sub>H<sub>12</sub>O<sub>4</sub>Na]<sup>+</sup> ([M + Na]<sup>+</sup>): 219.0628, found 219.0622.

#### Peroxide

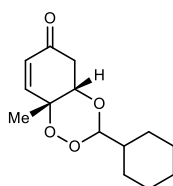
- **<sup>1</sup>H NMR** (400 MHz, CDCl<sub>3</sub>): δ 9.98 (s, 1H), 6.85 (d, *J* = 10.3 Hz, 2H), 6.30 (d, *J* = 10.3 Hz, 2H), 2.40 (t, *J* = 7.5 Hz, 2H), 2.09 (s, 3H), 1.98 (t, *J* = 7.5 Hz, 2H).
- **<sup>13</sup>C NMR** (101 MHz, CDCl<sub>3</sub>): δ 207.5, 185.7, 149.0, 131.0, 80.7, 37.3, 30.1, 29.1.
- **HRMS** (ESI) *m/z* calc for [C<sub>10</sub>H<sub>12</sub>O<sub>4</sub>Na]<sup>+</sup> ([M + Na]<sup>+</sup>): 219.0628, found 219.0622.

### 3-Isopropyl-8a-methyl-4a,8a-dihydrobenzo[e][1,2,4]trioxin-6(5H)-one. (5) <sup>[S4]</sup>



- The product was purified using flash chromatography column and eluted with a mixture of EtOAc/Cyclohexane (1:4)
- White solid
- **<sup>1</sup>H NMR** (400 MHz, CDCl<sub>3</sub>) δ= 6.84 (dd, *J* = 10.4, 2.8 Hz, 1H), 6.06 (dd, *J* = 10.4, 0.8 Hz, 1H), 5.00 (d, *J* = 5.1 Hz, 1H), 4.15 (q, *J* = 2.9 Hz, 1H), 2.78 – 2.64 (m, 2H), 1.76 (pd, *J* = 6.9, 5.0 Hz, 1H), 1.33 (s, 3H), 0.88 (d, *J* = 6.9 Hz, 6H).
- **<sup>13</sup>C NMR** (101 MHz, CDCl<sub>3</sub>) δ = 195.3, 151.2, 129.7, 107.2, 77.9, 76.5, 41.1, 31.0, 20.7, 16.7 (2×C).
- **HRMS** (ESI *m/z*): calc for C<sub>11</sub>H<sub>16</sub>O<sub>4</sub> [M+Na]<sup>+</sup>: 235.0941, found: 235.0934.

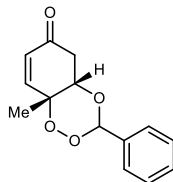
### 3-Cyclohexyl-8a-methyl-4a,8a-dihydrobenzo[e][1,2,4]trioxin-6(5H)-one. (6) <sup>[S4]</sup>



- The product was purified using flash chromatography column and eluted with a mixture of EtOAc/Cyclohexane (1:4)
- White solid
- **<sup>1</sup>H NMR** (400 MHz, CDCl<sub>3</sub>) δ 6.84 (dd, *J* = 10.4, 2.8 Hz, 1H), 6.07 (dd, *J* = 10.3, 0.9 Hz, 1H), 5.02 (d, *J* = 5.4 Hz, 1H), 4.14 (q, *J* = 3.0 Hz, 1H), 2.70 (t, *J* = 2.9 Hz, 2H), 1.74 – 1.58 (m, 6H), 1.33 (s, 3H), 1.22 – 0.98 (m, 5H).
- **<sup>13</sup>C NMR** (101 MHz, CDCl<sub>3</sub>) δ 195.3, 151.3, 129.7, 106.7, 78.0, 76.5, 41.2, 40.5, 27.1, 26.3, 25.8 (2×C), 20.7.

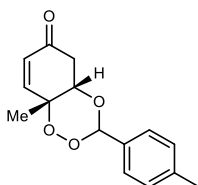
- **HRMS** (ESI  $m/z$ ): calc for  $C_{14}H_{20}O_4$   $[M+Na]^+$ : 275.1254, found: 275.1254.

**8a-Methyl-3-phenyl-4a, 8a-dihydrobenzo[e][1,2,4]trioxin-6(5H)-one. (7)**



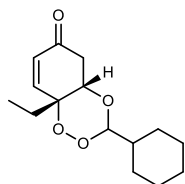
- The product was purified using flash chromatography column and eluted with a mixture of EtOAc/Cyclohexane (1:4)
- White solid
- **$^1H$  NMR** (400 MHz,  $CDCl_3$ )  $\delta$  = 7.43 – 7.33 (m, 5H), 6.95 (dd,  $J$  = 10.4, 2.8 Hz, 1H), 6.22 (s, 1H), 6.17 (dd,  $J$  = 10.4, 1.0 Hz, 1H), 4.41 (q,  $J$  = 2.9 Hz, 1H), 2.86 (ddd,  $J$  = 17.5, 3.0, 1.1 Hz, 1H), 2.79 (dd,  $J$  = 17.5, 3.0 Hz, 1H), 1.44 (s, 3H).
- **$^{13}C$  NMR** (101 MHz,  $CDCl_3$ )  $\delta$  = 195.0, 151.2, 133.6, 130.4, 129.9, 128.6 (2 $\times$ C), 127.3 (2 $\times$ C), 103.8, 78.1, 77.1, 41.2, 20.8.
- **HRMS** (ESI,  $m/z$ ): calc for  $C_{14}H_{14}O_4$   $[M+Na]^+$ : 269.0784, found: 269.0783.

**8a-Methyl-3-(*p*-tolyl)-4a,8a-dihydrobenzo[e][1,2,4]trioxin-6(5H)-one. (8)**



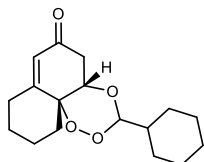
- The product was purified using flash chromatography column and eluted with a mixture of EtOAc/Cyclohexane (1:4)
- White solid
- **$^1H$  NMR** (400 MHz,  $CDCl_3$ )  $\delta$  7.29 (d,  $J$  = 8.2 Hz, 2H), 7.16 (d,  $J$  = 7.9 Hz, 2H), 6.94 (dd,  $J$  = 10.3, 2.8 Hz, 1H), 6.18 (s, 1H), 6.16 (d,  $J$  = 10.3 Hz 1H), 4.39 (q,  $J$  = 2.9 Hz, 1H), 2.88 – 2.75 (m, 2H), 2.34 (s, 3H), 1.43 (s, 3H).
- **$^{13}C$  NMR** (101 MHz,  $CDCl_3$ )  $\delta$  = 195.0, 151.3, 140.5, 130.8, 129.9, 129.3 (2 $\times$ C), 127.2 (2 $\times$ C), 103.8, 80.0, 77.1, 41.2, 21.5, 20.8.
- **HRMS** (ESI,  $m/z$ ): calc for  $C_{15}H_{16}O_4$ ,  $[M+Na]^+$ : 283.0941, found: 283.0942.

### 3-Cyclohexyl-8a-ethyl-4a,8a-dihydrobenzo[e][1,2,4]trioxin-6(5H)-one. (9)



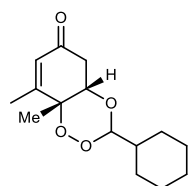
- The crude was purified with eluent (Cyclohexane/EtOAc) by autosampler Flash Chromatography after solvent removal.
- Off-white solid
- **<sup>1</sup>H NMR** (400 MHz, CDCl<sub>3</sub>) δ 6.90 (dd, *J* = 10.4, 2.7 Hz, 1H), 6.10 (d, *J* = 10.5 Hz, 1H), 4.99 (d, *J* = 5.5 Hz, 1H), 4.18 (q, *J* = 2.9 Hz, 1H), 2.68 (d, *J* = 3.0 Hz, 2H), 1.79 (dt, *J* = 15.2, 7.5 Hz, 1H), 1.74 – 1.57 (m, 7H), 1.49 (tdt, *J* = 11.6, 6.0, 3.1 Hz, 1H), 1.17 – 1.04 (m, 3H), 1.00 (t, *J* = 7.6 Hz, 3H).
- **<sup>13</sup>C NMR** (101 MHz, CDCl<sub>3</sub>) δ 195.5, 150.9, 130.0, 106.6, 80.0, 75.3, 41, 40.5, 28.8 (2×C), 27.0 (2×C), 26.3, 25.7, 7.3.
- **HRMS** (ESI, *m/z*): calc for C<sub>15</sub>H<sub>22</sub>O<sub>4</sub> [M+H]<sup>+</sup>: 267.1596, found: 267.1574.

### 3-Cyclohexyl-4a,5,8,9,10,11-hexahydro-6H-naphtho[1,8a-e][1,2,4]trioxin-6-one. (10)



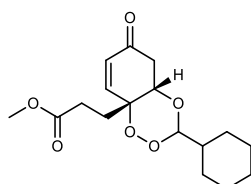
- The crude was purified with eluent (Cyclohexane/EtOAc) by autosampler Flash Chromatography after solvent removal
- Yellow oil
- **<sup>1</sup>H NMR** (400 MHz, CDCl<sub>3</sub>) δ 5.99 (t, *J* = 1.3 Hz, 1H), 5.02 (d, *J* = 5.5 Hz, 1H), 4.04 (t, *J* = 3.0 Hz, 1H), 2.83 – 2.70 (m, 1H), 2.73 – 2.58 (m, 2H), 2.29 (dt, *J* = 12.1, 3.6 Hz, 1H), 2.12 – 2.03 (m, 1H), 1.98 – 1.90 (m, 1H), 1.71 – 1.65 (m, 4H), 1.42 (s, 9H), 1.32 – 1.22 (m, 2H).
- **<sup>13</sup>C NMR** (101 MHz, CDCl<sub>3</sub>) δ 195.8, 163.6, 125.1, 106.2, 79.2, 75.5, 42.1, 40.5, 34.7, 32.2, 29.7, 29.0, 27.1, 27.0, 26.3, 25.7, 20.2.
- **HRMS** (ESI, *m/z*): calc for C<sub>17</sub>H<sub>24</sub>O<sub>4</sub> [M+H]<sup>+</sup>: 293.1747, found: 293.1749.

### 3-Cyclohexyl-8,8a-dimethyl-4a,8a-dihydrobenzo[e][1,2,4]trioxin-6(5H)-one. (11)



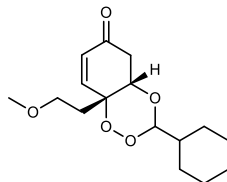
- The product was purified using flash chromatography column and eluted with a mixture of EtOAc/Cyclohexane (3:7)
- Yellow oil
- **<sup>1</sup>H NMR** (400 MHz, CDCl<sub>3</sub>): δ 5.92 (s, 1H), 4.99 (d, *J* = 5.3 Hz, 1H), 4.08 (t, *J* = 2.9 Hz, 1H), 2.66 (d, *J* = 2.9 Hz, 2H), 2.01 (s, 3H), 1.62 (m, , 5H), 1.46 (m, 1H), 1.28 (s, 3H), 1.05 (m, 5H).
- **<sup>13</sup>C NMR** (101 MHz, CDCl<sub>3</sub>): δ 194.8, 161.3, 127.7, 106.5, 79.7, 77.0, 41.1, 40.3, 26.9, 26.2, 25.6, 20.0, 18.3.
- **HRMS** (ESI) *m/z* calc for [C<sub>15</sub>H<sub>22</sub>O<sub>4</sub>Na]<sup>+</sup> ([M + Na]<sup>+</sup>): 289.1410, found 289.1423.

### Methyl 3-(3-cyclohexyl-6-oxo-5,6-dihydrobenzo[e][1,2,4]trioxin-8a(4aH)-yl)propanoate (12)



- The product was purified using flash chromatography column and eluted with a mixture of EtOAc/Cyclohexane (1:20)
- Yellow oil
- **<sup>1</sup>H NMR** (400 MHz, CDCl<sub>3</sub>): δ 6.84 (dd, *J* = 10.5, 2.9 Hz, 1H), 6.12 (dd, *J* = 10.5, 0.9 Hz, 1H), 4.99 (d, *J* = 5.4 Hz, 1H), 4.16 (q, *J* = 2.9 Hz, 1H), 3.68 (s, 3H), 2.76 (dd, *J* = 17.7, 2.9 Hz, 1H), 2.70 (ddd, *J* = 17.7, 2.9, 0.9 Hz, 1H), 2.54 (ddd, *J* = 16.4, 9.9, 6.2 Hz, 1H), 2.42 (ddd, *J* = 16.4, 10.0, 6.0 Hz, 1H), 2.10 (ddd, *J* = 14.8, 9.9, 6.0 Hz, 1H), 2.01 (ddd, *J* = 14.8, 10.0, 6.2 Hz, 1H), 1.74 – 1.56 (m, 5H), 1.49 (tdt, *J* = 11.5, 5.4, 3.2 Hz, 1H), 1.27 – 0.97 (m, 5H).
- **<sup>13</sup>C NMR** (101 MHz, CDCl<sub>3</sub>): δ 195.0, 172.9, 149.4, 130.7, 106.7, 79.0, 75.3, 52.1, 40.9, 40.4, 30.5, 27.3, 27.0, 26.3, 25.7.
- **HRMS** (ESI) *m/z* calc for [C<sub>17</sub>H<sub>24</sub>O<sub>6</sub>Na]<sup>+</sup> ([M + Na]<sup>+</sup>): 347.1465, found 347.1467.

**3-Cyclohexyl-8a-(2-methoxyethyl)-4a,8a-dihydrobenzo[e][1,2,4]trioxin-6(5H)-one. (13)**

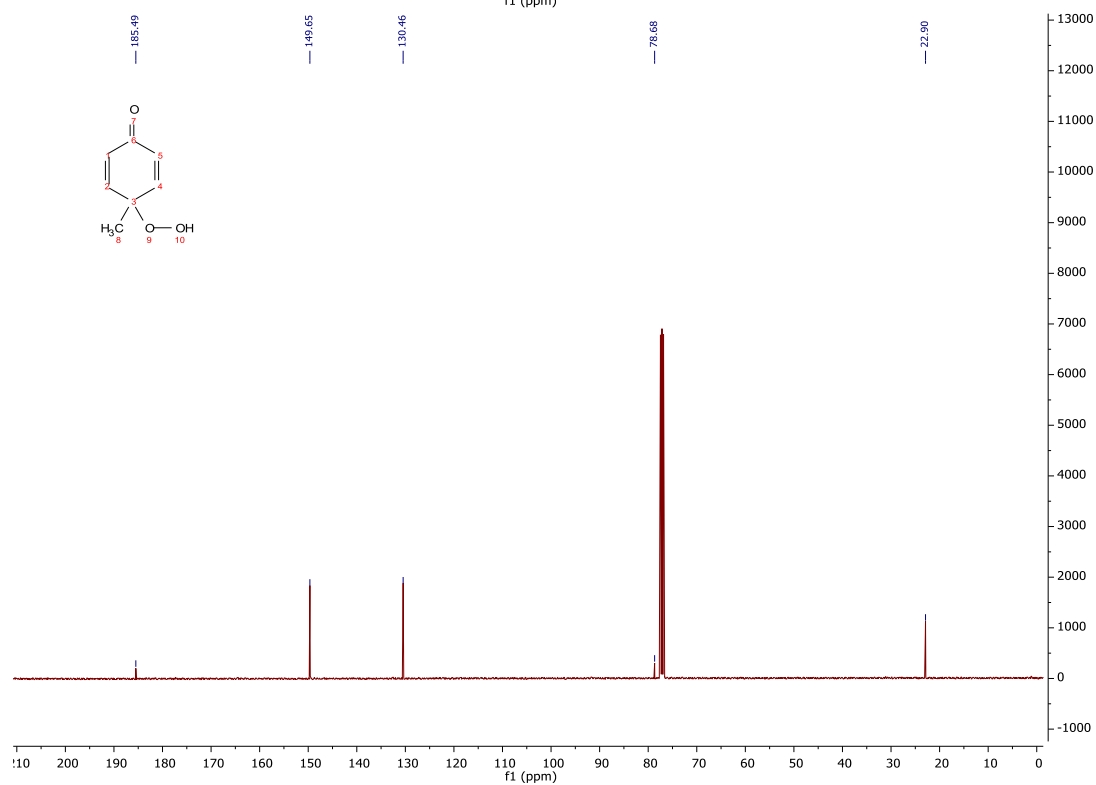
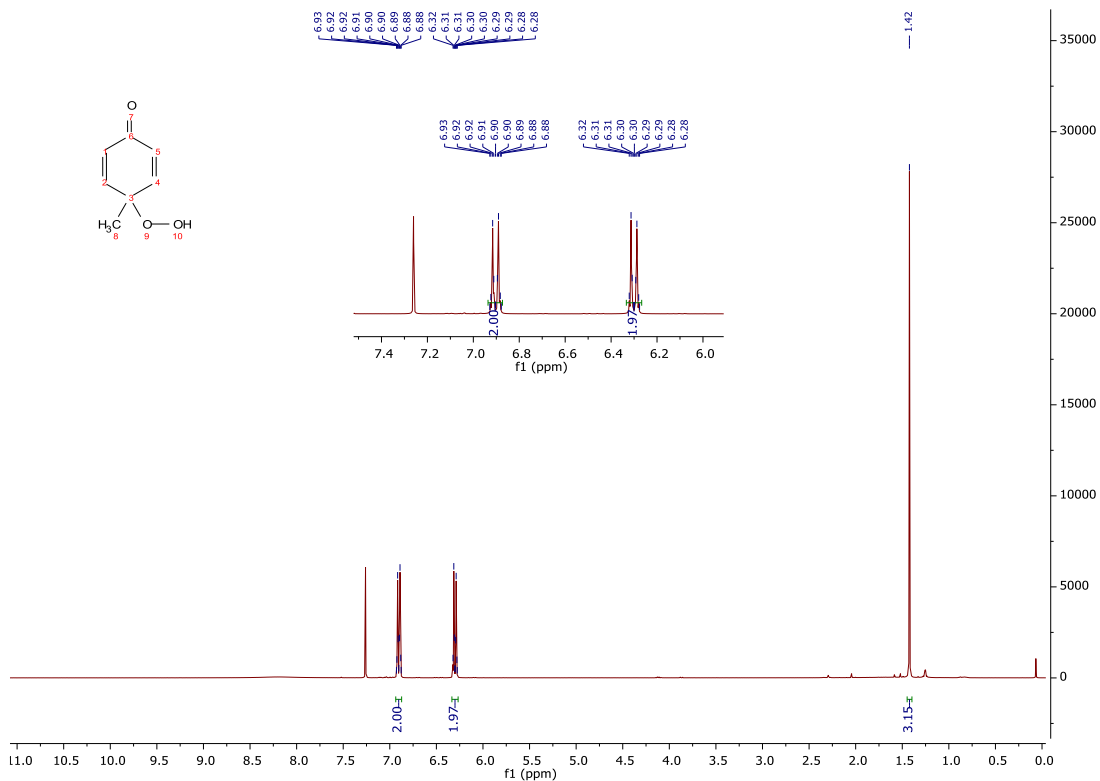


- The product was purified using flash chromatography column and eluted with a mixture of EtOAc/Cyclohexane (1:20)
- Yellow oil
- **<sup>1</sup>H NMR** (400 MHz, CDCl<sub>3</sub>) δ 6.85 (dd, *J* = 10.4, 2.8 Hz, 1H), 6.07 (dd, *J* = 10.4, 1.2 Hz, 1H), 4.99 (d, *J* = 5.4 Hz, 1H), 4.26 (q, *J* = 3.0 Hz, 1H), 3.58 – 3.40 (m, 2H), 3.29 (s, 3H), 2.76 (dd, *J* = 17.6, 3.0 Hz, 1H), 2.66 (ddd, *J* = 17.6, 3.0, 1.2 Hz, 1H), 2.05 – 1.84 (m, 2H), 1.78 – 1.56 (m, 5H, Ar), 1.52 – 1.43 (m, 1H, Ar), 1.24 – 0.97 (m, 5H, Ar).
- **<sup>13</sup>C NMR** (101 MHz, CDCl<sub>3</sub>): δ 195.6, 150.5, 129.8, 106.6, 79.4, 75.3, 66.5, 58.7, 40.9, 40.4, 35.7, 27.0, 26.2, 25.7.

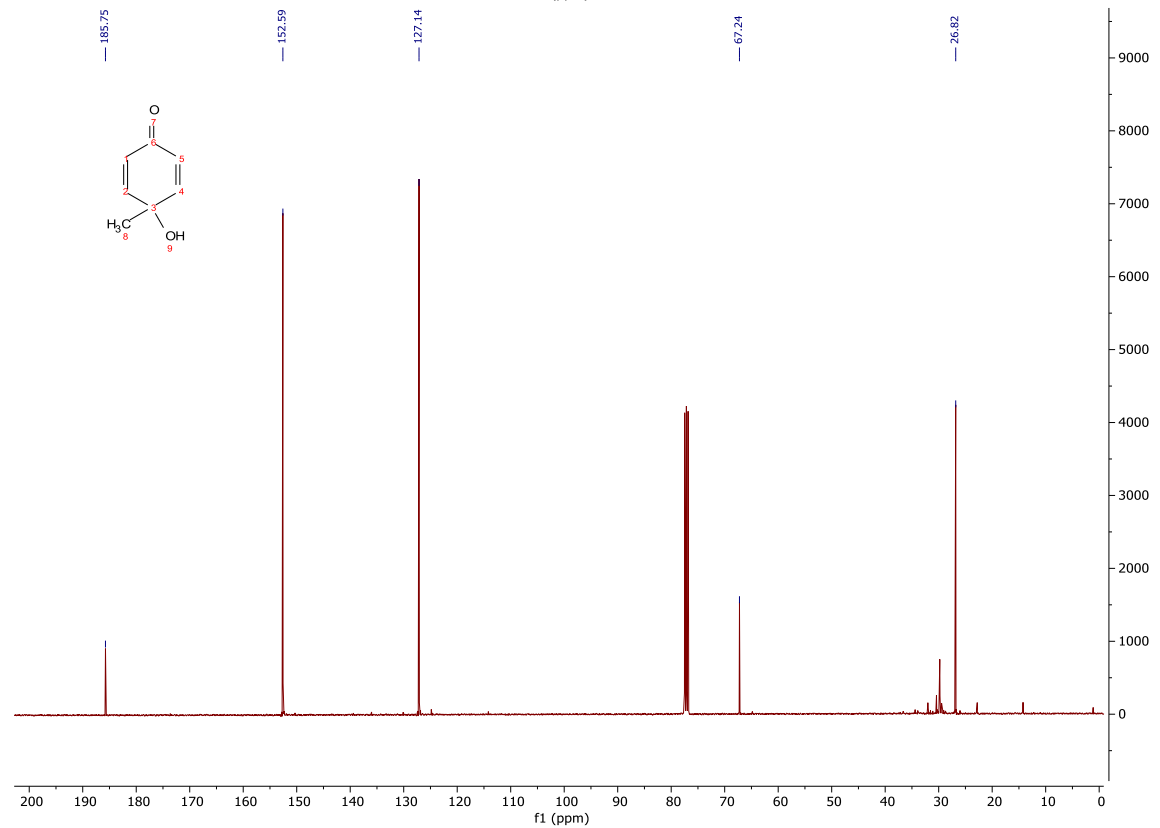
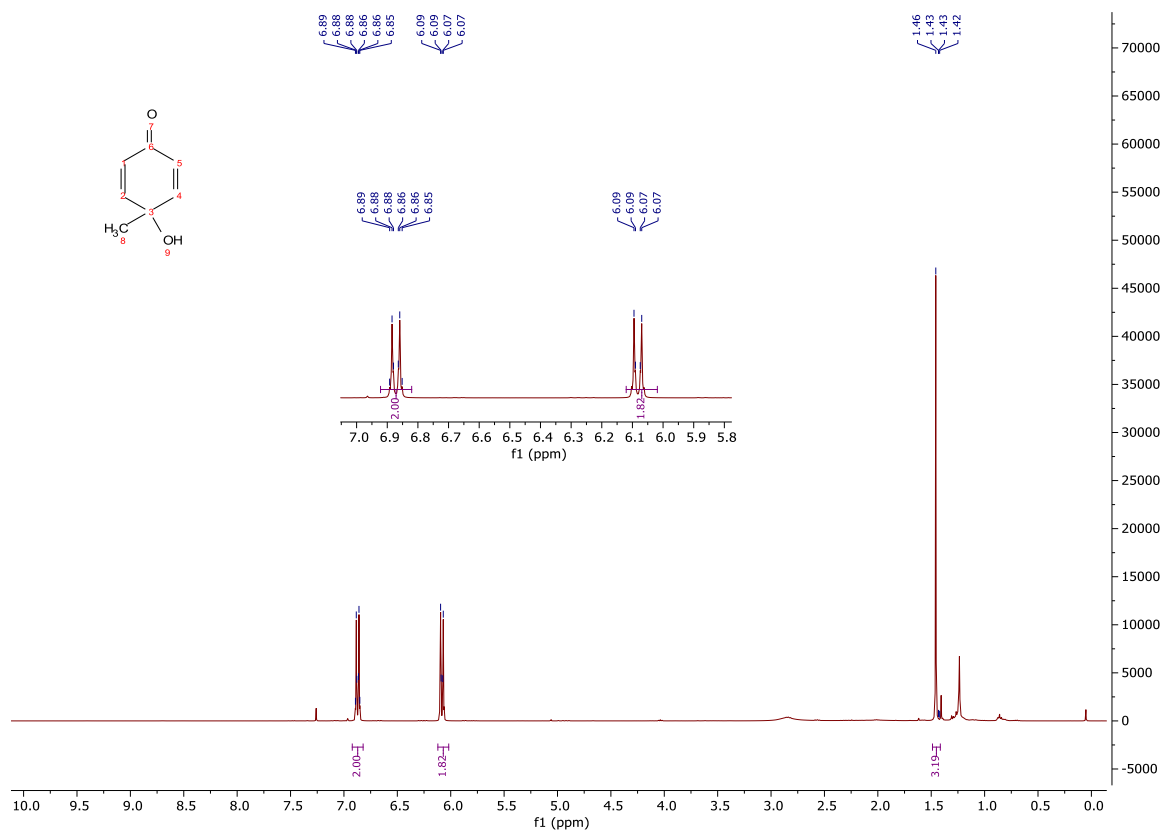
**HRMS** (ESI) *m/z* calc for [C<sub>16</sub>H<sub>28</sub>N<sub>1</sub>O<sub>5</sub>]<sup>+</sup> ([M + NH<sub>4</sub>]<sup>+</sup>): 314.1962, found 314.1966.

# NMR Spectra

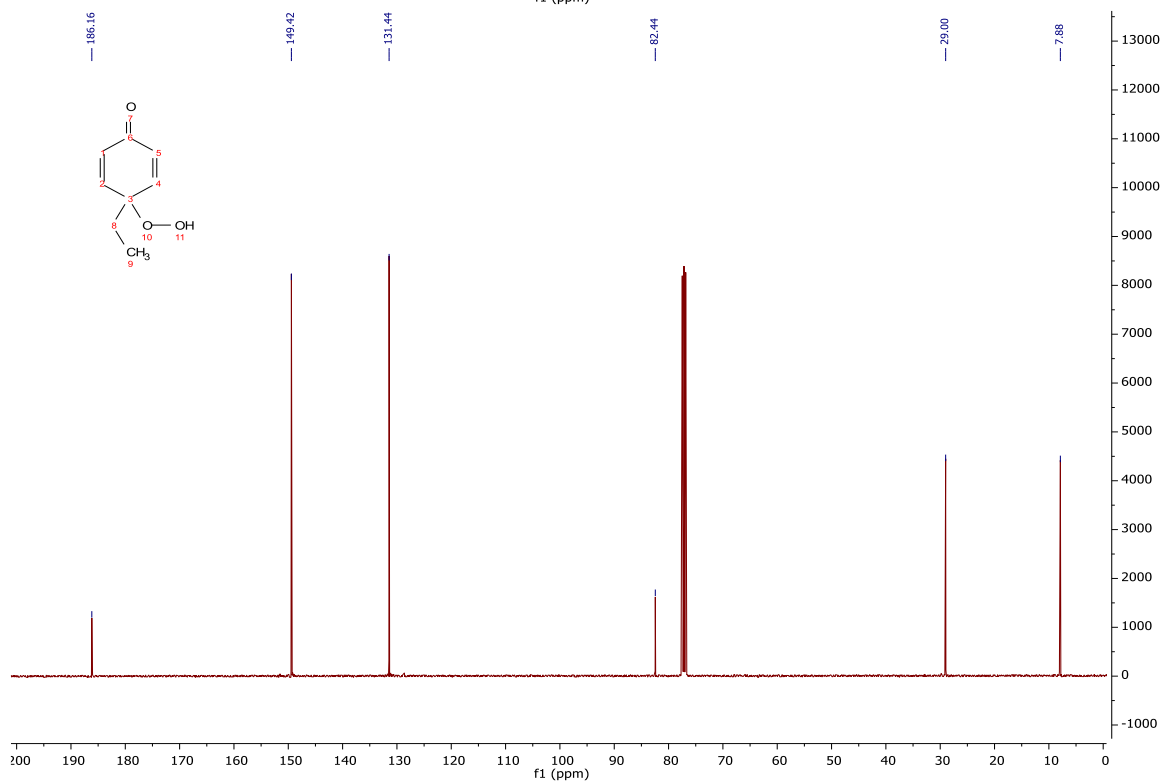
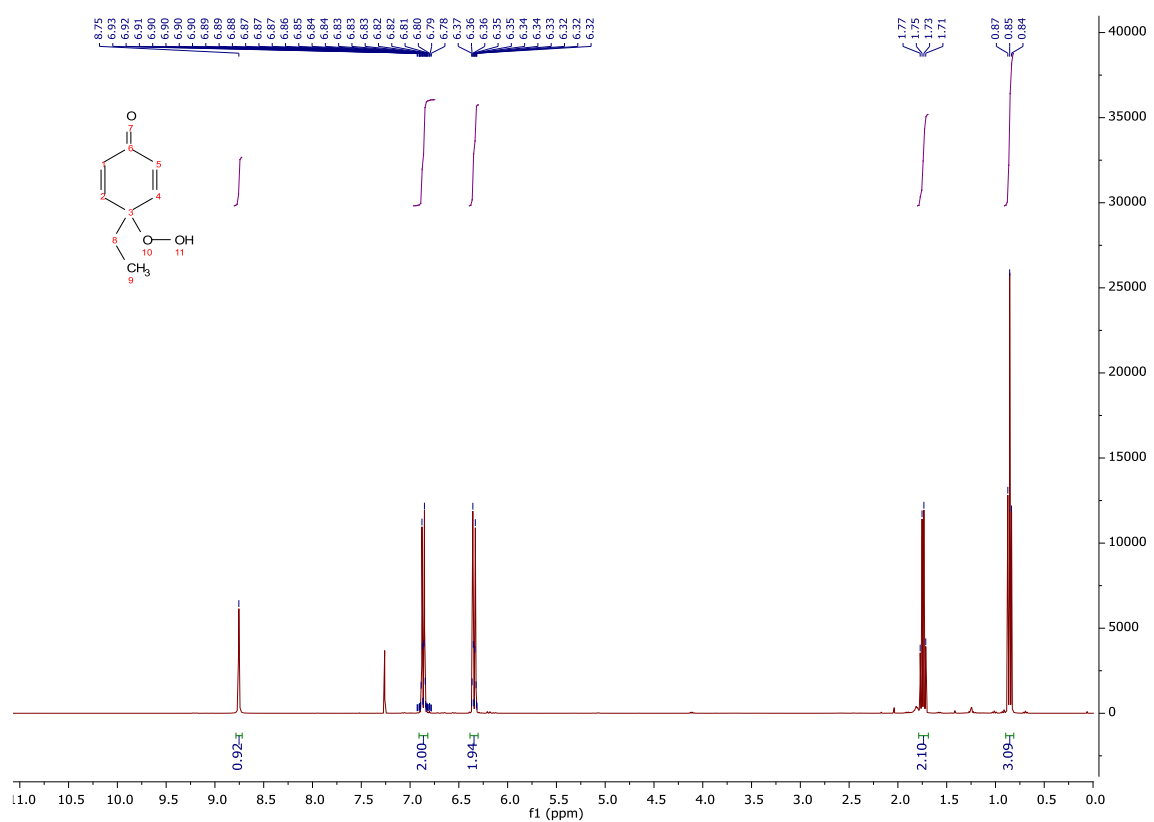
## 4-Hydroperoxy-4-methylcyclohexa-2,5-dien-1-one. (2a)



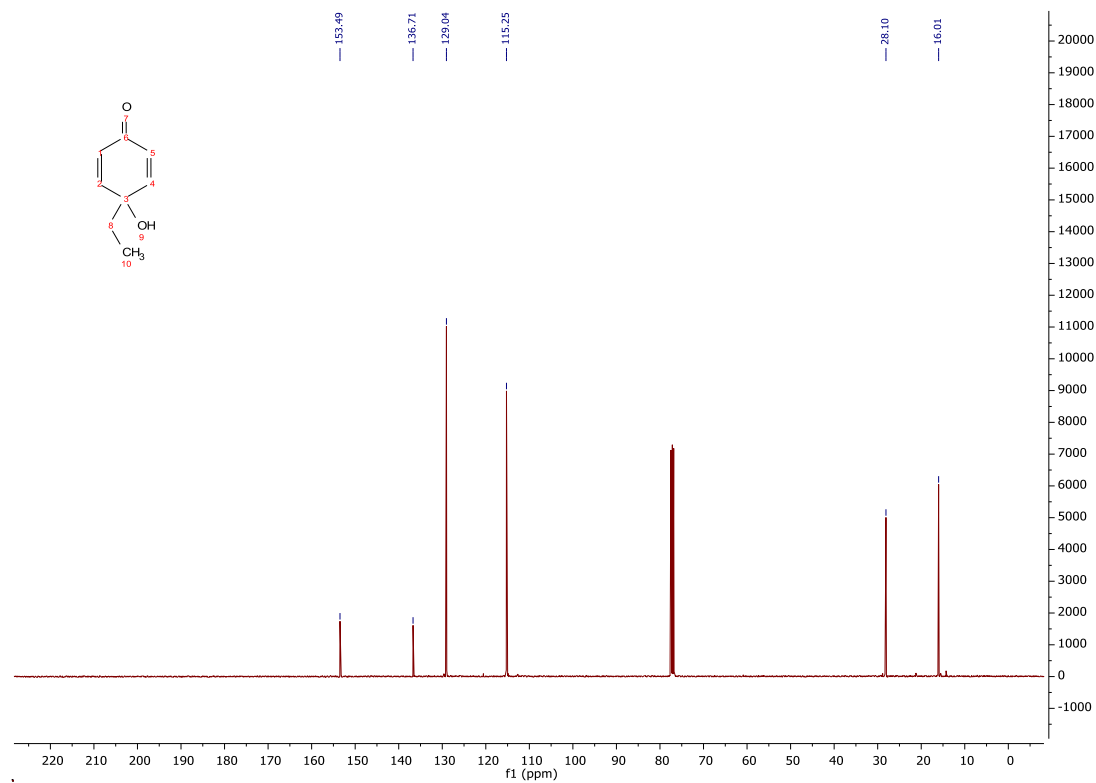
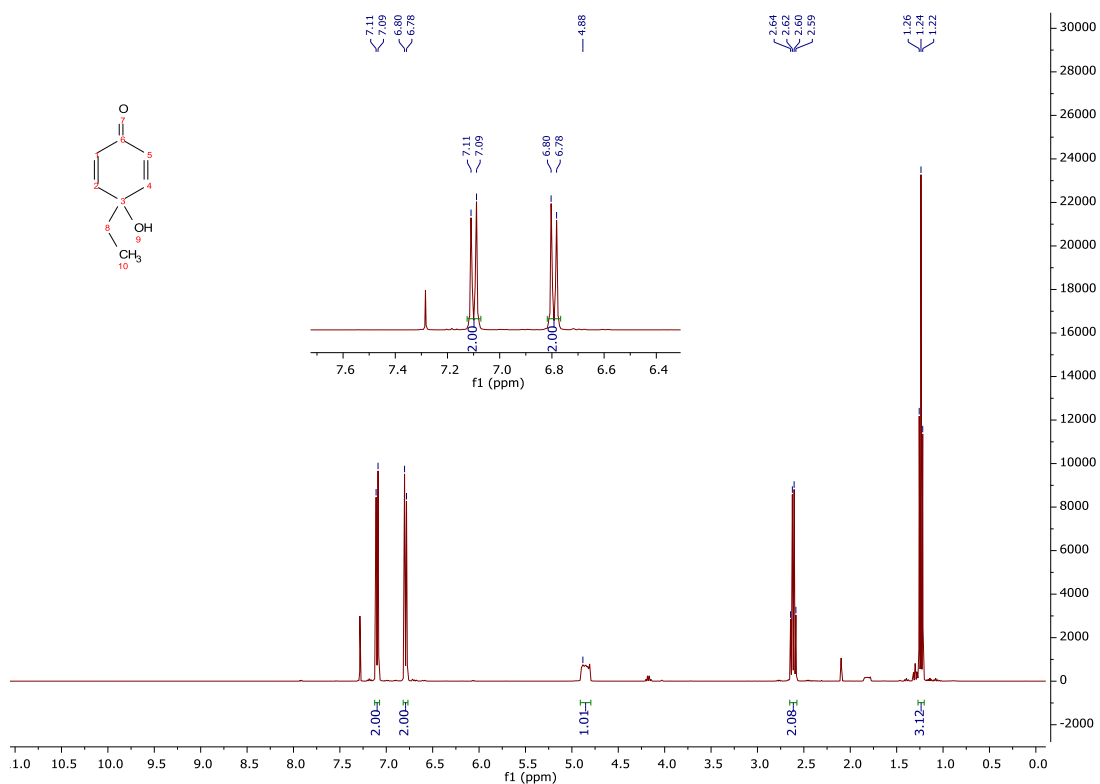
# 4-Hydroxy-4-methylcyclohexa-2,5-dien-1-one. (3a)



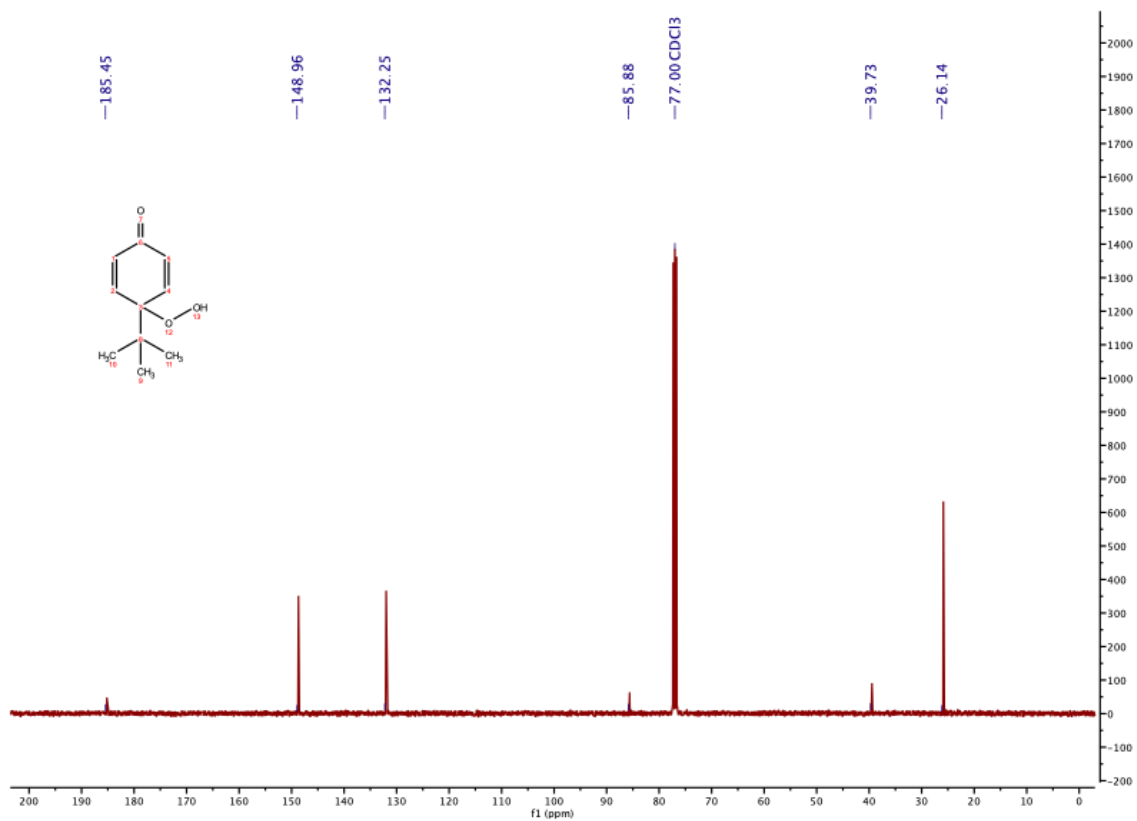
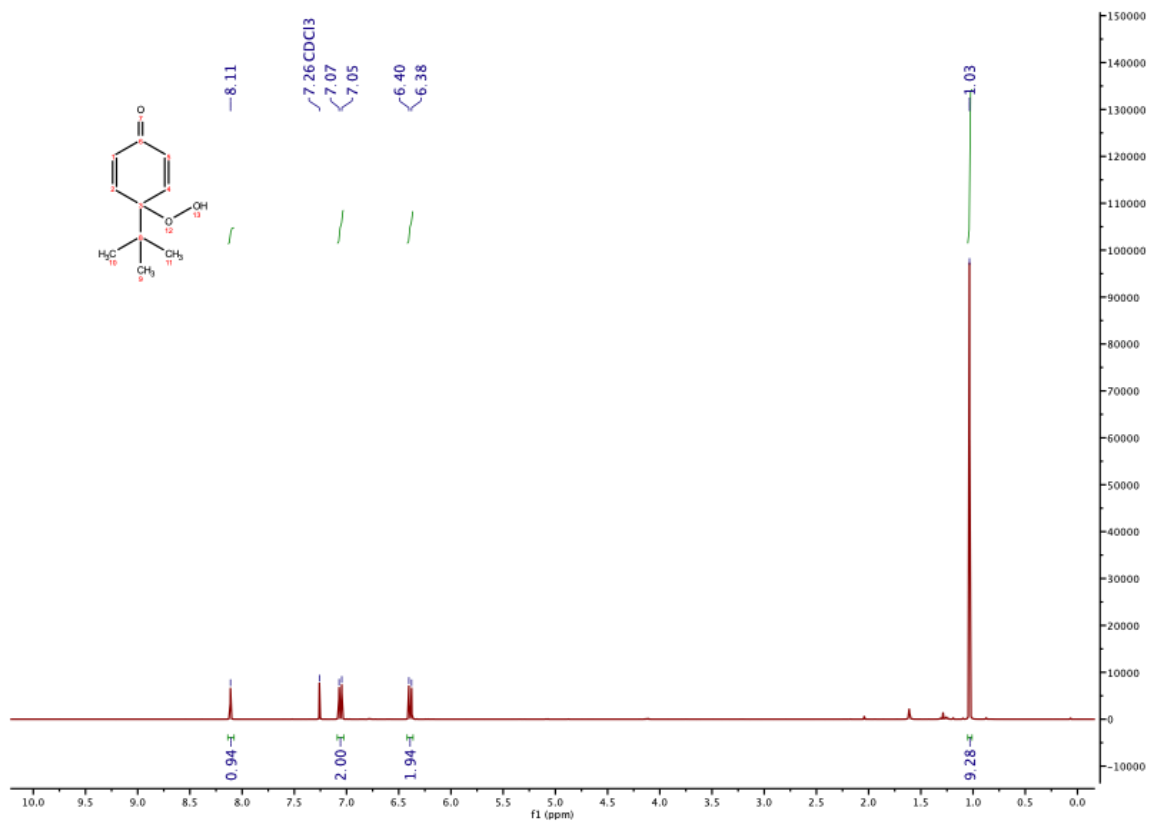
# 4-Ethyl-4-hydroperoxycyclohexa-2,5-dien-1-one. (2b)



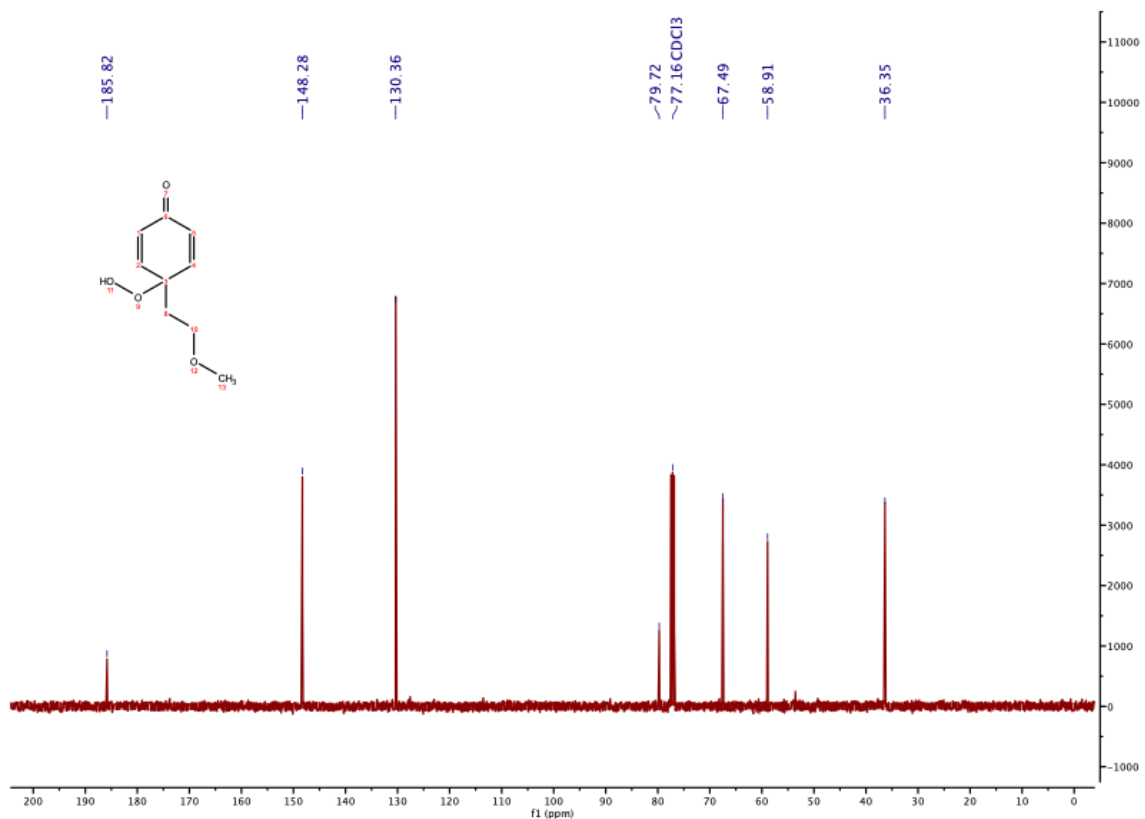
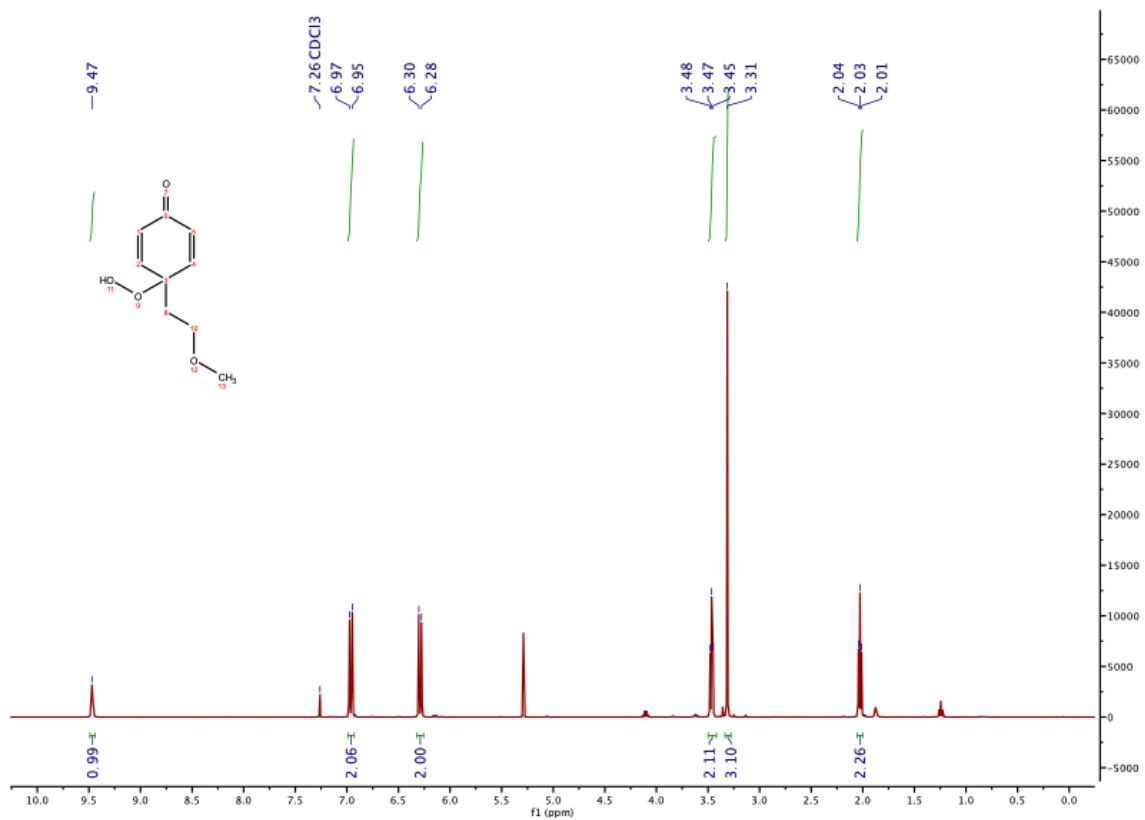
# 4-Ethyl-4-hydroxycyclohexa-2,5-dien-1-one (3b)



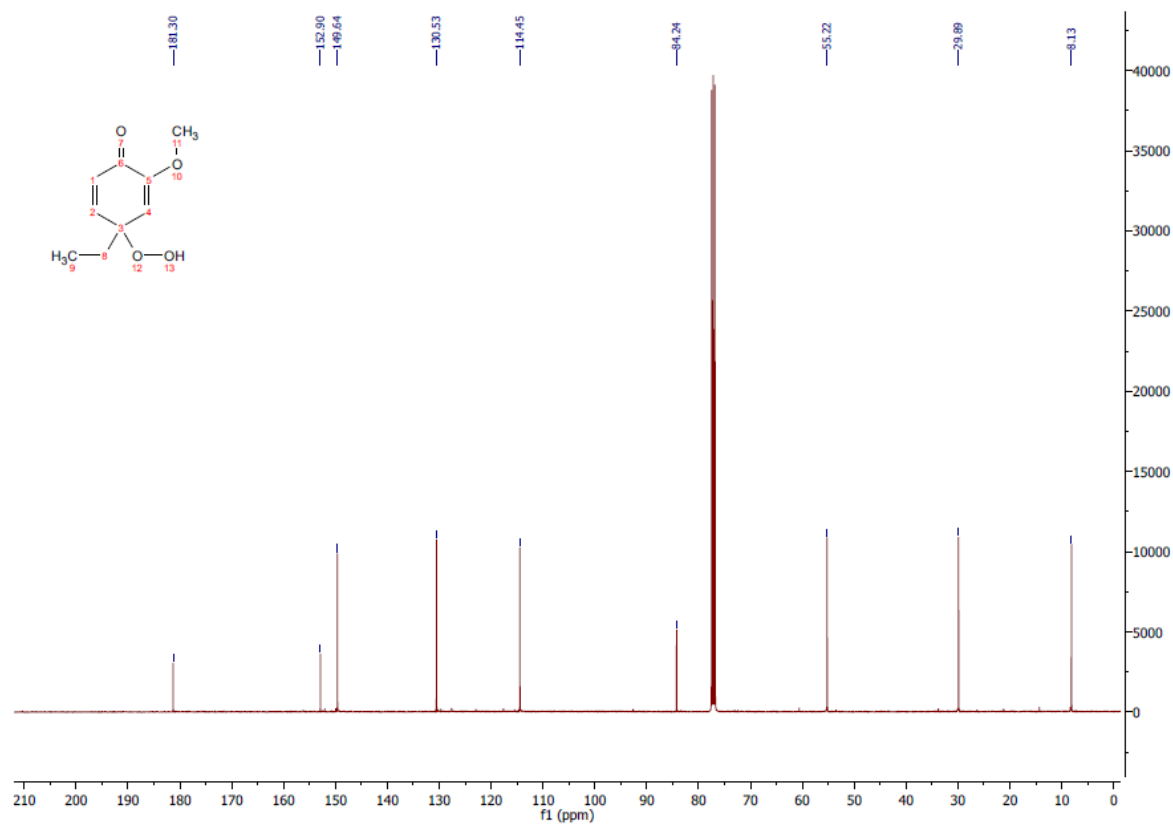
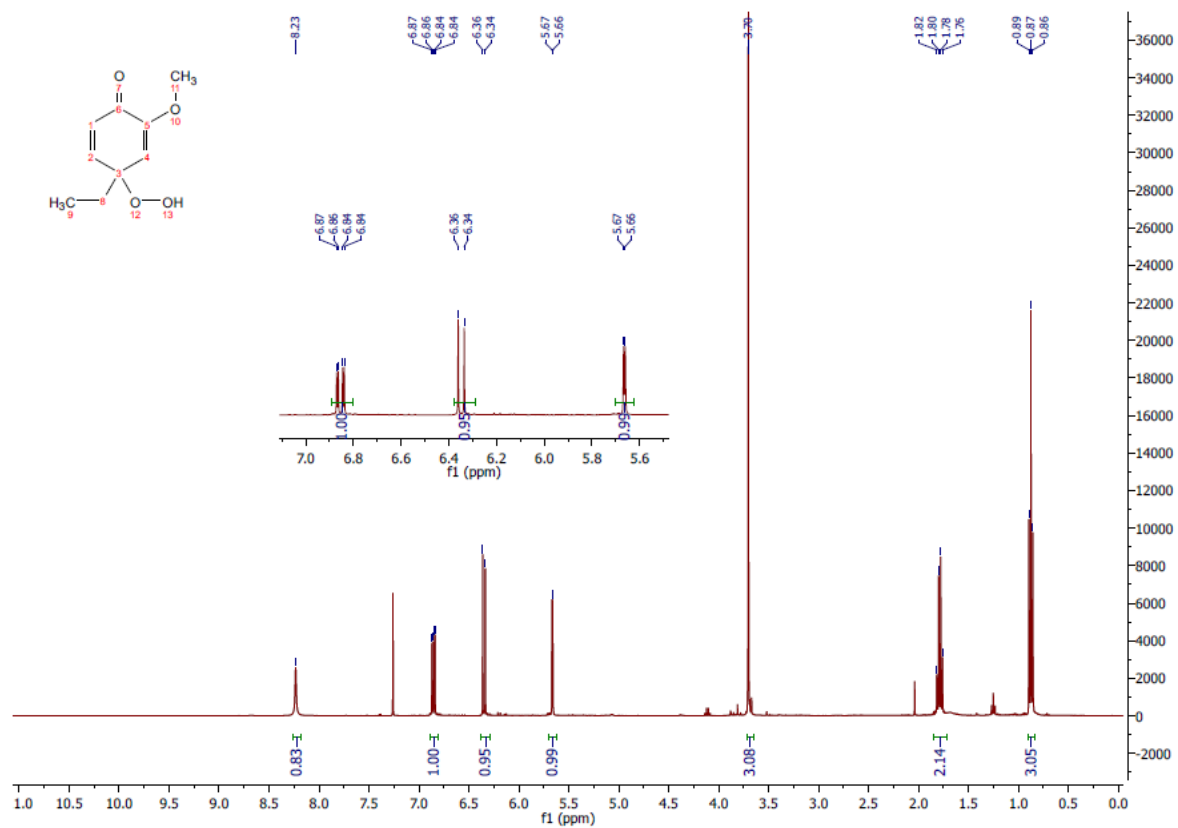
# 4-(*tert*-Butyl)-4-hydroperoxycyclohexa-2,5-dien-1-one. (2c)



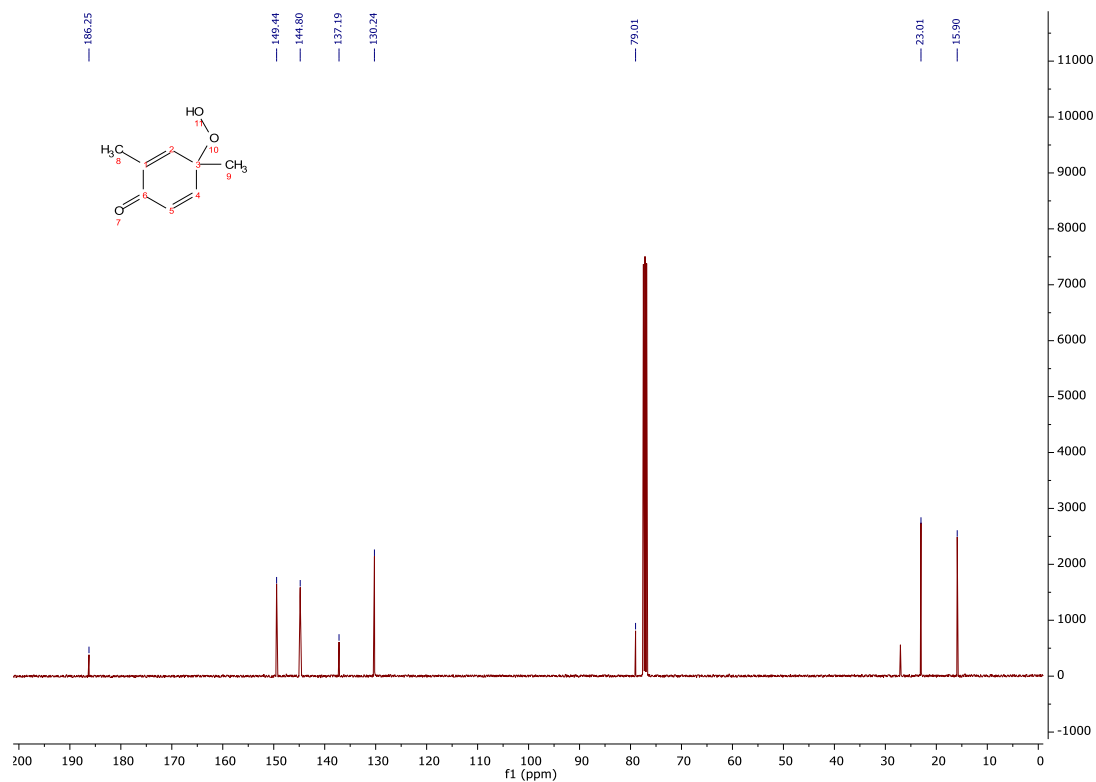
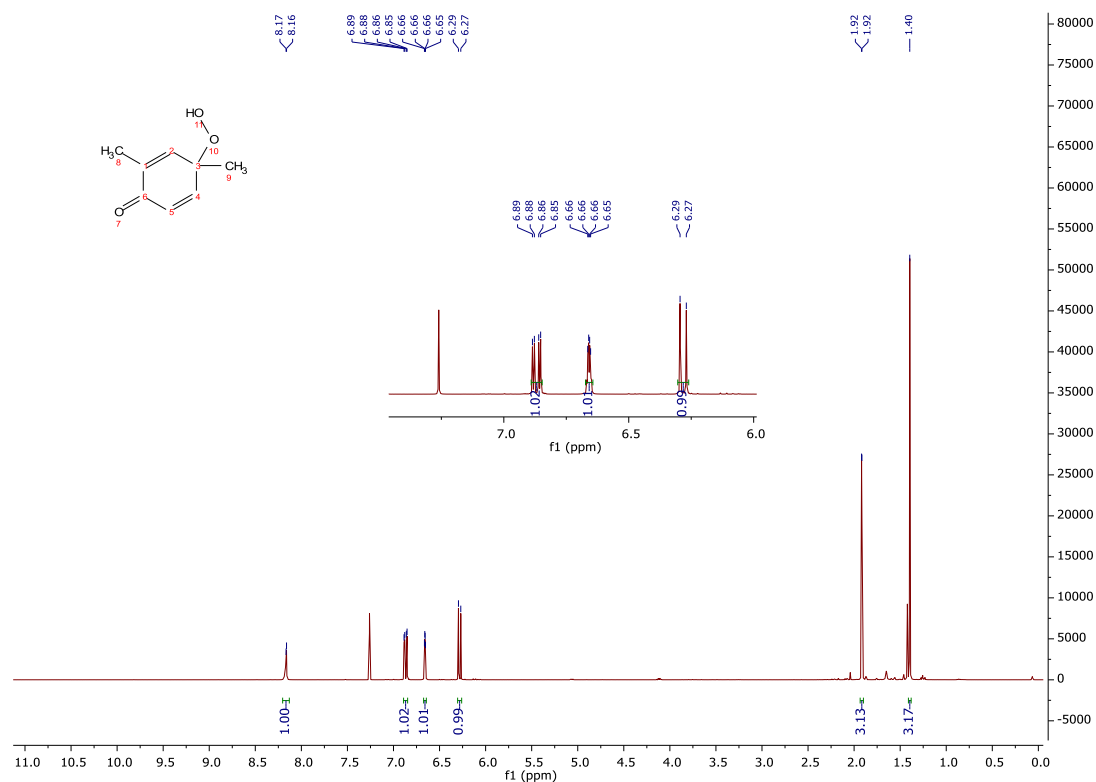
# 4-Hydroperoxy-4-(2-methoxyethyl)cyclohexa-2,5-dien-1-one. (2d)



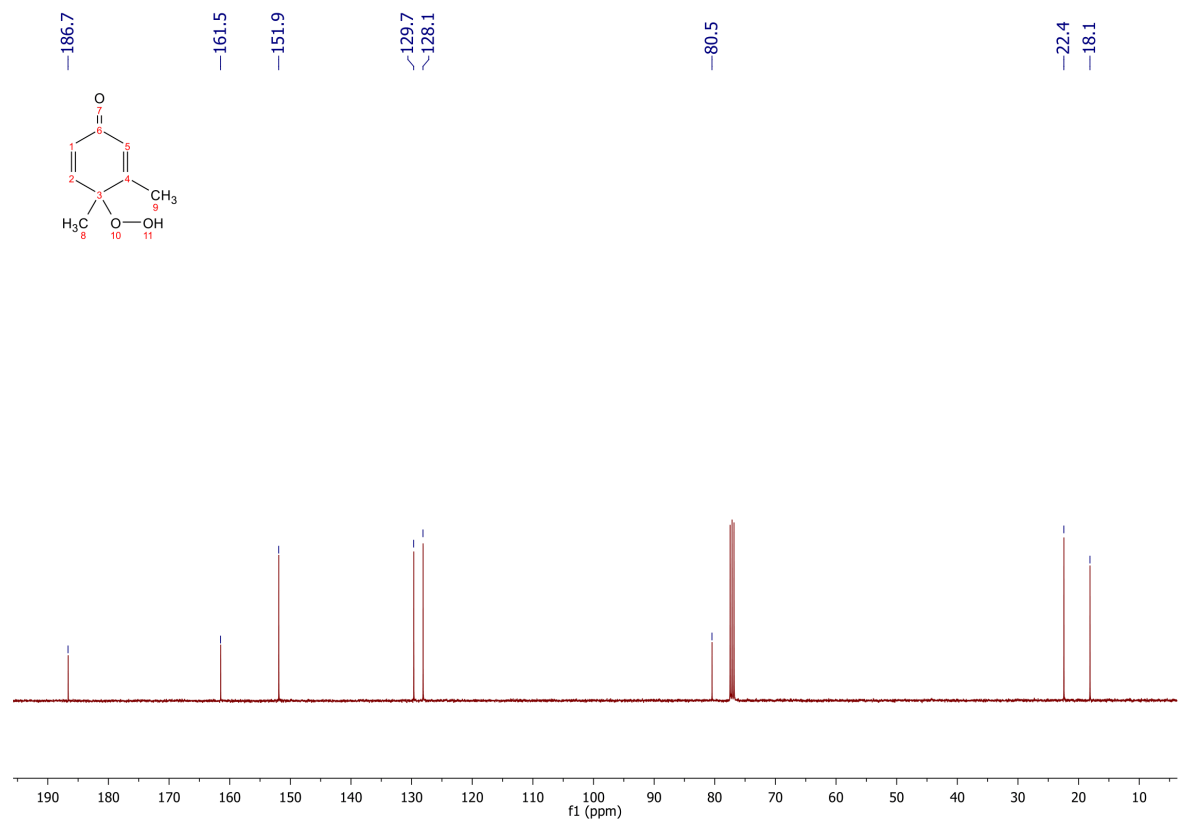
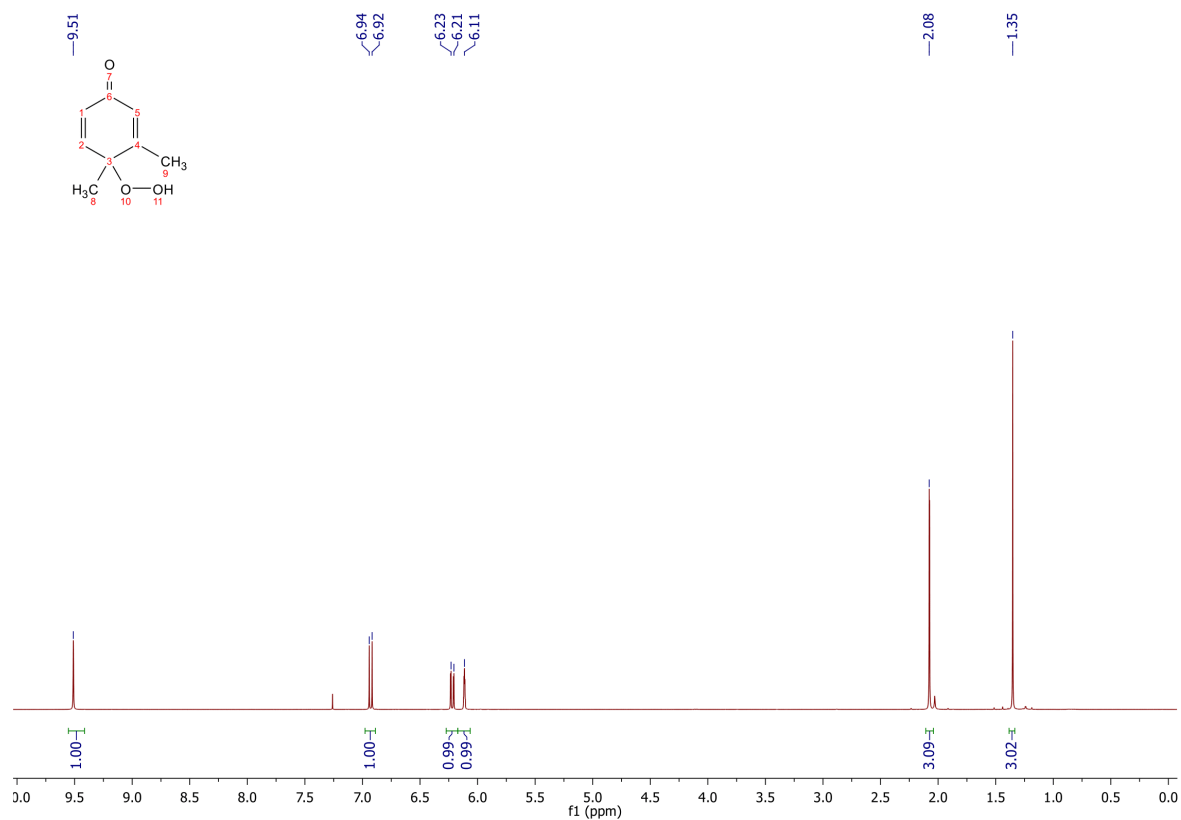
# 4-Ethyl-4-hydroperoxy-2-methoxycyclohexa-2,5-dien-1-one. (2e)



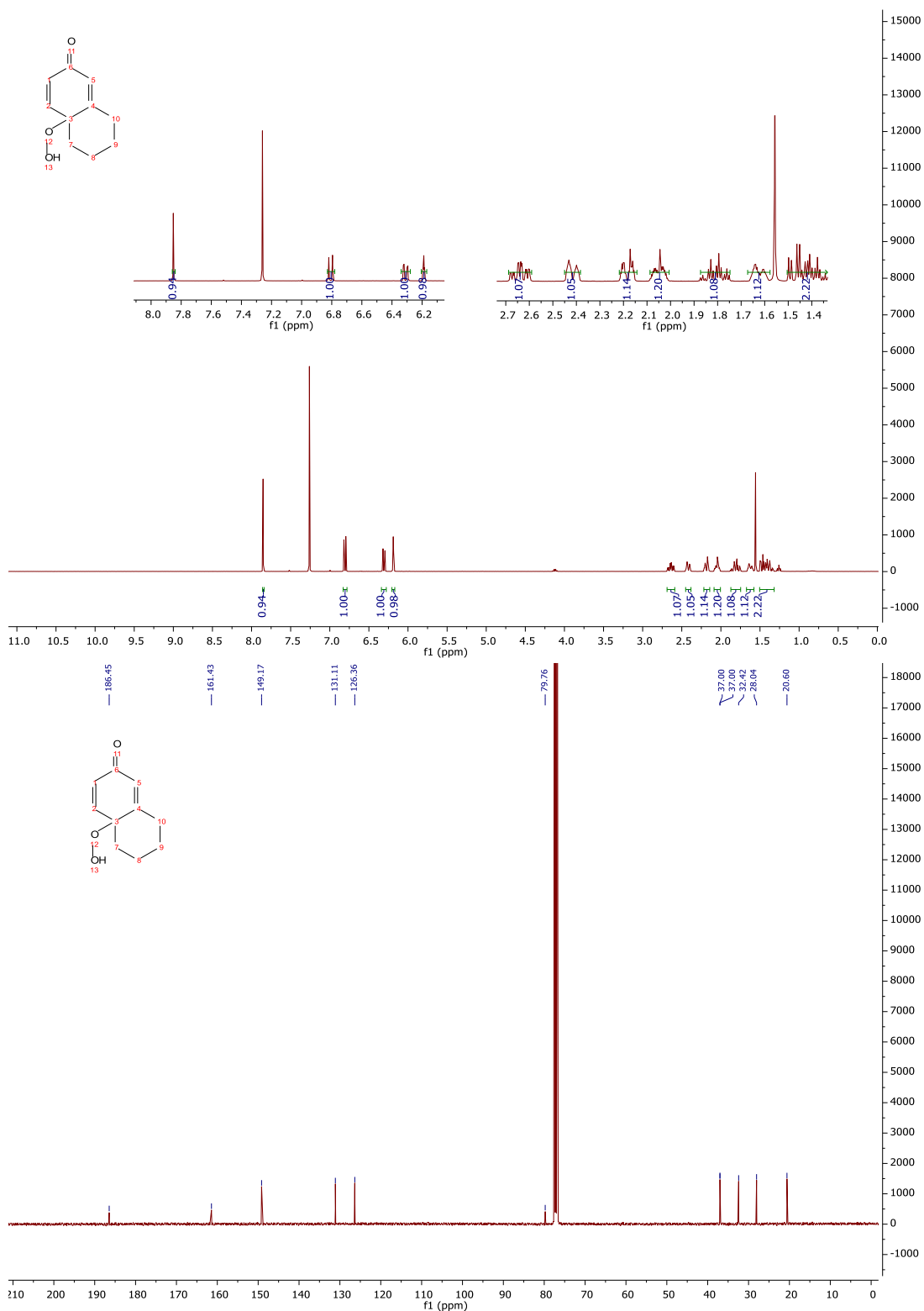
# 4-Hydroperoxy-2,4-dimethylcyclohexa-2,5-dien-1-one. (2f)



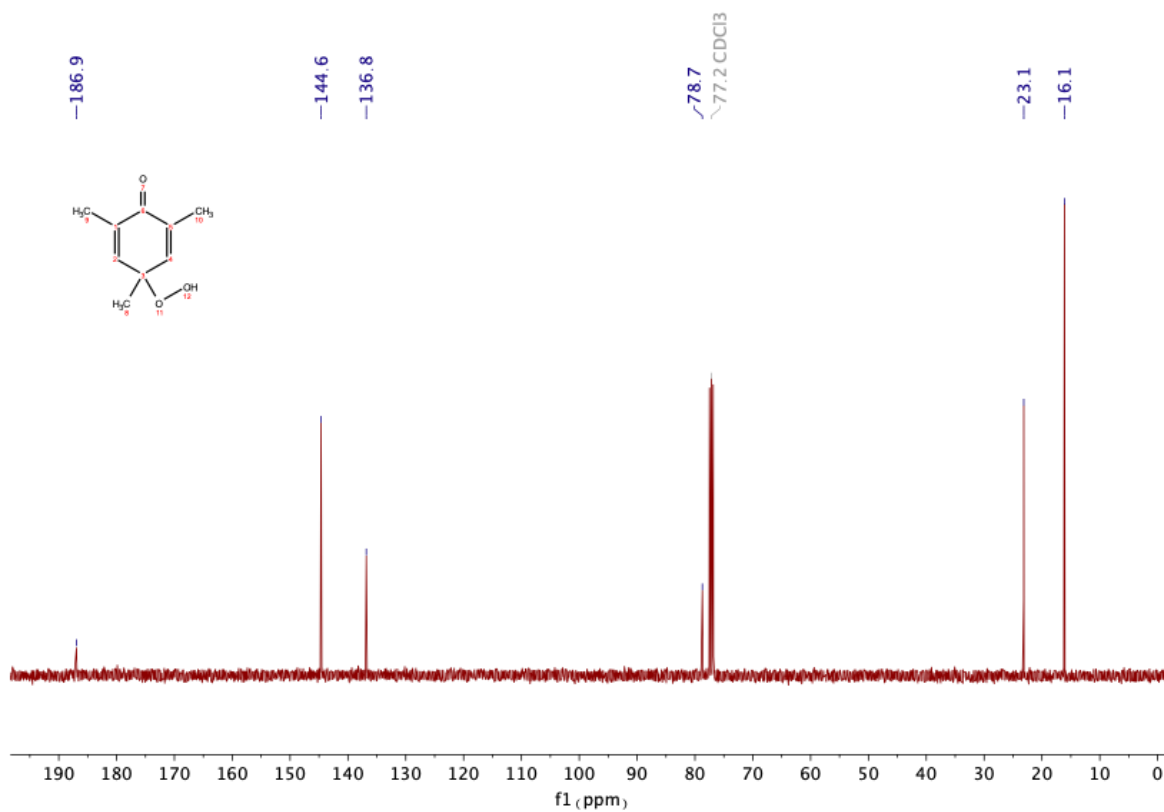
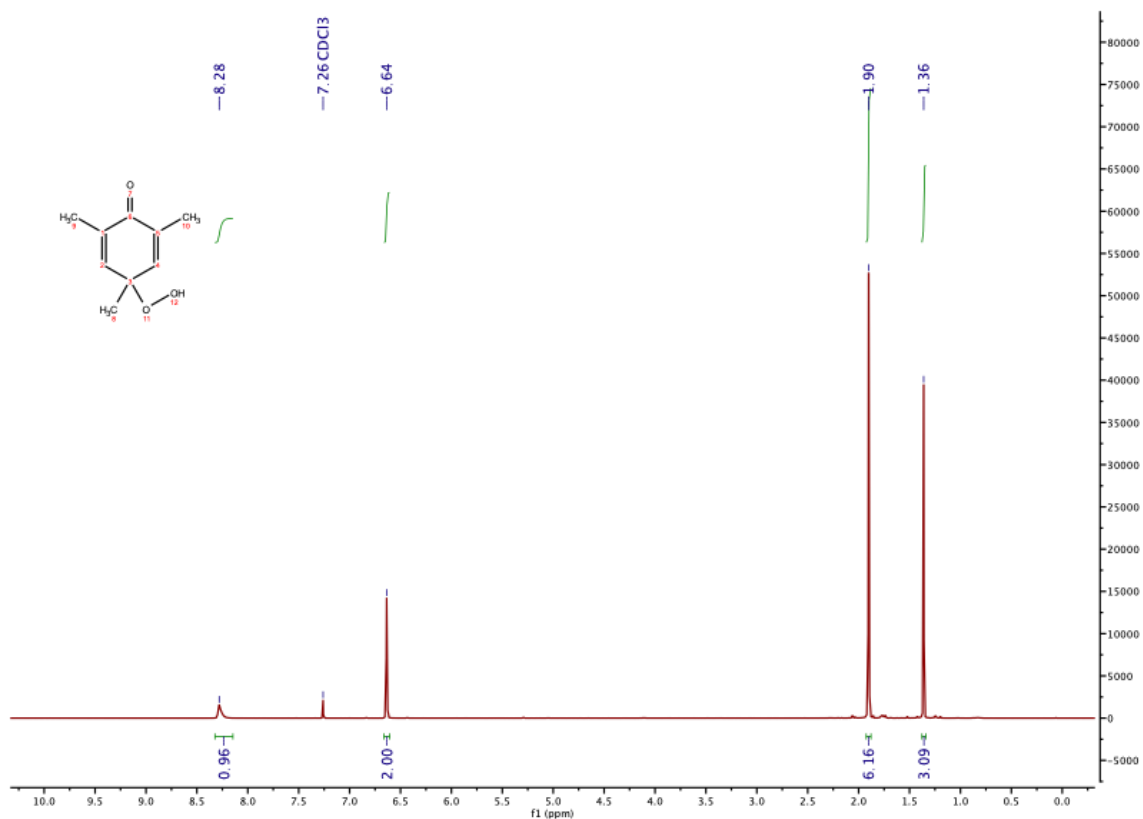
# 4-Hydroperoxy-3,4-dimethylcyclohexa-2,5-dien-1-one (2g)



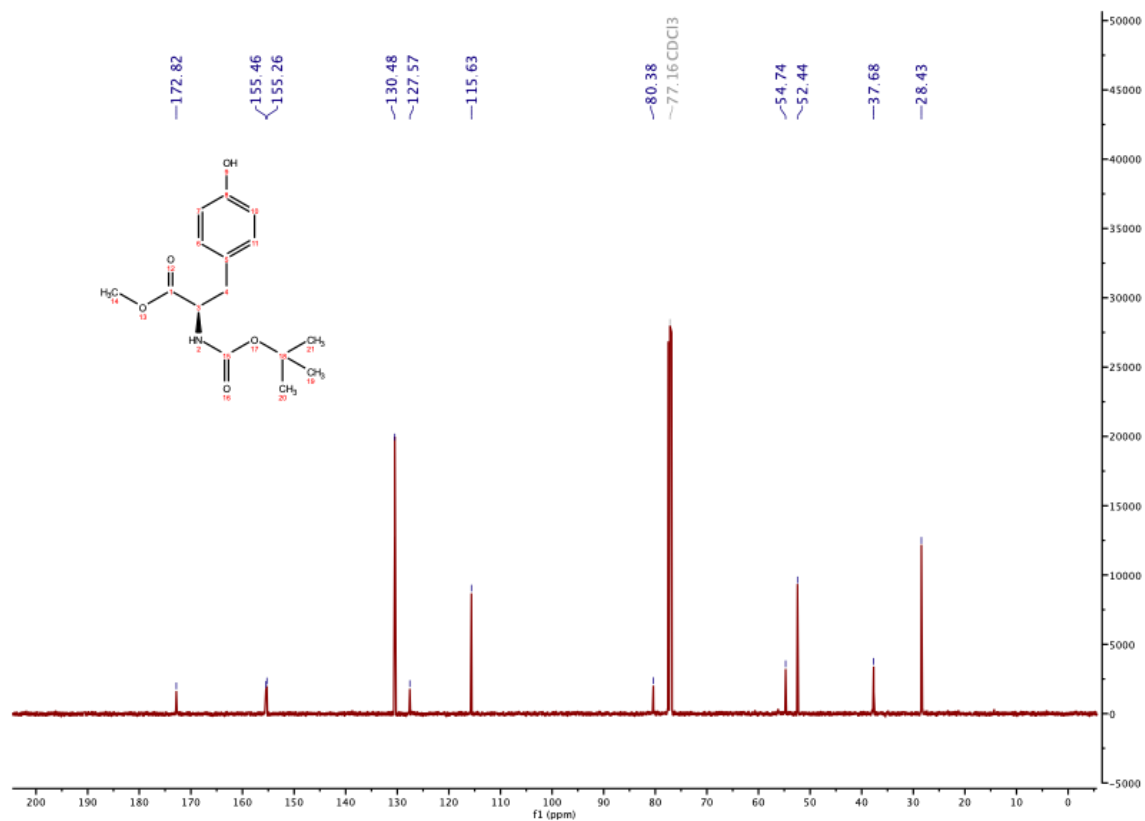
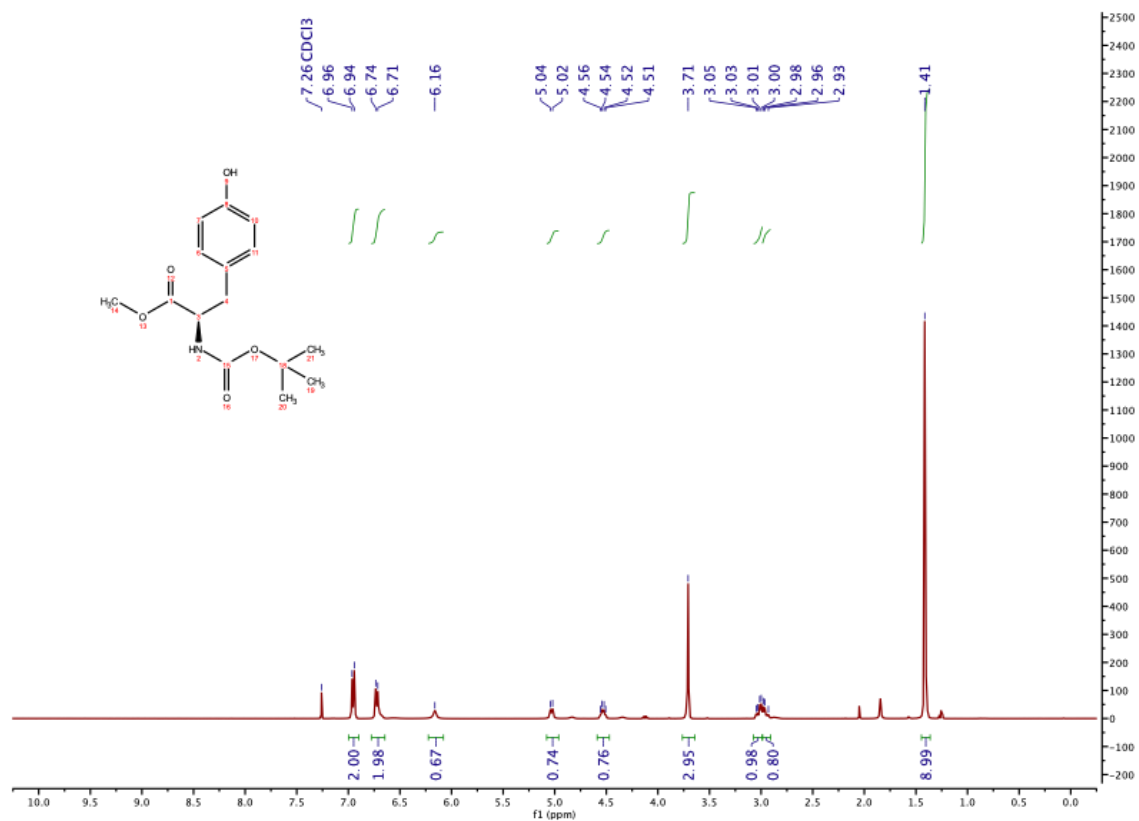
# 4a-Hydroperoxy-5,6,7,8-tetrahydronaphthalen-2(4aH)-one. (2h)



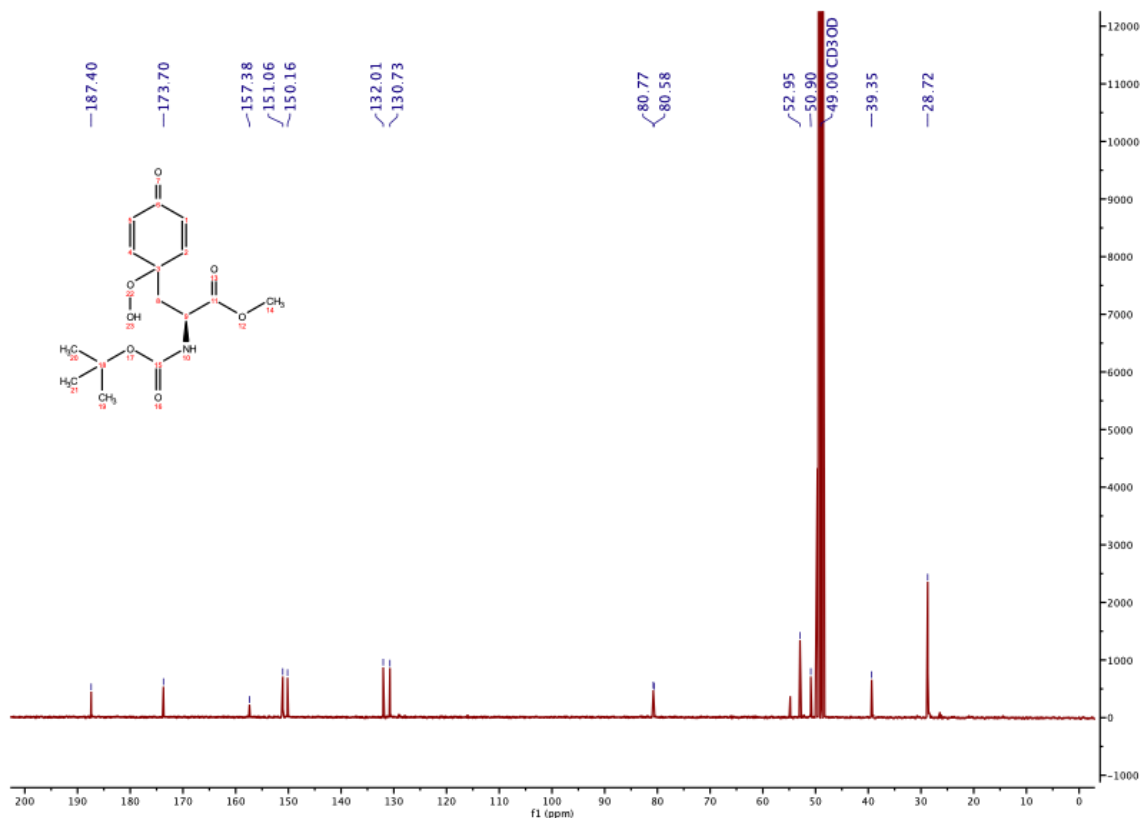
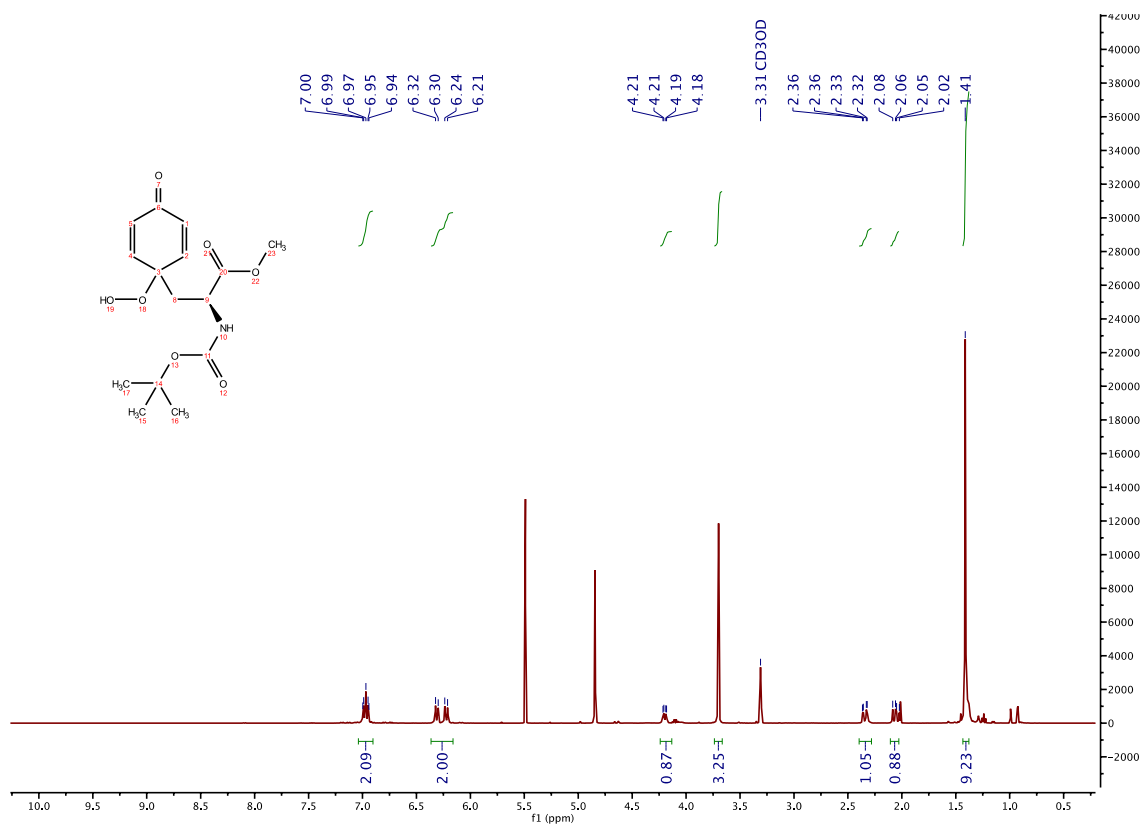
# 4-Hydroperoxy-2,4,6-trimethylcyclohexa-2,5-dien-1-one. (2i)



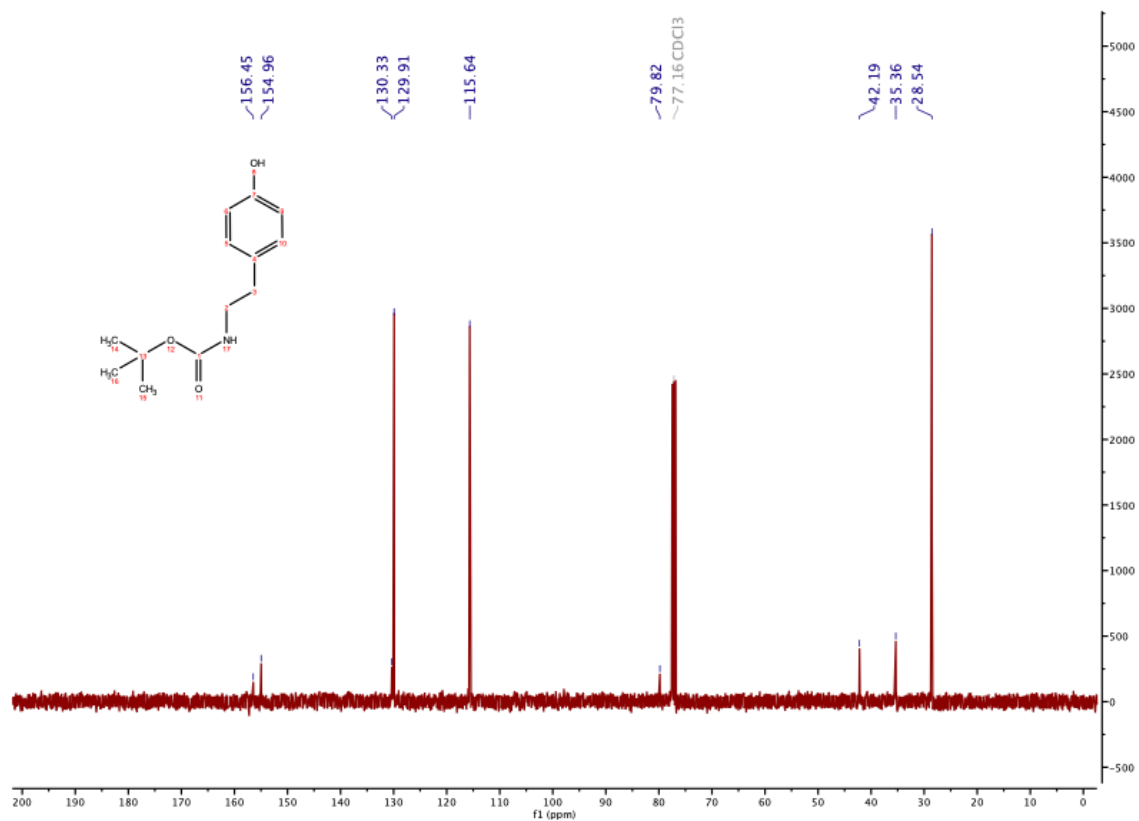
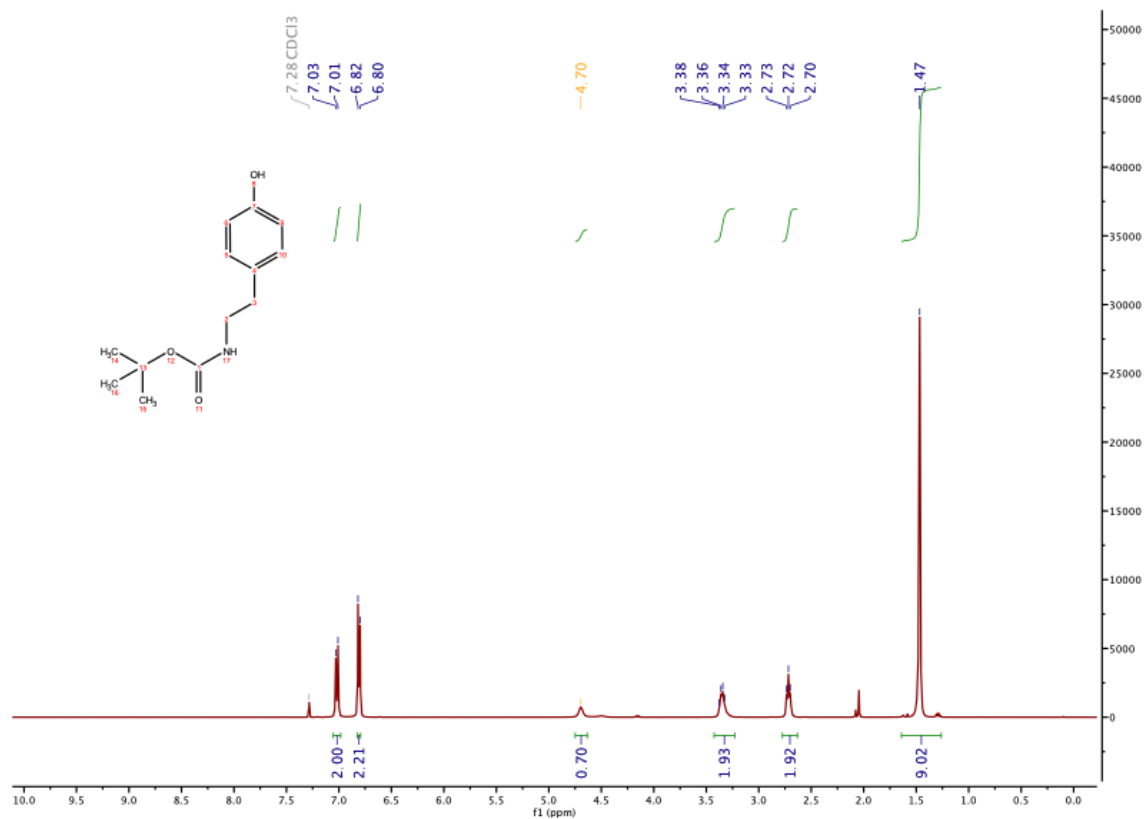
# Methyl (*tert*-butoxycarbonyl)-*L*-tyrosinate. (1j)



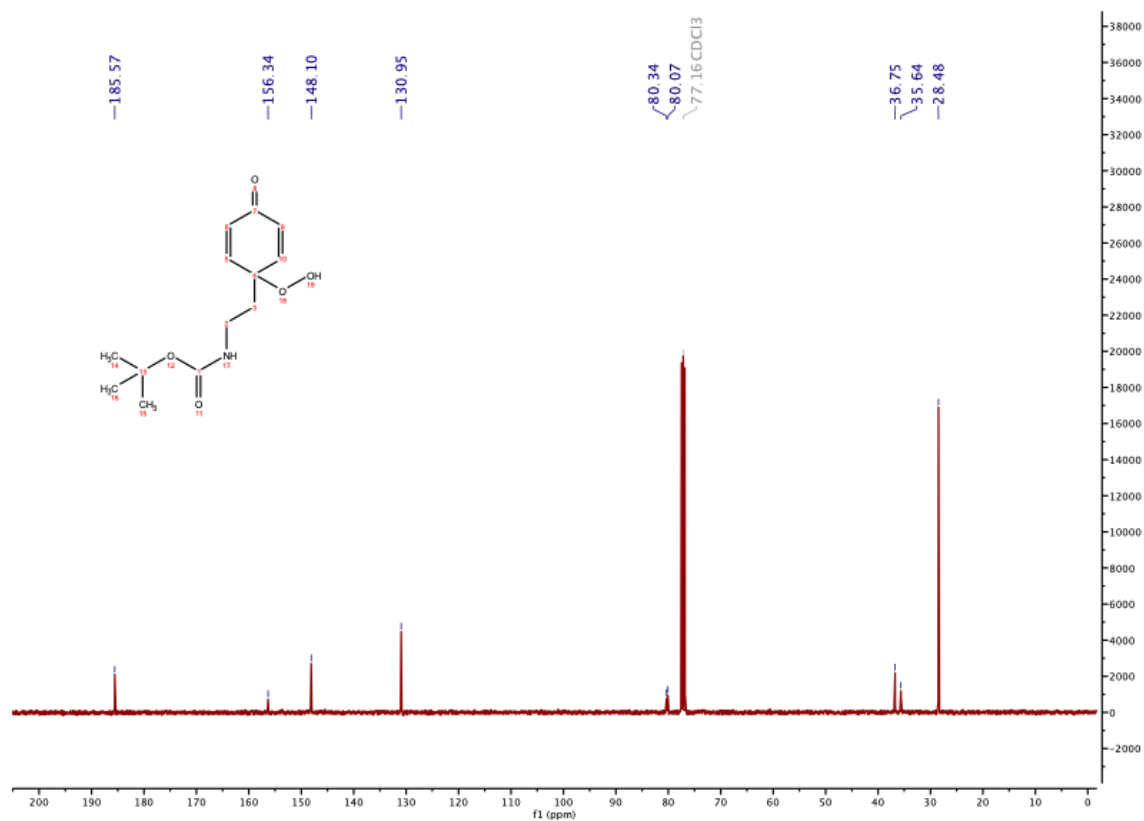
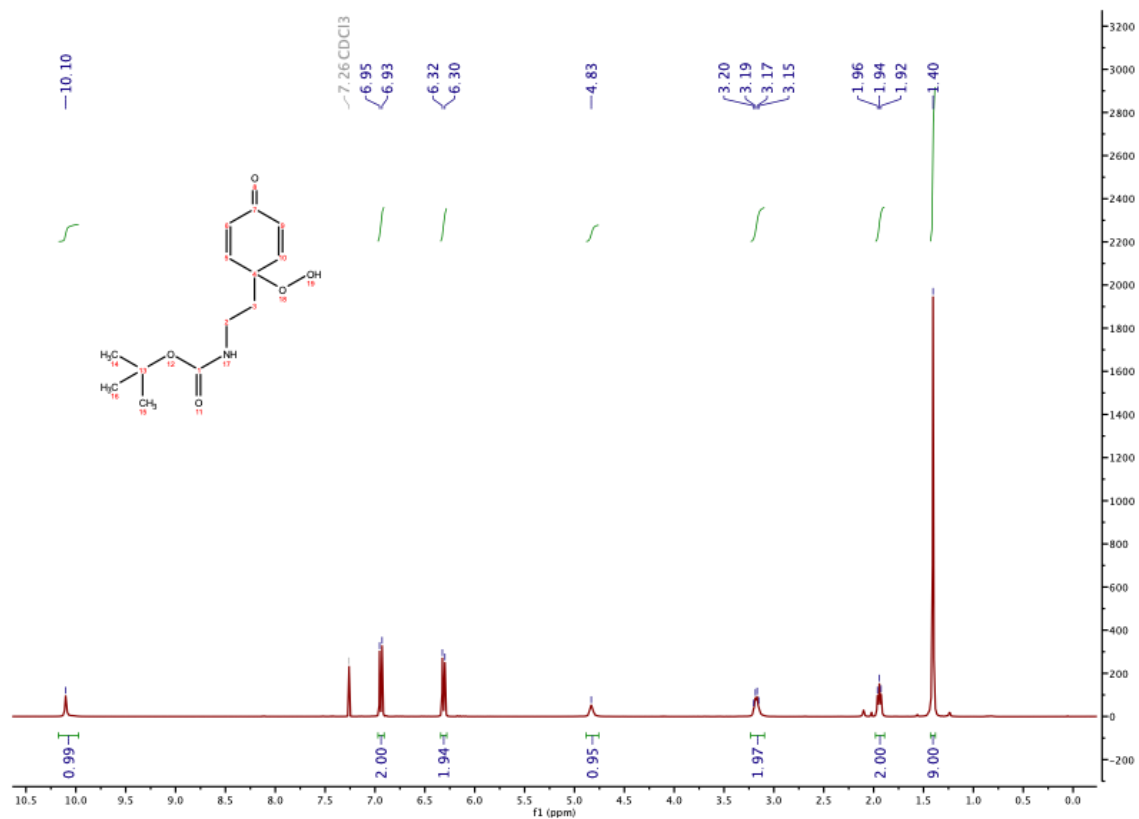
**Methyl (S)-2-((tert-butoxycarbonyl)amino)-3-(1-hydroperoxy-4-oxocyclohexa-2,5-dien-1-yl)propanoate. (2j)**



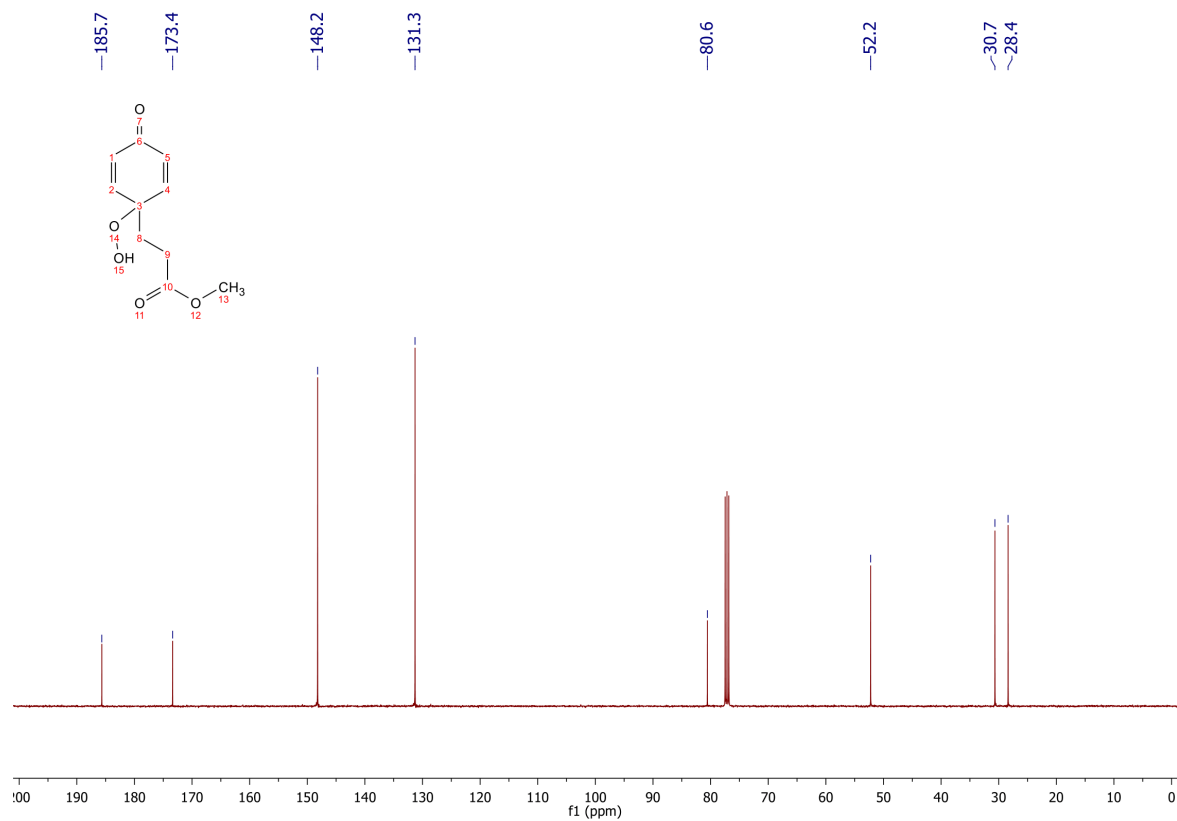
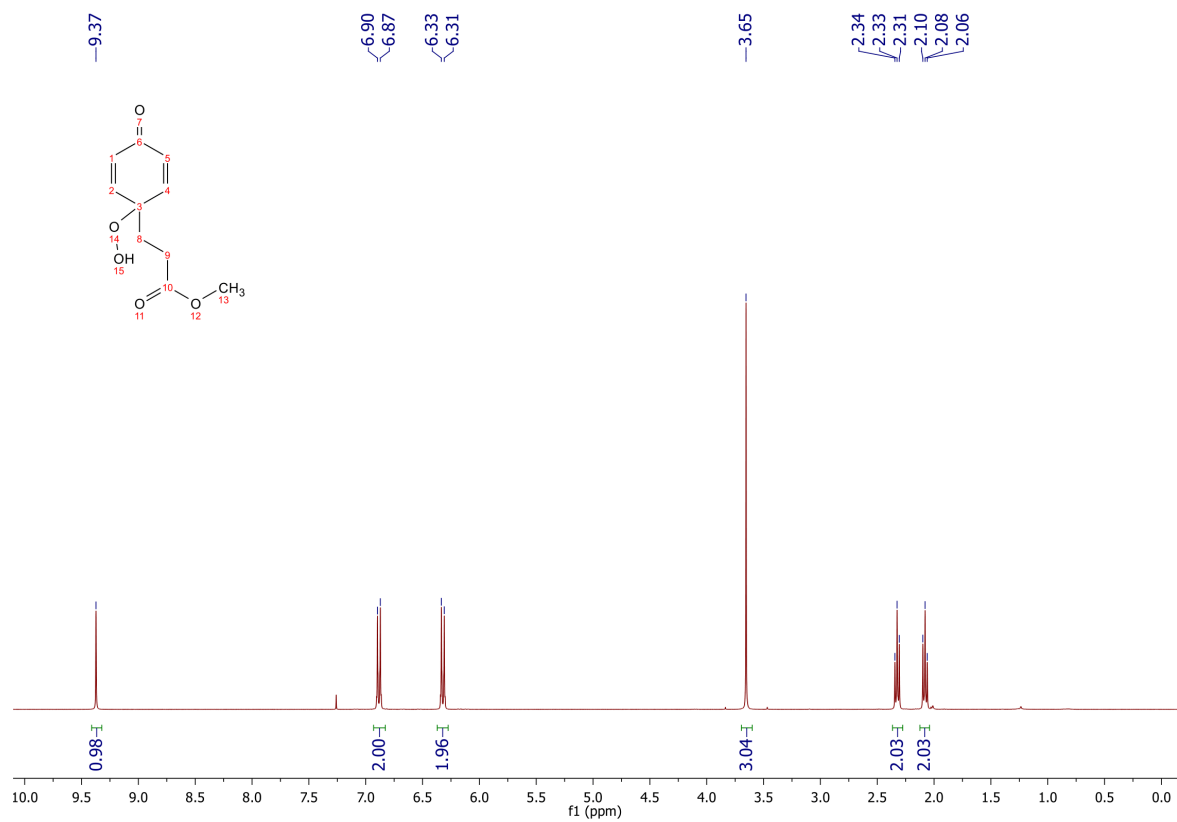
**tert-Butyl (4-hydroxyphenethyl) carbamate. (1k)**



**tert-Butyl (2-(1-hydroperoxy-4-oxocyclohexa-2,5-dien-1-yl)ethyl) carbamate. (2k)**



# Methyl 3-(1-hydroperoxy-4-oxocyclohexa-2,5-dien-1-yl)propanoate. (2I)

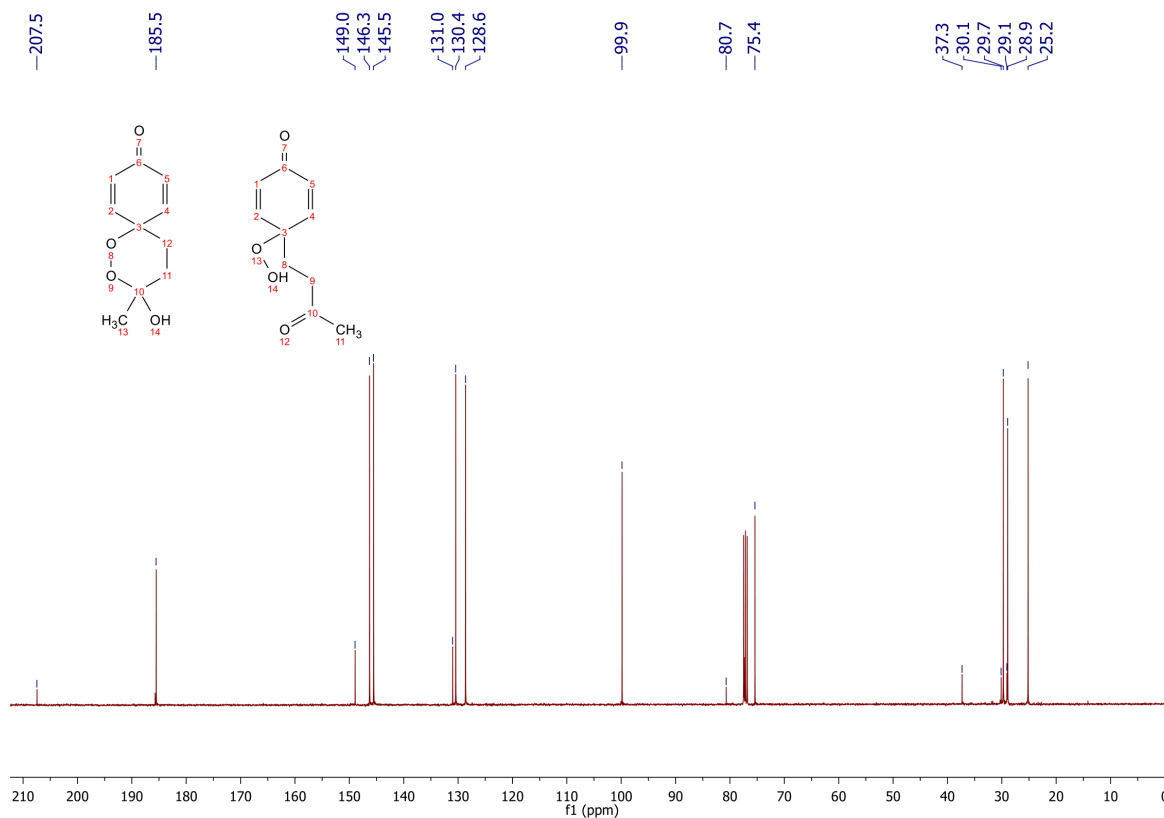
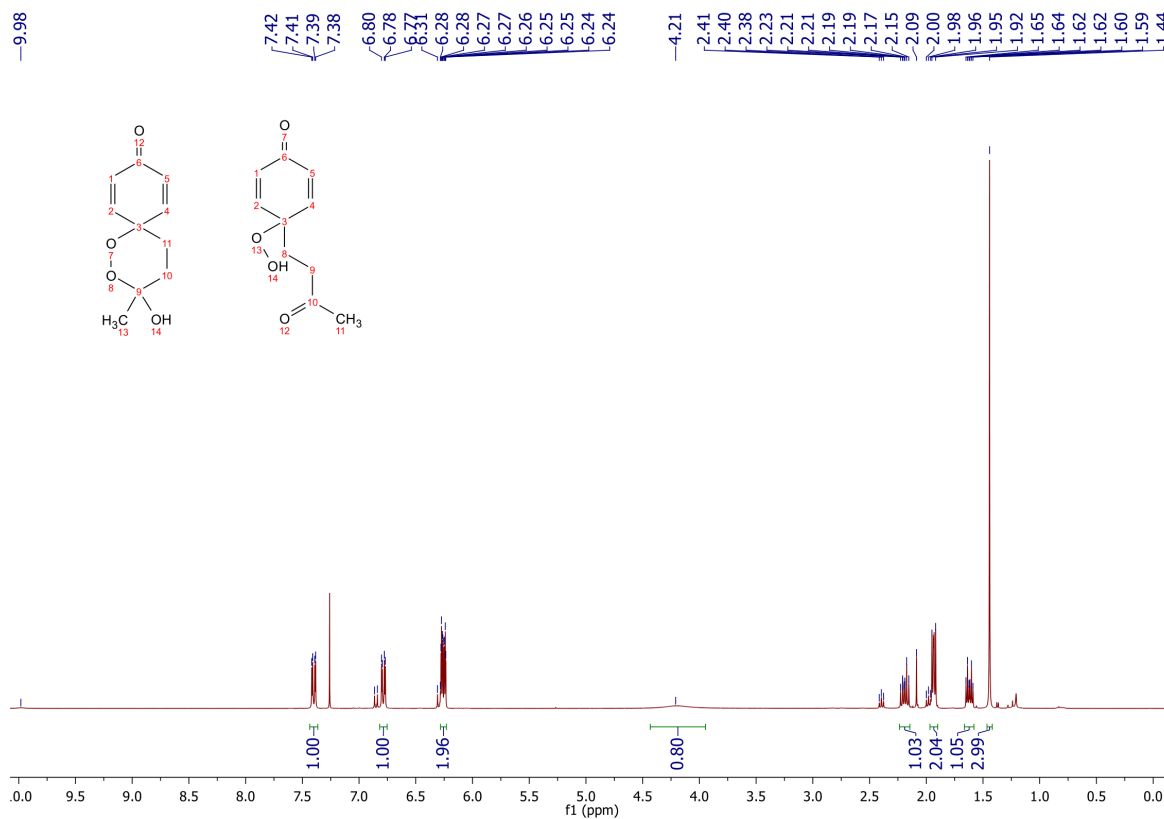


3-Hydroxy-3-methyl-1,2-dioxaspiro[5.5]undeca-7,10-dien-9-one

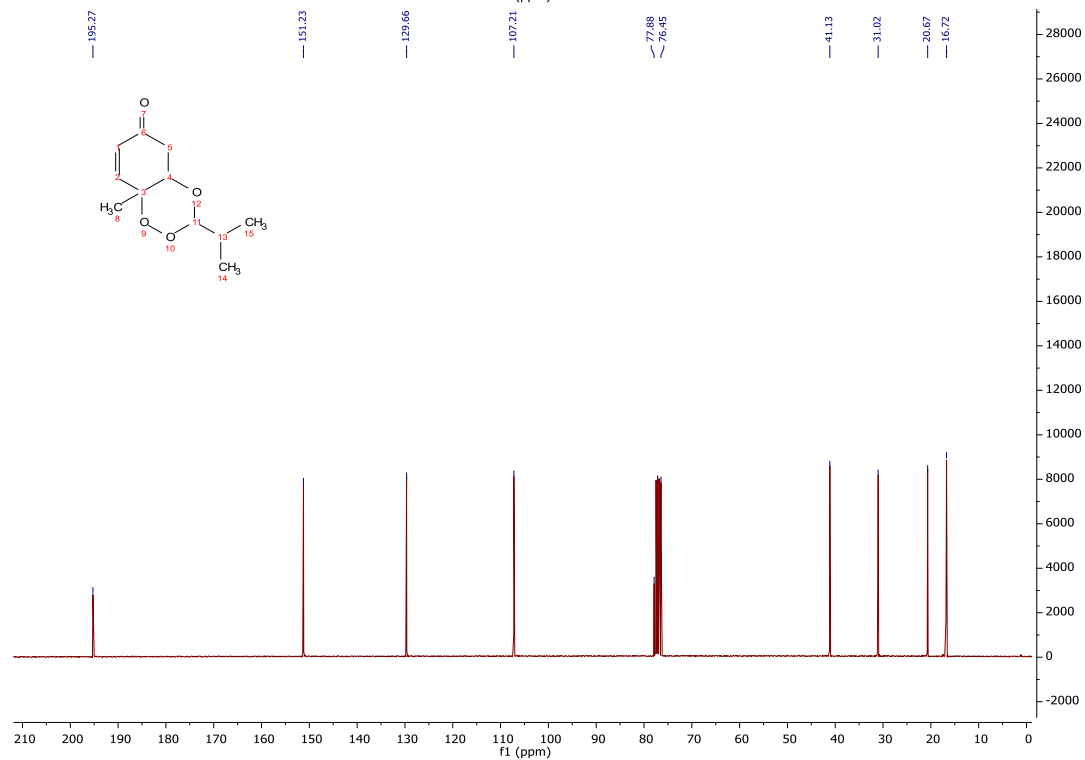
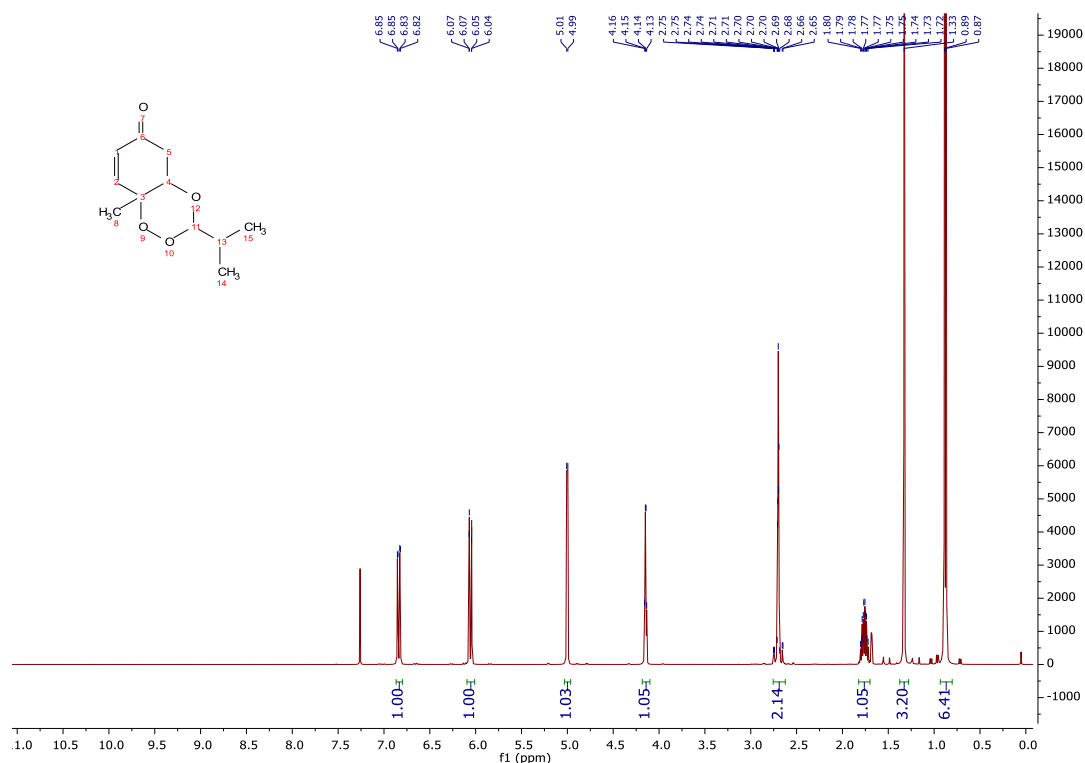
/

4-

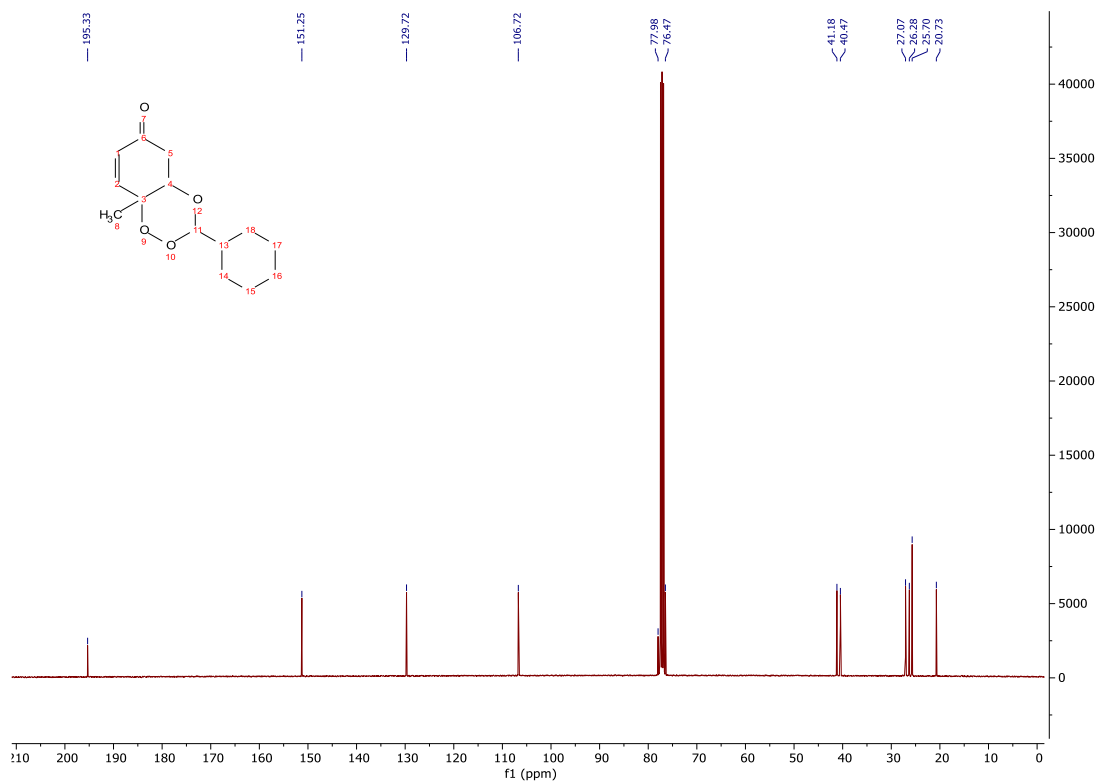
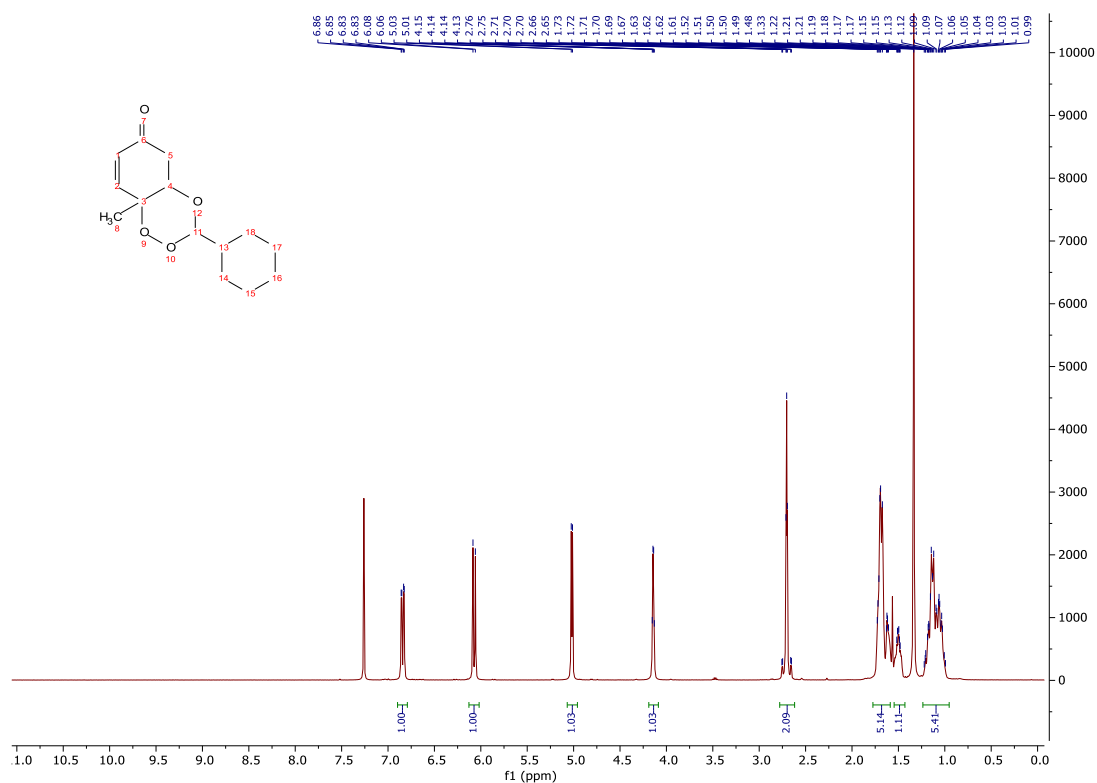
Hydroperoxy-4-(3-oxobutyl)cyclohexa-2,5-dien-1-one. (2m)



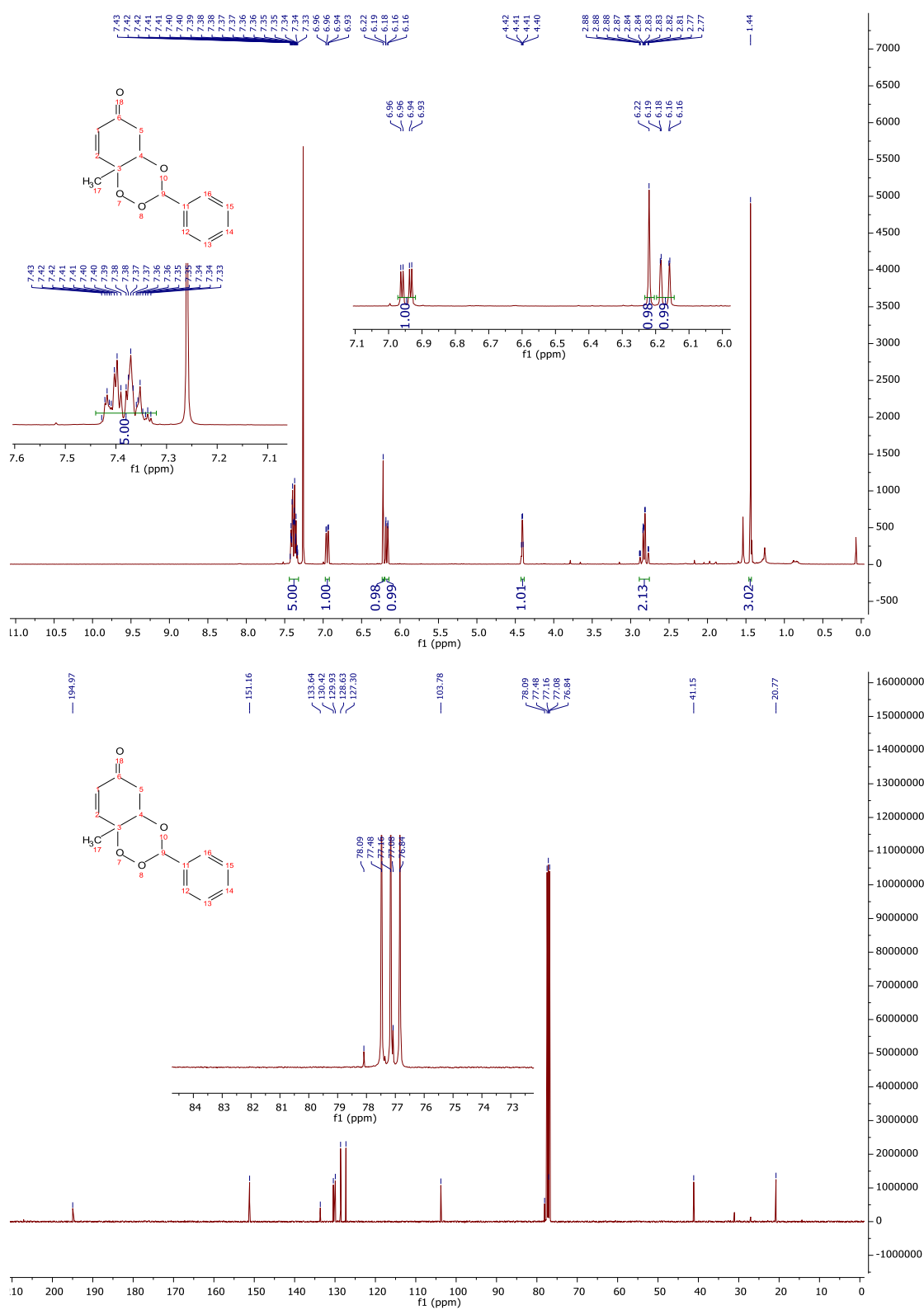
### 3-Isopropyl-8a-methyl-4a,8a-dihydrobenzo[e][1,2,4]trioxin-6(5H)-one. (5)



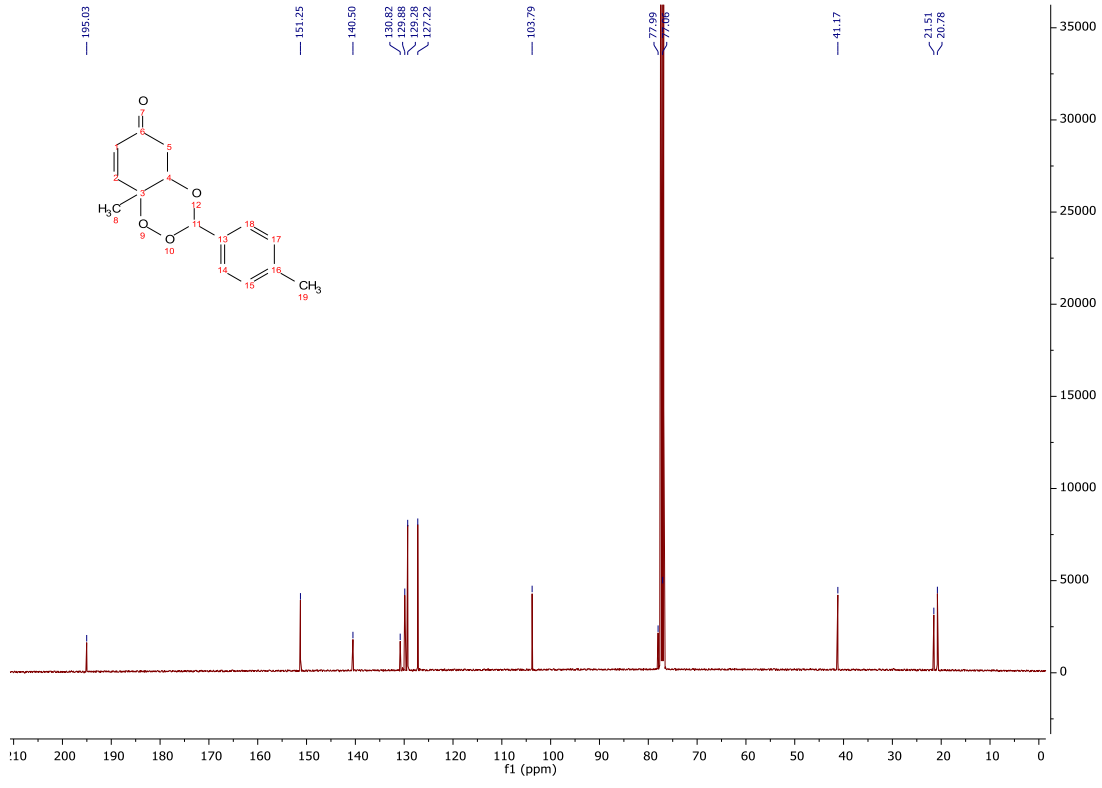
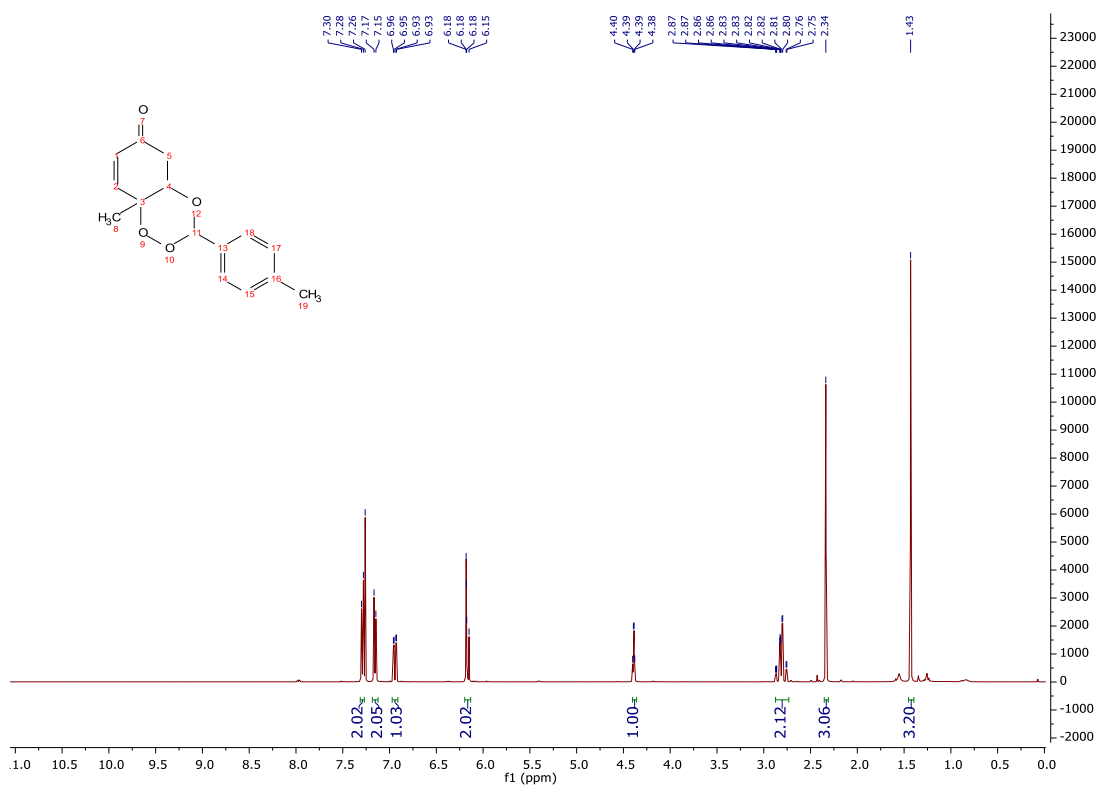
### 3-Cyclohexyl-8a-methyl-4a, 8a-dihydrobenzo[e][1,2,4]trioxin-6(5H)-one. (6)



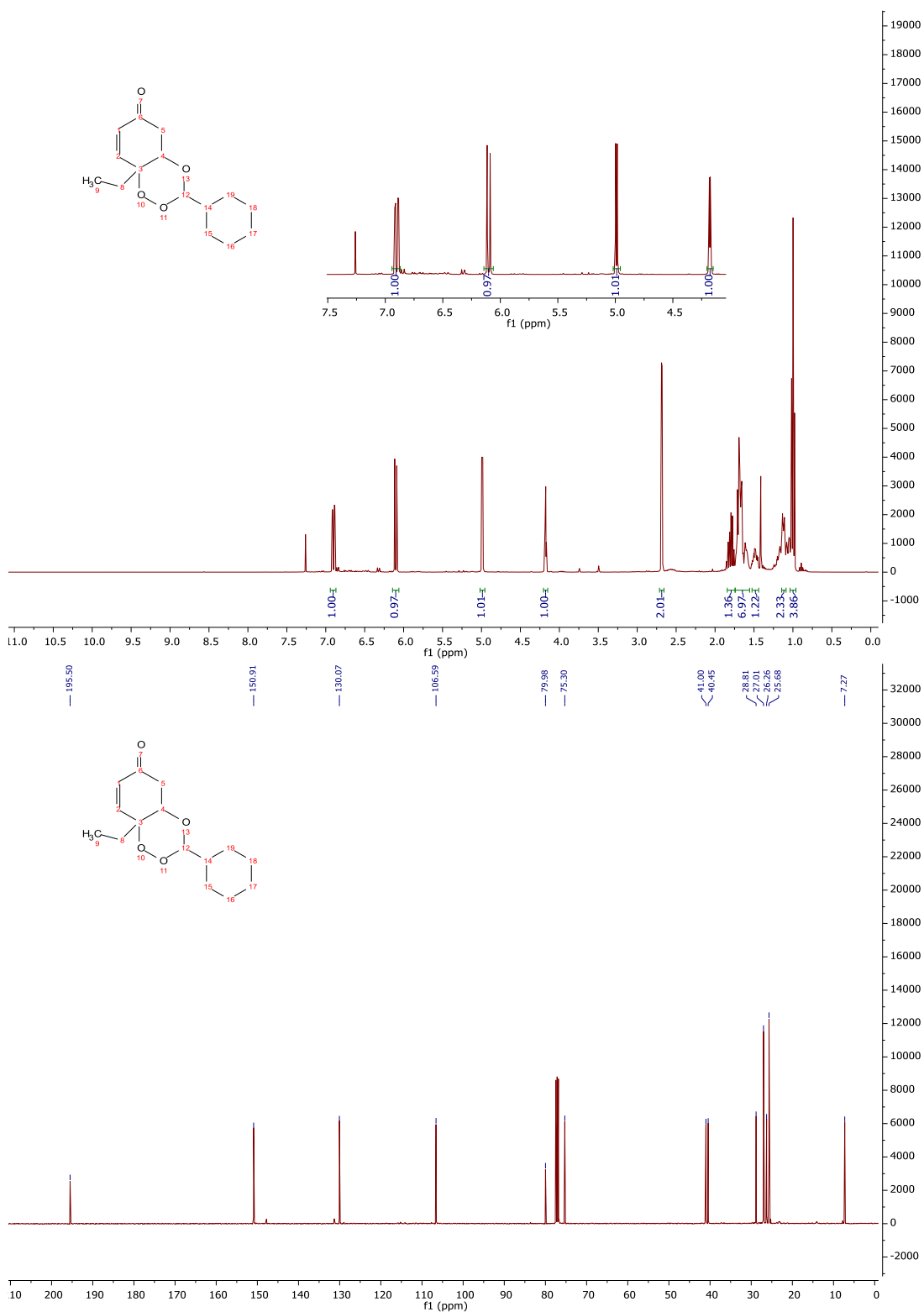
# 8a-Methyl-3-phenyl-4a, 8a-dihydrobenzo[e][1,2,4]trioxin-6(5H)-one. (7)



**8a-Methyl-3-(p-tolyl)-4a,8a-dihydrobenzo[e][1,2,4]trioxin-6(5H)-one. (8)**

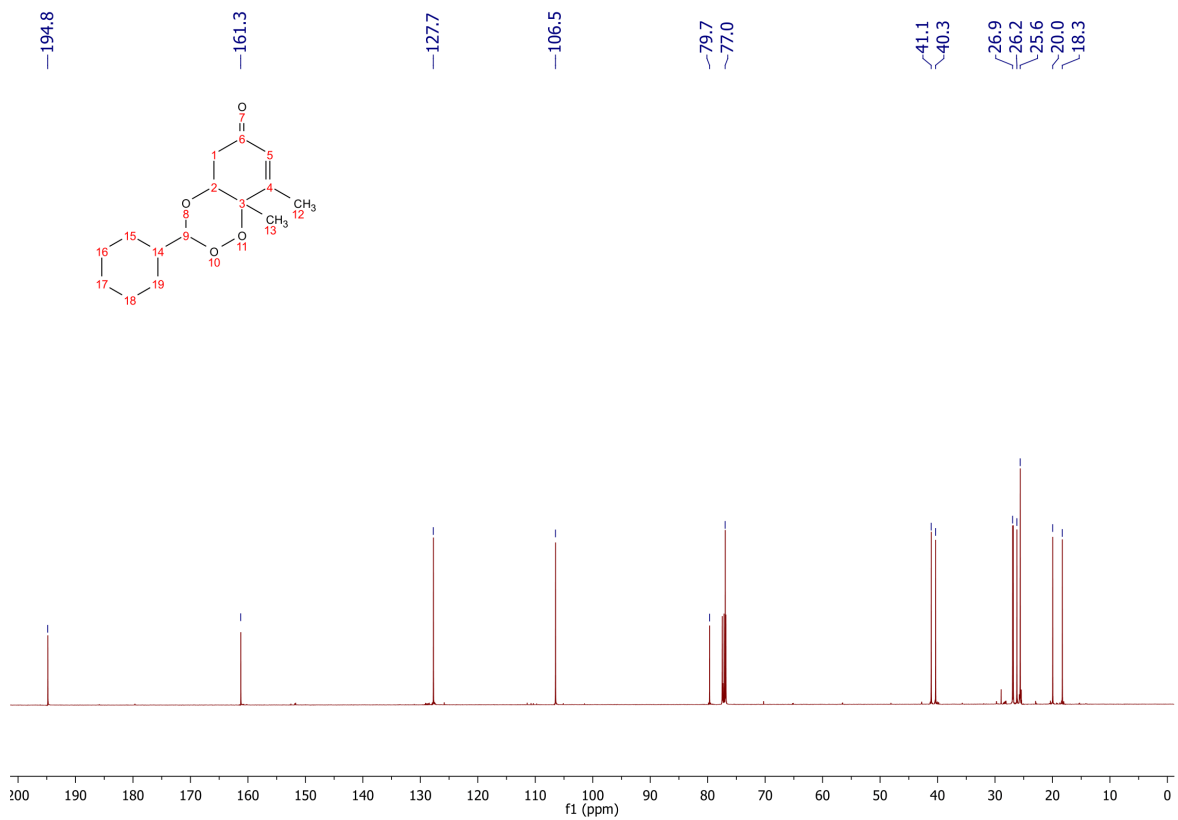
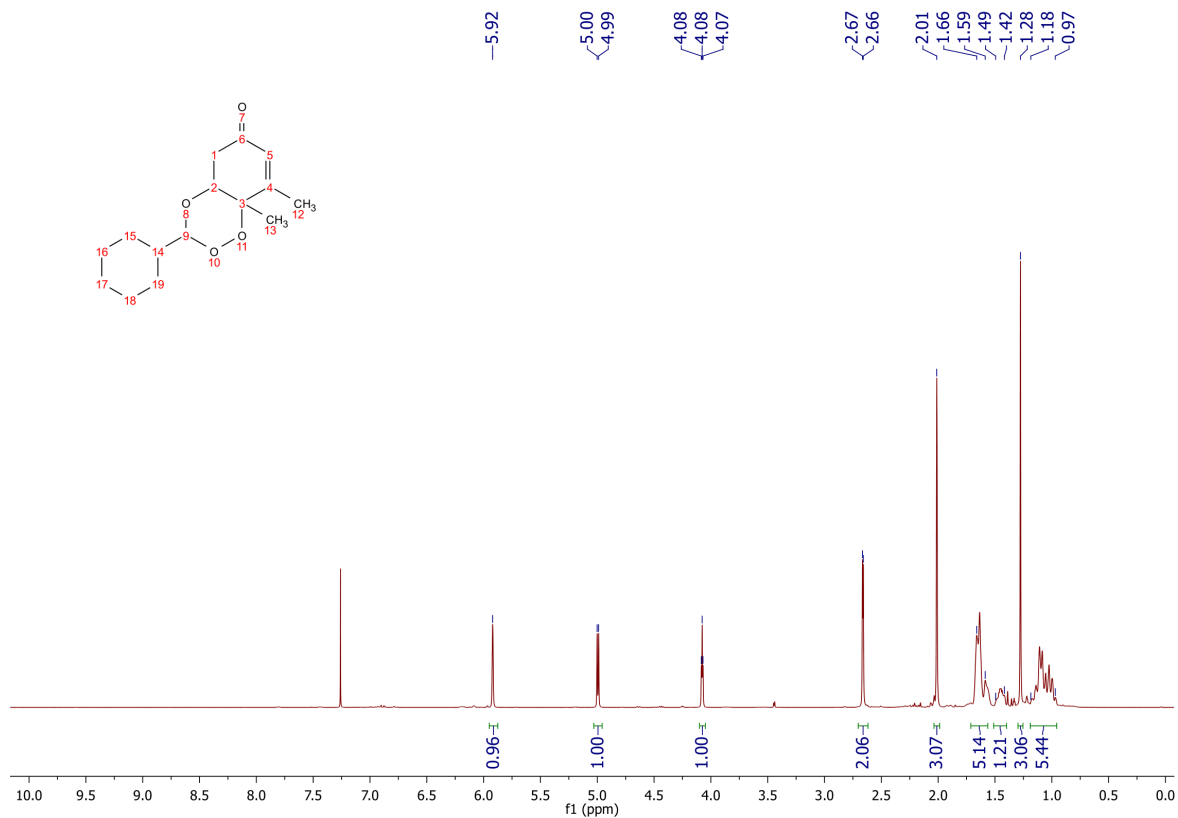


### 3-Cyclohexyl-8a-ethyl-4a,8a-dihydrobenzo[e][1,2,4]trioxin-6(5H)-one. (9)

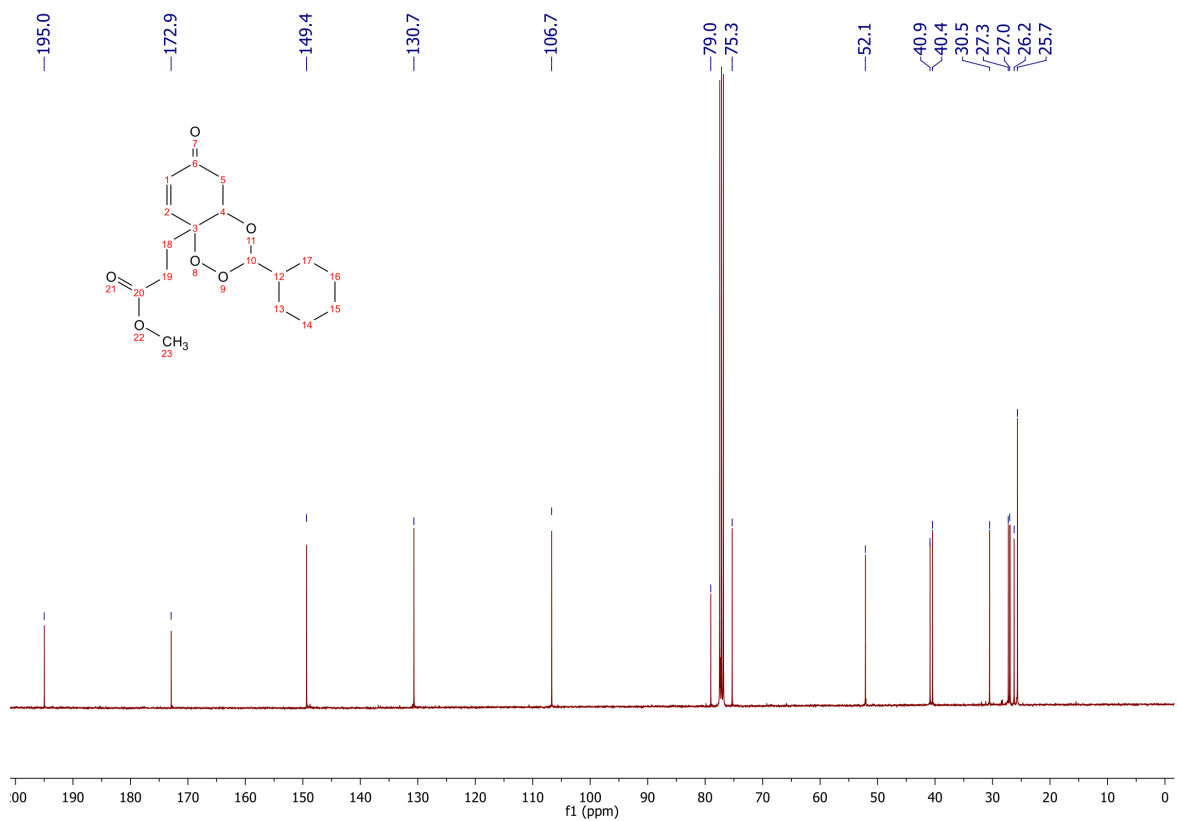
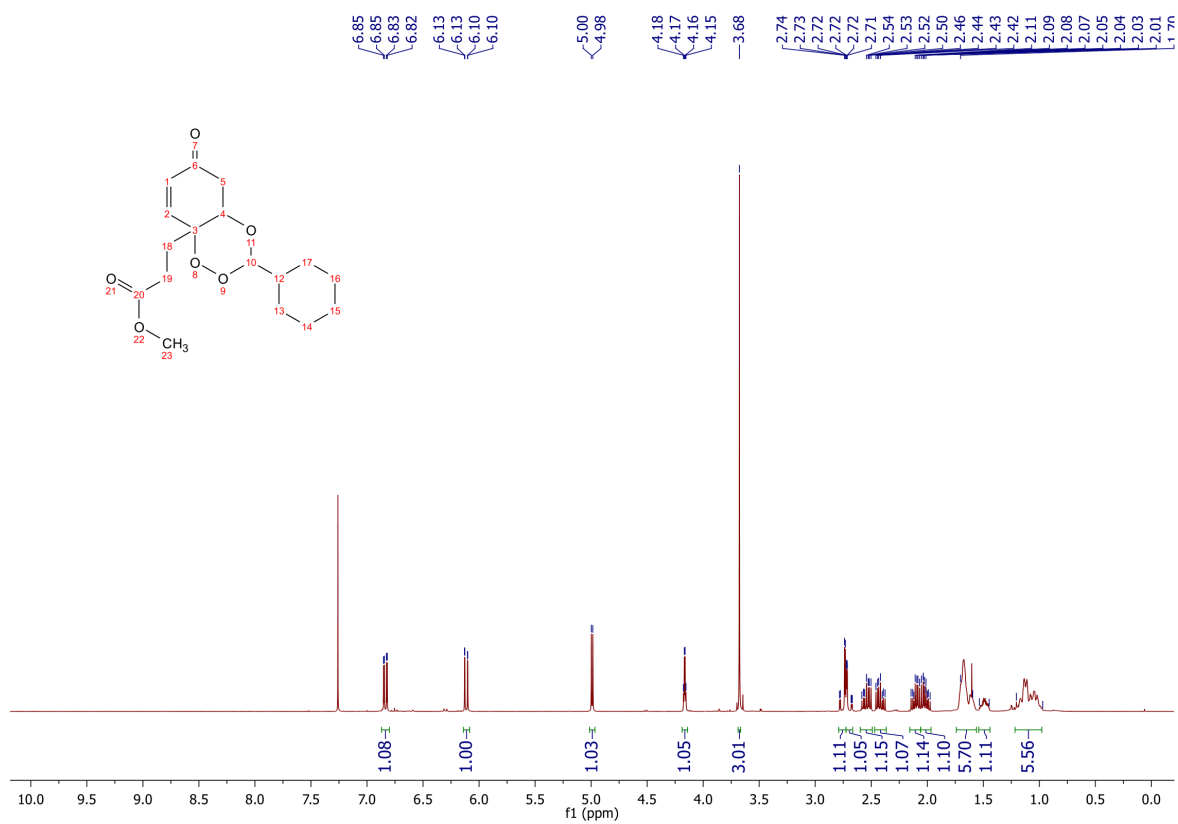




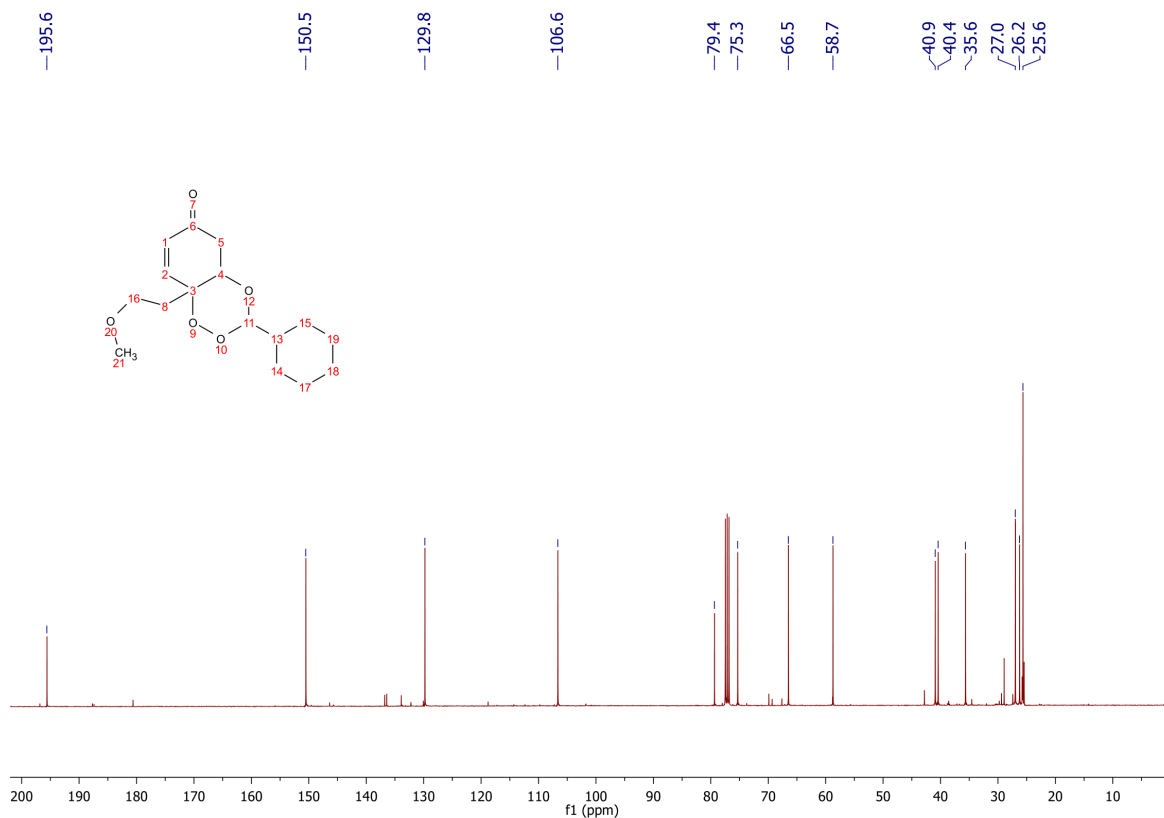
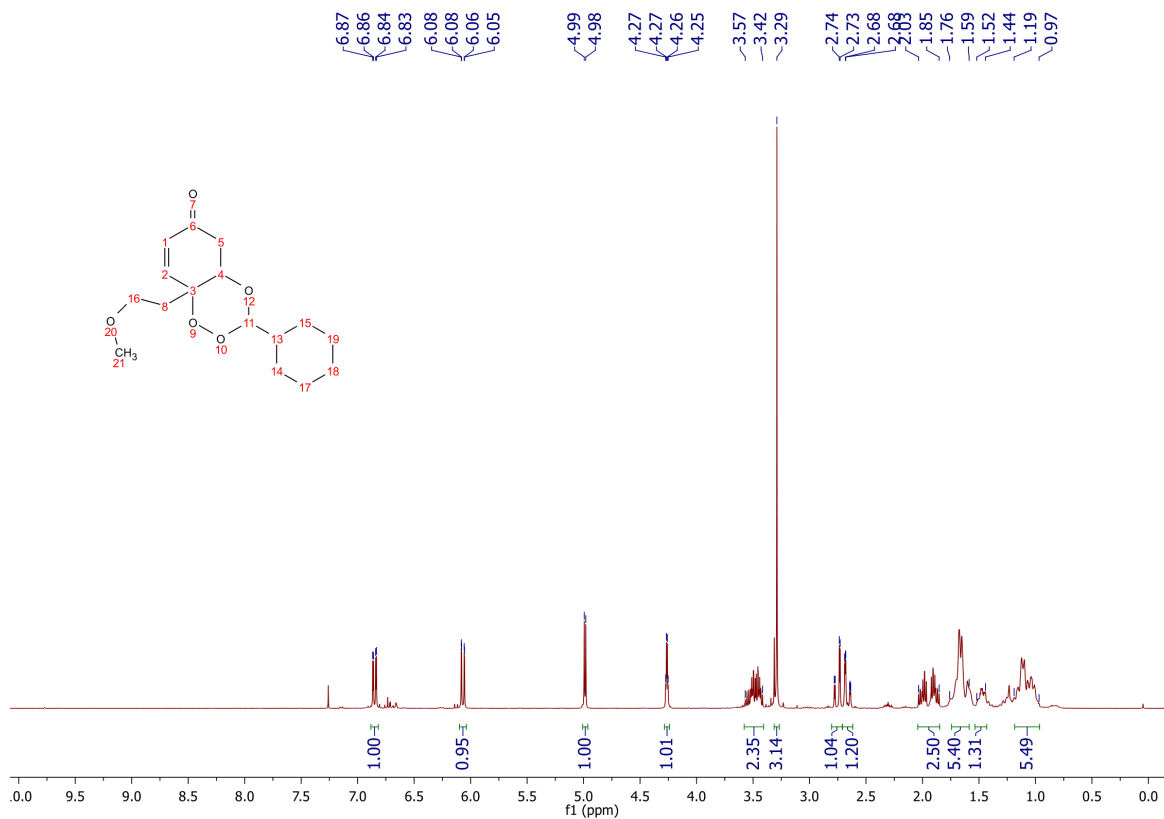
**3-Cyclohexyl-8,8a-dimethyl-4a,8a-dihydrobenzo[e][1,2,4]trioxin-6(5H)-one. (11)**



**Methyl 3-(3-cyclohexyl-6-oxo-5,6-dihydrobenzo[e][1,2,4]trioxin-8a(4aH)-yl)propanoate. (12)**



**3-Cyclohexyl-8a-(2-methoxyethyl)-4a,8a-dihydrobenzo[e][1,2,4]trioxin-6(5H)-one. (13)**



## Crystallography Data

### Crystal (2a)

Single crystals of  $C_7H_8O_3$  [**2a**] were grown by slow evaporation from ethyl acetate solution.

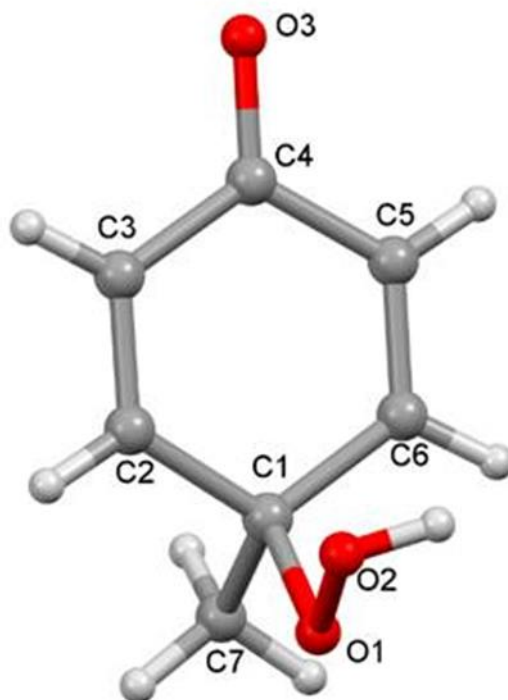


**Table S5.** Bond lengths for **2a**.

Atom	Atom	Length/Å	Atom	Atom	Length/Å
C1	C2	1.4729(19)	C4	C5	1.4997(18)
C1	C6	1.4691(18)	C4	C7	1.5307(19)
C1	O10	1.2351(16)	C4	O8	1.4506(16)
C2	C3	1.335(2)	C5	C6	1.3333(19)
C3	C4	1.4981(18)	O8	O9	1.4643(14)

**Table S6.** Hydrogen Bonds for **2a**.

D	H	A	d(D-H)/Å	d(H-A)/Å	d(D-A)/Å	D-H-A/°
O9	H9	O101	0.848(16)*	1.960(16)	2.7946(14)	167(2)

\*O9-H9 Distance restrained to a value of 0.84 Å (esd 0.02 Å)

## Crystal (2b)

Single crystals of C<sub>8</sub>H<sub>10</sub>O<sub>3</sub> [**2b**] were grown by slow evaporation from ethyl acetate solution.

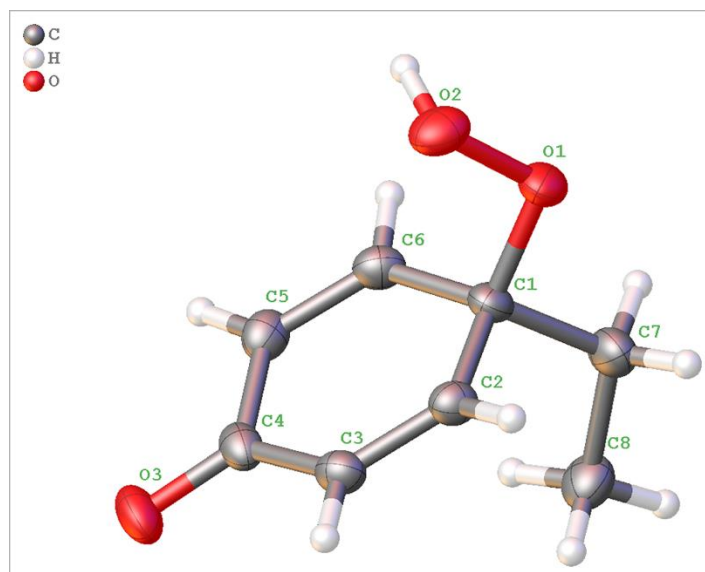


**Table S7.** Bond Lengths for **4**.

Atom	Atom	Length/Å	Atom	Atom	Length/Å
O1	O2	1.4654(14)	C1	C2	1.4947(17)
O1	C1	1.4415(13)	C1	C7	1.5481(18)
O3	C4	1.2359(15)	C4	C3	1.4654(18)
C5	C4	1.4629(18)	C3	C2	1.3302(17)
C5	C6	1.3302(17)	C7	C8	1.5180(18)
C1	C6	1.4949(17)			

## Crystal (2h)

Single crystals of C<sub>10</sub>H<sub>12</sub>O<sub>3</sub> [2h] were grown by slow evaporation from methanol solution.

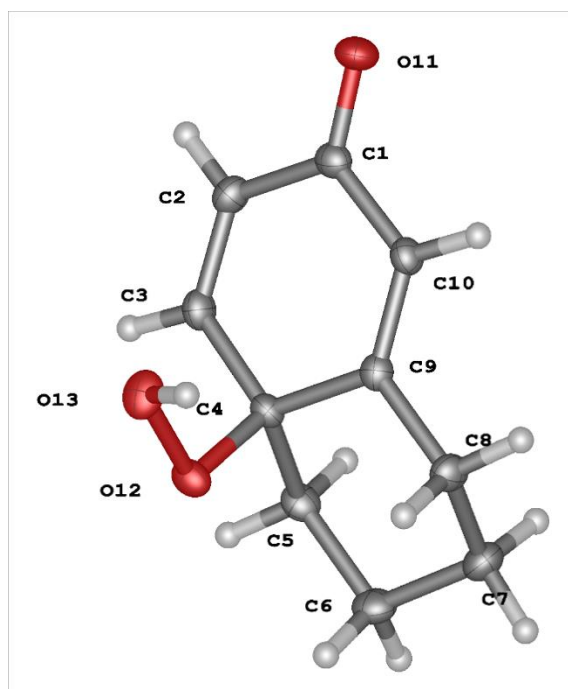


**Table S8.** Bond Lengths for 10.

Atom	Atom	Length/Å	Atom	Atom	Length/Å
C1	C2	1.4663(15)	C4	O12	1.4475(12)
C1	C10	1.4631(15)	C5	C6	1.5274(16)
C1	O11	1.2360(13)	C6	C7	1.5230(16)
C2	C3	1.3291(16)	C7	C8	1.5386(15)
C3	C4	1.4969(14)	C8	C9	1.4998(14)
C4	C5	1.5405(14)	C9	C10	1.3373(15)
C4	C9	1.5135(14)	O12	O13	1.4651(10)

## Crystal (6)

Single crystals of C<sub>14</sub>H<sub>20</sub>O<sub>4</sub> [6] were obtained after recrystallisation from diethyl ether solution.

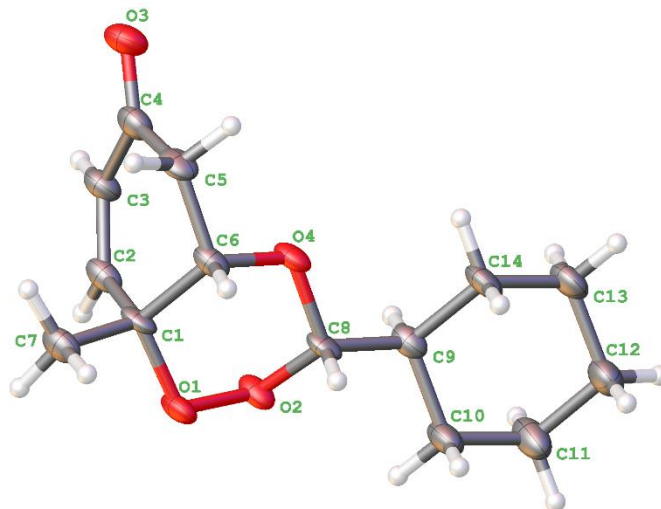


**Table S9.** Bond Lengths for 17.

Atom	Atom	Length/Å	Atom	Atom	Length/Å
O1	O2	1.467(4)	C3	C4	1.471(7)
O1	C1	1.455(5)	C4	C5	1.506(7)
O2	C8	1.426(5)	C5	C6	1.520(6)
O3	C4	1.230(6)	C8	C9	1.515(6)
O4	C6	1.439(5)	C9	C10	1.529(6)
O4	C8	1.416(5)	C9	C14	1.529(6)
C1	C2	1.501(6)	C10	C11	1.526(7)
C1	C6	1.529(6)	C11	C12	1.528(7)
C1	C7	1.522(6)	C12	C13	1.522(7)
C2	C3	1.335(6)	C13	C14	1.523(7)

## Single Crystal X-ray Diffraction Experimental

Single crystals were selected and mounted using Fomblin® (YR-1800 perfluoropolyether oil) on a polymer-tipped MiTeGen MicroMount™ and cooled rapidly to 120 K in a stream of cold N<sub>2</sub> using an Oxford Cryosystems open flow cryostat.<sup>[S8]</sup> Single crystal X-ray diffraction data were collected on either an Oxford Diffraction GV1000 (AtlasS2 or TitanS2 CCD area detector, mirror-monochromated Cu-K $\alpha$  radiation source;  $\lambda$  = 1.54184 Å,  $\omega$  scans) or a Rigaku OD XtaLAB PRO MM007 (PILATUS3 R 200K Hybrid Pixel Array detector, mirror-monochromated Cu-K $\alpha$  radiation source;  $\lambda$  = 1.54184 Å,  $\omega$  scans). Cell parameters were refined from the observed positions of all strong reflections and absorption corrections were applied using a Gaussian numerical method with beam profile correction (CrysAlisPro).<sup>[S9]</sup> Structures were solved within Olex2<sup>[S10]</sup> by dual space iterative methods (SHELXT)<sup>[S11]</sup> and all non-hydrogen atoms refined by full-matrix least-squares on all unique F<sup>2</sup> values with anisotropic displacement parameters (SHELXL).<sup>[S12]</sup> Structures were checked with checkCIF.<sup>[S13]</sup> CCDC-2004817-2004820 contains the supplementary data for these compounds. These data can be obtained free of charge from The Cambridge Crystallographic Data Centre via [www.ccdc.cam.ac.uk/data\\_request/cif](http://www.ccdc.cam.ac.uk/data_request/cif).

**TableS10.** Single Crystal X-ray Diffraction Experimental Data

Structure	2a	2b	2h	6
<b>Chemical formula</b>	C <sub>7</sub> H <sub>8</sub> O <sub>3</sub>	C <sub>8</sub> H <sub>10</sub> O <sub>3</sub>	C <sub>10</sub> H <sub>12</sub> O <sub>3</sub>	C <sub>14</sub> H <sub>20</sub> O <sub>4</sub>
<b>M<sub>r</sub></b>	140.13	154.16	180.20	252.30
<b>Crystal system</b>	Monoclinic	Orthorhombic	Monoclinic	Monoclinic
<b>Space group</b>	<i>P2<sub>1</sub>/c</i>	<i>Pbca</i>	<i>P2<sub>1</sub>/n</i>	<i>P2<sub>1</sub>/c</i>
<b>a, b, c (Å)</b>	10.1442 (5), 10.4033 (5), 6.3880 (3)	7.13195 (11), 11.8244 (2), 18.2107 (3)	8.29297 (16), 7.41007 (12), 14.8813 (3)	5.8033 (5), 38.0676 (19), 6.4898 (5)
<b>a, b, g (°)</b>	90, 104.154 (5), 90	90, 90, 90	90, 105.2902 (19), 90	90, 115.253 (10), 90
<b>V (Å<sup>3</sup>)</b>	653.68 (6)	1535.72 (5)	882.11 (3)	1296.70 (19)
<b>Z</b>	4	8	4	4
<b>Radiation</b>	Cu Ka	Cu Ka	Cu Ka	Cu Ka
<b>m (mm<sup>-1</sup>)</b>	0.95	0.85	0.83	0.77
<b>Crystal size (mm)</b>	0.22 × 0.17 × 0.10	0.32 × 0.11 × 0.05	0.32 × 0.21 × 0.11	0.57 × 0.13 × 0.03
<b>Temperature (K)</b>	120(1)	120(1)	120(1)	120(1)
<b>Diffraction, detector</b>	Oxford Diffraction SuperNova, Titan S2	Rigaku OD XtalLAB PRO MM007, PILATUS3 R 200K	Oxford Diffraction SuperNova, Atlas S2	Oxford Diffraction SuperNova, Titan S2
<b>T<sub>min</sub>, T<sub>max</sub></b>	0.636, 1.000	0.745, 1.000	0.679, 1.000	0.473, 1.000
<b>No. of measured, independent and observed [<i>I</i> &gt; 2<i>s</i>(<i>I</i>)] reflections</b>	2408, 1257, 1141	8244, 1612, 1525	9460, 1783, 1671	16445, 2323, 2043
<b>R<sub>int</sub></b>	0.022	0.027	0.021	0.079
<b>(sin <i>q</i>/<i>l</i>)<sub>max</sub> (Å<sup>-1</sup>)</b>	0.620	0.634	0.624	0.601
<b>R[<i>F</i><sup>2</sup> &gt; 2<i>s</i>(<i>F</i><sup>2</sup>)], wR(<i>F</i><sup>2</sup>), S</b>	0.038, 0.105, 1.10	0.037, 0.100, 1.06	0.033, 0.088, 1.04	0.110, 0.294, 1.14
<b>No. of reflections</b>	1257	1612	1783	2323
<b>No. of parameters</b>	95	104	121	164
<b>No. of restraints</b>	1	1	0	0
<b>Dρ<sub>max</sub>, Dρ<sub>min</sub> (e Å<sup>-3</sup>)</b>	0.27, -0.24	0.26, -0.17	0.28, -0.20	0.64, -0.42
<b>CCDC Deposit</b>	2004817	2004818	2004819	2004820

## Single Crystal X-ray Diffraction Refinement Details

All hydrogen atoms in the structures of **2a**, **2b**, **2h** and **6** were observed in the electron density maps. Alkyl and aryl hydrogen atoms were geometrically placed and refined with riding models. The peroxide hydrogen atoms in **2a**, **2b**, and **2h** were refined; hydrogen atoms H9 and H2 in structures **2a** and **2b** respectively were restrained to have O-H bond lengths of 0.84 Å (DFIX). The isotropic displacement parameters of all peroxy-hydrogen atoms were fixed at values of 1.5 times  $U_{eq}$  of their parent oxygen atoms.

**TableS11.** Hydrogen Bond Parameters

Structure	<i>D</i> —H... <i>A</i>	<i>D</i> —H (Å)	H... <i>A</i> (Å)	<i>D</i> ... <i>A</i> (Å)	<i>D</i> —H... <i>A</i> (°)
<b>2a</b>	O9—H9...O10	0.848 (16)	1.960 (16)	2.7946 (14)	167 (2)
<b>2b</b>	O2—H2...O3	0.871 (15)	1.909 (15)	2.7775 (13)	174.5 (18)
<b>2h</b>	O13—H13...O11	0.883 (18)	1.878 (18)	2.7470 (12)	167.5 (16)

## References

- [S1] Fulmer, G. R.; Miller, A. J. M.; Sherden, N. H.; Gottlieb, H. E.; Nudelman, A.; Stoltz, B. M.; Bercaw, J. E.; Goldberg, K. I. NMR chemical shifts of trace impurities: common laboratory solvents, organics, and gases in deuterated solvents relevant to the organometallic chemist. *Organometallics*, **2010**, *29*, 2176–2179.
- [S3] Sunasee, R.; Cliven, D. L. J. Desymmetrization of 4-hydroxy-2,5-cyclohexadienones by radical cyclization: synthesis of optically pure  $\gamma$ -lactones. *Chem. Commun.* **2010**, *46*, 701–703.
- [S4] Rubush, D. M.; Morges, M. A.; Rose, B. J.; Thamm, D. H.; Rovis, T. An asymmetric synthesis of 1,2,4-trioxane anticancer agents via desymmetrization of peroxyquinols through a brønsted acid catalysis cascade. *J. Am. Chem. Soc.* **2012**, *134*, 13554–13557.
- [S5] Carreño, M. C.; González-López, M.; Urbano, A. Oxidative de-aromatization of *para*-alkyl phenols into *para*-peroxyquinols and *para*-quinols mediated by oxone as a source of singlet oxygen. *Angew. Chem. Int. Ed.* **2006**, *45*, 2737–2741.
- [S6] Broo, A.; Holm, P.; Judkins, R.; Li, L.; Lindstedt-Alstermark, E.-L.; Sandberg, P.; M. Swanson, M.; Weidolf, L.; Mrickmann, K.; AstraZeneca AB. Non-anilinic derivatives of isothiazol-3(2H)-one 1,1-dioxides as liver X receptor modulators. Patent WO2006073366A1, 2006.
- [S7] Page, P. C. B.; Buckley, B. R.; Farah, M. M.; Blacker, A. J. Binaphthalene-derived iminium salt catalysts for highly enantioselective asymmetric epoxidation. *Eur. J. Org. Chem.* **2009**, *20*, 3413–3426.
- [S8] Cosier, J.; Glazer, A. M. A nitrogen-gas-stream cryostat for general X-ray diffraction studies. *J. Appl. Cryst.* **1986**, *19*, 105–107.
- [S9] Rigaku Oxford Diffraction, (2018), CrysAlisPro Software system, version 1.171.40.45a, Rigaku Corporation, Oxford, UK.
- [S10] Dolomanov, O. V.; Bourhis, L. J.; Gildea, R. J.; Howard, J. A. K.; Puschmann, H. OLEX2: a complete structure solution, refinement and analysis program. *J. Appl. Cryst.* **2009**, *42*, 339–341.
- [S11] Sheldrick, G. M. SHELXT - Integrated space-group and crystal-structure determination. *Acta Cryst.*, 2015, **A71**, 3-8.
- [S12] Sheldrick, G. M. Crystal structure refinement with SHELXL. *Acta Cryst.*, 2015, **C71**, 3-8.
- [S13] “CheckCIF” can be found under <http://checkcif.iucr.org>